Chemical characterization and biomarker fingerprinting of Deepwater Horizon oil spill residues

by

Fang Yin

A dissertation submitted to the Graduate Faculty of
Auburn University
in partial fulfillment of the
requirements for the Degree of
Environmental Engineering, Doctor of Philosophy

Auburn, Alabama
August 1, 2015

Keywords: Oil spill, Deepwater Horizon, petroleum biomarkers, oil fingerprinting, polycyclic aromatic hydrocarbons, tar balls

Approved by

T. Prabhakar Clement (Chair), Professor of Civil Engineering
Mark O. Barnett, Professor of Civil Engineering
Joel S. Hayworth, Associate Professor of Civil Engineering
Ming-Kuo Lee, Professor of Geosciences

Abstract

On April 20th, 2010, the Deepwater Horizon (DWH), a semi-submersible drilling rig, located about 120 miles off the coast of Alabama, exploring for oil in the Gulf of Mexico (GOM), experienced a catastrophic blowout and exploded. This event resulted in one of the largest marine oil spill disasters in U.S. history. Until the leaked oil gusher was capped on July 15th, 2010, approximately 4.9 million barrels of crude oil was released into the waters of GOM. About 40 days after the accident, the spilled oil started to wash along the shorelines of Florida, Alabama, Mississippi and Louisiana. The State of Alabama has approximately 50 km of sandy shoreline that are classified as amenity beaches. These beaches are priceless due to their economic and environmental values. To understand the environmental impacts of DWH oil on these amenity beaches, our group has been continuously monitoring this 50 km region over the past five years. The overall goal of this study is to characterize and fingerprint the field samples collected from these monitoring efforts.

In the first part of this study we compare the chromatographic signatures of petroleum biomarkers present in DWH source crude, three other reference crude oils, emulsified mousse that arrived on Alabama's shoreline in June 2010, and seven tar balls collected from Alabama beaches from 2011 to 2012. Characteristic of hopane and sterane fingerprints show that all the tar ball samples originated from DWH oil. The

diagnostic ratios of various hopanes indicated an excellent match. Quantitation data for C30αβ-hopane concentration levels show that most of the weathering observed in DWH-related tar balls found on Alabama's beaches is likely the result of natural evaporation and dissolution processes that occurred when the oil was transported across the Gulf of Mexico, prior to beach deposition. Based on the physical and biomarker characterization data presented in this study we conclude that virtually all fragile, sticky, brownish tar balls currently found on Alabama shoreline originated from the DWH oil spill.

In the second part of this study we present a four-year dataset to characterize the temporal evolution of various polycyclic aromatic hydrocarbons (PAHs) and their alkylated homologs trapped in the residual oil buried along the shoreline. Field samples analyzed include the first arrival oil collected from Perdido Bay, Alabama in June 2010, and multiple oil spill samples collected until August 2014. Our field data show that, as of August 2014, DWH oil is still trapped along Alabama's beaches as submerged oil, predominately in the form of surface residual oil balls (SRBs). Chemical characterization data show that various PAHs present in the spilled oil (MC252 crude) weathered by about 45% to 100% when the oil was floating over the open ocean system in the Gulf of Mexico. Light PAHs, such as naphthalenes, were fully depleted whereas heavy PAHs, such as chrysenes were only partially depleted by about 45%. However, the depletion rates of PAHs appear to have decreased significantly once the oil was buried within the partially-closed SRB environment. Depletion levels of several heavy PAHs have almost remained constant over the past 4 years. Our data also show that evaporation was the most likely weathering mechanism for PAH removal when the oil was floating over the ocean, although photo-degradation and other physico-chemical processes could have

contributed to some additional weathering. Chemical data presented in this study indicate that the submerged oil containing various heavy PAHs (for example, parent and alkylated chrysenes) is likely to remain in the beach system for several years.

In the third part of this study we have analyzed the first-arrival oil spill residues collected from two Gulf of Mexico (GOM) beach systems following two recent oil spills: the 2014 Galveston Bay (GB) oil spill and the 2010 Deepwater Horizon (DWH) oil spill. This is the first study to provide field observations and chemical characterization data for the 2014 GB oil spill. The primary purpose of this chapter is to present the similarities and differences between these two oil spills. Our data show that both oil spills had similar shoreline deposition patterns; however, the physical and chemical characteristics of their residues differed considerably.

In the final section we summarize the key outcomes of this research effort and also point out some future research directions.

Acknowledgments

I would like to express my sincere thanks to my advisor, Dr. Prabhakar Clement, for his patient guidance and mentorship during my stay at Auburn University. All the way from when I was starting the graduate program in the Department of Civil Engineering, through to the degree completion today, I am deeply influenced by Dr. Clement's sincere work attitude, active scientific thinking, humorous personality and down-to earth humility; I truly appreciate the opportunity to work with him. I would also like to thank my committee members Dr. Mark O. Barnett, Dr. Joel Hayworth and Dr. Ming-Kuo Lee, and my dissertation university reader Dr. Muralikrishnan Dhanasekaran, for their valuable comments and suggestions.

Special thanks to my colleagues, Gerald John and Yuling Han, for helping me with project design, instrumental exploration, experimental preparation and enrichment of our office life.

My other Auburn colleagues Farhad Jazaei, Dr. Jagadish Torlapati, Dr. Sunwoo Chang, Dr. Gautham Jeppu and Katie Nemec deserve appreciation for their supports in making our group experience fruitful and fun. I would like to acknowledge Dr. Vanisree Mulabagal for her help and support with various analytical experiments.

Finally, my great gratitude goes to my wife, Qi Cheng, who made innumerable sacrifices to complete all my endeavors, to my parents who gave the selfless contributions to my life, and to my friends who provided generous support during my

difficulties. I want to thank the City of Orange Beach, Alabama, USA, the National Science Foundation (NSF), Samuel Ginn College of Engineering, Auburn University, and Marine Environmental Sciences Consortium (MESC) for funding this research.

Table of Contents

List of Tables

List of Figures

List of Abbreviations

ITOPF	International Tanker Owners Pollution Federation
MC252	Macondo Prospect 252
DWH	Deepwater Horizon
GOM	Gulf of Mexico
SOMs	Submerged oil mats
SRBs	Surface residual balls
PAHs	Polycyclic aromatic hydrocarbons
BP	British Petroleum
USEPA	United States Environmental Protection Agency
NRC	National research council
OSAT	Operational science advisory team
LP	Lagoon Pass
OB	Orange Beach
BS	Bon Secour National Wildlife Refuge
FM	Fort Morgan
EI	Electron ionization
SIM	Single ion monitoring
MRM	Multiple reaction monitoring

TS	Time segment
CE	Collision energy
SS	Surrogate standard
IS	Internal standard
RRF	Relative response factor
LOD	Limit of detection
LOQ	Limit of quantitation
SD	Standard deviation
LWO	Laboratory-weathered oil samples
OWO	Ocean-weathered oil samples
DL	Below detection limit
C0-P	C_0-Phenanthrene
C1-P	C_1-Phenanthrenes
C2-P	C_2-Phenanthrenes
C3-P	C_3-Phenanthrenes
C4-P	C_4-Phenanthrenes
C0-D	C_0-Dibenzothiophene
C1-D	C_1-Dibenzothiophenes
C2-D	C_2-Dibenzothiophenes
C3-D	C_3-Dibenzothiophenes
C0-F	C_0-Fluorene
C1-F	C_1-Fluorenes
C2-F	C_2-Fluorenes

C3-F	C_3-Fluorenes
C0-C	C_0-Chrysene
C1-C	C_1-Chrysenes
C2-C	C_2-Chrysenes
C3-C	C_3-Chrysenes
C4-C	C_4-Chrysenes
B(a)A	Benzo(*a*)anthracene
B(b)F	Benzo(*b*)fluoranthene
B(k)F	Benzo(*k*)fluoranthene
B(j)F	Benzo(*j*)fluoranthene
B(e)P	Benzo(*e*)pyrene
B(a)P	Benzo(*a*)pyrene
B(ghi)P	Benzo(*ghi*)perylene
Anth	Anthracene
Flan	Fluoranthene
Py	Pyrene
Pery	Perylene
D(a,c)An	Dibenz(*a*,*c*)anthracene
D(a.h)An	Dibenz(*a*,*h*)anthracene
I(1,2,3-cd)Py	Indeno(1,2,3,-*cd*)pyrene

Chapter 1

Introduction

1.1 Occurrences of marine oil spills

Oil spills are one of common pollution sources released into the marine environment. They are mainly caused by mistakes from human activities that result in offshore tanker spills, oil platform spills, and drilling rig/well spills. The International Tanker Owners Pollution Federation (ITOPF) (2015) documented that there have been 1355 medium sized oil spills (7 to 700 tons) and 459 large sized oil spills (>700 tons) occurred from 1970 to 2014. According to a recent article (Fingas, 2012a), about 15 spills per day occur in the navigable water systems in United States. Also, about 12 oil spills occur per day in Canada, of which one spill per day occurs in navigable waters. In China, about 2635 oil spills were reported from 1973 to 2006, of which about 69 medium to large sized oil spills (>50 tons) were documented. On an average about 537 tons of oil originated from these accidents in China (Wang et al., 2014). Fortunately, according to published studies (Anderson and LaBelle, 2000; Burgherr, 2007; ITOPF, 2015), both in terms of volume and number, the statistics indicate a reducing trend in oil spill events in recent years. However, due to their potential to induce long-term negative impacts to the marine ecosystems, every oil spill is unacceptable, especially the large ones. The recent

2010 Deepwater Horizon oil spill that discharged about 663 million tons of oils into the Gulf of Mexico is the largest oil spill in U.S. history. The long term damages caused by this oil spill event is not fully known to date.

1.2 Fate and behavior of marine oil spills

The actual fate and behavior of oil discharged into ocean environment would depend on the oil's physical and chemical properties, local weather conditions and other environmental parameters. The common physicochemical processes occurring in marine environments have been well documented in previous studies (NRC, 2003; Sebastião and Guedes Soares, 1995; Thibodeaux et al., 2011; Wolfe et al., 1994). The key processes include evaporation, water-in-oil emulsification, photo-oxidation, dissolution, and biodegradation.

1.2.1 Evaporation

Due to the density and polarity differences between oil and seawater, oil is expected to float on the surface once it is released into marine waters. Evaporation processes will begin once the floating oil is exposed to the open atmosphere. Within several hours, light or medium crude oils can volatilize up to 40 to 70 % (in terms of volume). In contrast, heavy or refined oils can volatilize only by about 10% of their volume (NRC, 2003). Previous experimental data (Fingas, 1999; Fingas, 2012b) show that wind speed, exposed oil area, thickness of oil layer might not have a significant effect on the rate of oil evaporation. According to published literature (Fingas, 1999;

Fingas, 2013; NRC, 2003), the most important parameters that control oil evaporation rate are temperature and time. In general, the rate of evaporative loss will be proportional to the ambient temperature and air exposure time.

1.2.2 Water-in-oil emulsification process

Emulsification is another important ocean weathering process that impacts oil spills. Emulsification is mostly the result of mixing by turbulent currents and/or strong wave actions. Mixing promotes the capture of water droplets into the oil phase and forms a thick emulsion known as "chocolate mousse" or "oil mousse". Oil mousse can trap up to 85% of water and could expand the net oil volume by 3 to 5 times more than the original spill volume (NRC, 2003). Also, oil emulsion can dramatically change the physico-chemical properties of the oil. For example, with increase in water content, the net density of emulsified oil can become close to water density. This increase in density will enhance the chance of oil sinking into the water column, which can greatly complicate the cleanup efforts. Emulsification can also significantly decrease evaporation rates and also reduce the efficiency of chemical dispersants (Canevari, 1985). According to published data (McLean et al., 1998; NRC, 2003), the stability of an emulsified oil emulsion will be highly dependent on the amount of asphaltenes and resins in the oil. These studies have found that asphaltenes and resins can be accumulated at the oil-water boundary and hinder the re-coalescent process between the oil emulsion and new water droplets, which would result in the formation of stable oil emulsions.

1.2.3 Photo-oxidation

During most oil spill accidents, huge oil slicks will be formed as the result of oil spreading over the water. These floating slicks have large surface area indicating that they have a very high potential for reacting with solar radiation. During photochemical reactions, high polar oil products can be formed via solar radiation catalyzed reactions that occurring between petroleum chemicals and oxygen. These reactions can generate more water soluble products, and thus causing higher toxicity to the marine ecosystems. The potential toxic chemical derivatives formed could include hydroperoxides, ketones, aldehydes and oxygenated polycyclic aromatic hydrocarbons (PAHs) (Aeppli et al., 2012; Fathalla and Andersson, 2011; NRC, 2003). Photo-oxidation processes also might yield more high-molecular-weight oxyhydrocarbons that might considerably increase the persistence level of chemical residues trapped in offshore and nearshore ecosystems (Aeppli et al., 2012).

1.2.4 Dissolution

Dissolution of oil hydrocarbons into the water phase will be limited because of their differences in polarity levels. Dissolution is highly dependent on the oil properties and mixing conditions that exist at the oil-water boundary layer. Light crude oils have high fractions of low-molecular-weight aliphatic and aromatic hydrocarbons, which are more polar and can easily dissolve into water (NRC, 2003). Also, high turbulence levels could generate more contact area between water and oil thus could enhance solubility levels. Broadly, dissolution of oil would result in higher risk to marine species. However, in some oil spill cases, chemical dispersants are often used to increase dispersion and

decompose the spilled oil in to small droplets that can be easily dissolved within the water column. The usage of dispersants can also improve the efficiency of oil degradation by natural means and can potentially prevent the oil spill from reaching the shoreline.

1.2.5 Biodegradation

Biodegradation is a biochemical reaction that occurs between hydrocarbons present in the spilled oil and natural microorganisms. Biodegradation is the ultimate oil weathering process and it requires certain favorable environmental conditions including optimal water temperature, dissolved oxygen levels, pH conditions, and the availability of nutrients such as nitrogen and phosphorus. Biodegradation is the safest weathering process since it causes no secondary pollution to the environment. The biodegradation potential of a crude oil would depend on the types of petroleum hydrocarbons that are present in the original source. The most degradable hydrocarbons are linear alkanes, followed by branched alkanes, small aromatics hydrocarbons and cyclic alkanes (Das and Chandran, 2011). Several high-molecular-weight PAHs and polar compounds that contain nitrogen, sulfur and oxygen maybe difficult to biodegrade (Atlas and Bragg, 2009; Das and Chandran, 2011). The biodegradation pathways of oil hydrocarbons are initiated by various key enzymatic reactions that are catalyzed by oxygenases, peroxidases, dehydrogenases and hydrolases. These enzymes transform oil hydrocarbons into intermediate products during biodegradation. Since oil biodegradation is a safe and natural process, several types of bioremediation methods have been proposed for treating

nearshore contamination caused by different types of oil spill events (Atlas and Hazen, 2011; Bragg et al., 1994; Pritchard et al., 1992).

1.3 Chemicals of concern

Crude oils are natural fossil fuels formed by ancient organisms. They are a complex mixture of thousands of hydrocarbons and non-hydrocarbons. In general, the most abundant element in a crude oil is carbon (83-87%), followed by hydrogen (10-14%), sulphur (0.05%-6%), nitrogen (0.1-2%), oxygen (0.05-1.5%) and trace metals (less than 0.1%) (Helmenstine, 2014). The high percentages of carbon and hydrogen determine that hydrocarbons are the most dominant component in crude oils, which normally can be classified into paraffins (15-60%), napthenes (30-60%), aromatics (3-30%) and asphaltenes (remainder) (Helmenstine, 2014). Among them, the petroleum biomarkers (branched cycloalkanes), n-alkanes (straight chain paraffins) and polycyclic aromatic hydrocarbons (aromatics) are the most important class of petroleum hydrocarbons that been extensively studied in oil spill investigations. These compounds can be greatly useful for oil spill identification. They are also important indicators for assessing the detrimental effects of the oil to human and environment health.

1.3.1 Petroleum biomarkers - Hopanes and Steranes

Biomarkers are generally indicators used for fingerprinting oil spill samples. Biomarkers are accumulated when the oil was formed from former living organisms whose organic materials are preserved within source rocks over geologic times (Peters et

al., 2005). Their relative resistance to weathering allows them to be used as conservative markers and they are often referred to as "molecular fossils" (Peters and Moldowan, 1993). The chemical signatures of biomarkers can be used for tracking the source of a particular crude oil and also for quantifying its weathering rate in natural environments (Wang et al., 2001). Therefore, characterization of petroleum biomarkers is a critical step in oil spill studies. The composition of biomarkers in crude oils can vary widely depending primarily on the source and geological conditions of the reservoir (Idris et al., 2008; Peters et al., 2005). Comparing the fingerprints of biomarkers in oil residues with those from the original crude oil is a standard approach used in several oil spill assessment studies (Aeppli et al., 2014; Carmichael et al., 2012; Peters et al., 2005; Wang et al., 2006; Zakaria et al., 2001).

Hopanes and steranes are two important groups of biomarkers. They are branched cycloalkanes containing several carbon rings. The structural skeletons of hopanes and steranes are presented in Figure 1.1. Depending on the numbers of carbon atoms present, hopanes and steranes are named from C_{27} to C_{35} and C_{24} to C_{30}, respectively. Studies have shown that hopanes and steranes are abundant in weathered oils and can be used to quantify the degree of weathering (Aeppli et al., 2014; Douglas et al., 1996; Wang et al., 1999). Also, each crude oil can be easily identified according to its unique hopane and sterane patterns (Hostettler et al., 2013; Wang et al., 1999; Wang et al., 2006). Based on the position of hydrogen atom, α and β hydrogens are defined for these biomarker stereoisomers. As shown in Figure 1.1, the α hydrocarbons (dashed line) are located below the plane of the molecule, and the β hydrogens (wedge bond) are located above the plane of the molecule; note, this is illustrated using 17α(H), 21β(H)-

hopane molecule (Wang et al., 2006). Moreover, R and S are present for the two stereoisomers of C_{31}-C_{35} hopanes, which have an asymmetric center at carbon-22, referred as two homologous 22R- and 22S-hopanes (Figure 1.1). They can be eluted using a GC/MS method and the diagnostic ratios of $C_{31}(22S)/C_{31}(22S+22R)$, $C_{32}(22S)/C_{32}(22S+22R)$, $C_{33}(22S)/C_{33}(22S+22R)$, $C_{34}(22S)/C_{34}(22S+22R)$, and $C_{35}(22S)/C_{35}(22S+22R)$ can be calculated for fingerprinting the oil source. Similarly, in Figure 1.1, C_{27} to C_{29} steranes can have R and S assignments at carbon-20, which are referred as 20R- and 20S-steranes (Wang et al., 2006). Typical diagnostic ratios of these steranes (such as DiaC_{27}βα(20S)-sterane/DiaC_{27}βα(20R)-sterane) are also widely used in oil spill studies. These biomarkers provide an important approach for distinguishing oils, monitor the degree of oil weathering, and to quantify biodegradation processes under different environmental conditions (Wang and Fingas, 2003).

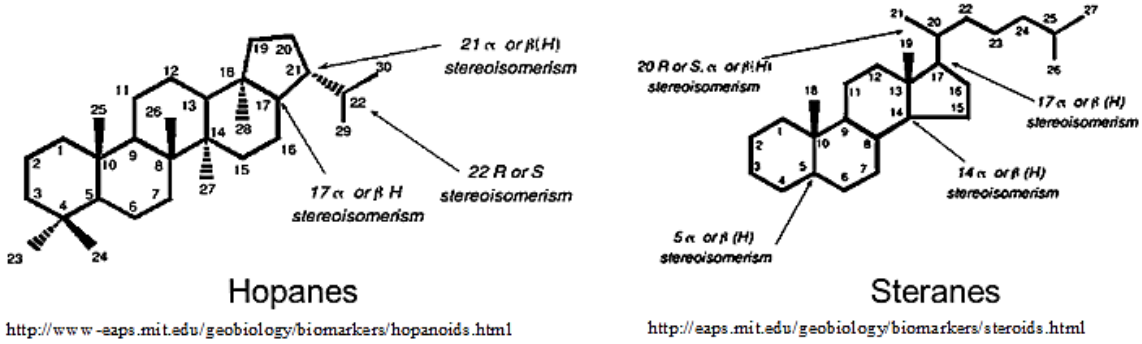

Figure 1.1 Molecular structures of hopanes and steranes

1.3.2 n-Alkanes

The n-alkanes are predominant hydrocarbon compounds that are commonly present in oil spill samples. They are composed of hydrogens and carbons with carbon-

carbon single bonds, which are known as “saturated” components of the oil. In oil spill studies, biological source of crude oils can be identified through n-alkanes, which typically show a higher abundance of the odd carbon-numbered alkanes than the even carbon-numbered alkanes (Wang et al., 1999). Also, the oil sources differentiation can be mapped from their n-alkanes elution range and their specific chromatogram patterns (Wang et al., 1999). Moreover, some important branched alkanes such as pristane and phytane are widely used with the C_{17} and C_{18} alkanes for oil sources identification; these include the diagnostic ratios of pristane/C_{17}, phytane/C_{18} and pristane/phytane (Chandru et al., 2008; Wang et al., 1999).

1.3.3 Polycyclic aromatic hydrocarbons

Contamination of coastal environment by oil residues can have major impact on ecological and socio-economic value of the system. Polycyclic aromatic hydrocarbons (PAHs) are one of the most important groups of toxic environmental contaminants present in oil spill residues that can directly impact human activities (Harvey, 1998; Neff, 1979). These groups of chemicals constitute a large class of organic substances with two or more fused aromatic rings (see Figure 1.2). Due to their mutagenic and carcinogenic properties (Michel et al., 2013; Mumtaz et al., 1996), PAHs are classified as hazardous organic compounds. To date, well over 100 PAHs have been identified, and sixteen of them have been classified as “priority pollutants” by the USEPA (1982). Many PAHs found in crude oil are highly recalcitrant in natural environments and hence can persist in the environment for a long period. For examples, the concentration levels of high molecular weight PAHs in the residues recovered 20 years after the *Arrow* oil spill

(which occurred in Nova Scotia, Canada in 1970) were nearly same as the levels found in their original reference oil (Wang et al., 1994c).

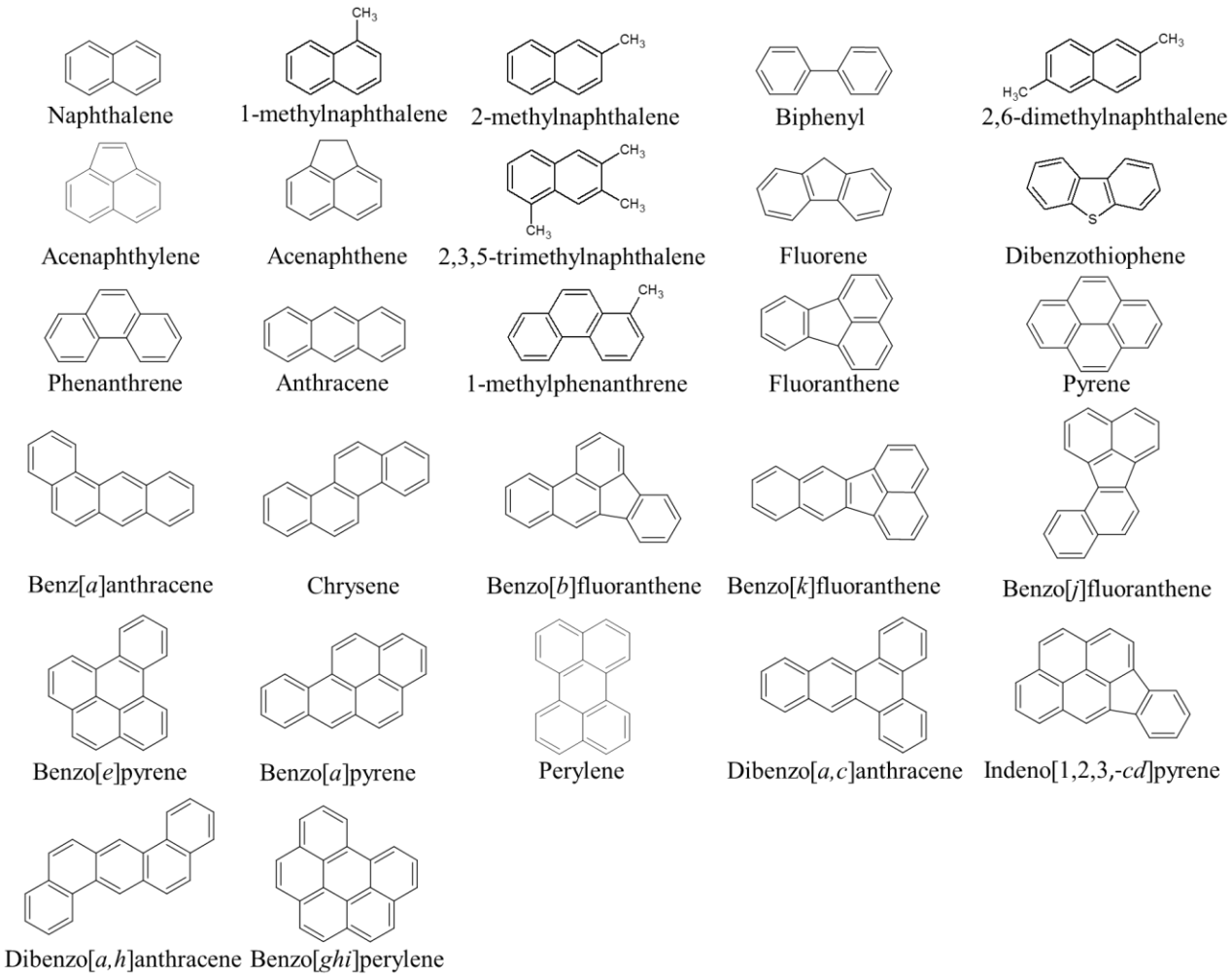

Figure 1.2 Molecular structures of the 27 target polycyclic aromatic hydrocarbons (PAHs)

1.4 Deepwater Horizon oil spill and the resulting coastal contamination

On April 20th, 2010, the Deepwater Horizon (DWH), a semi-submersible drilling rig while exploring for oil at the Macondo Prospect (MC252) in Gulf of Mexico (GOM), exploded and released large volume of light crude oil into GOM waters. Until the leaking well was capped on July 15th, 2010, approximately 4.9 million barrels of crude oil was released. Within a few weeks after the accident, ocean-weathered oil started to wash along the shorelines of Florida, Alabama, Mississippi and Louisiana. This weathered oil was predominantly in the form of water-in-oil emulsion (oil mousse), a highly viscous, buoyant and smelly material that experienced various ocean-weathering processes including evaporation, photo-oxidation, dissolution and biodegradation. After arriving in the nearshore environment, a portion of the mousse interacted with suspended solids and became denser and sank in the surf zone along the nearshore, forming submerged oil mats (SOMs). Figure 1.3 summarizes various nearshore processes that would have facilitated this sinking process. Over time, these SOMs have been buried and exposed as a result of coastal sediment dynamics. Their ultimate fate is largely unknown, although there is sufficient indirect evidence that tar mats are the primary source for the millions of oil spill residues (size ranging from several millimeters to 10 or more centimeters) that continue to be deposited along the shoreline till to-date. These residues are also known as tar balls, and also as surface residual balls (SRBs).

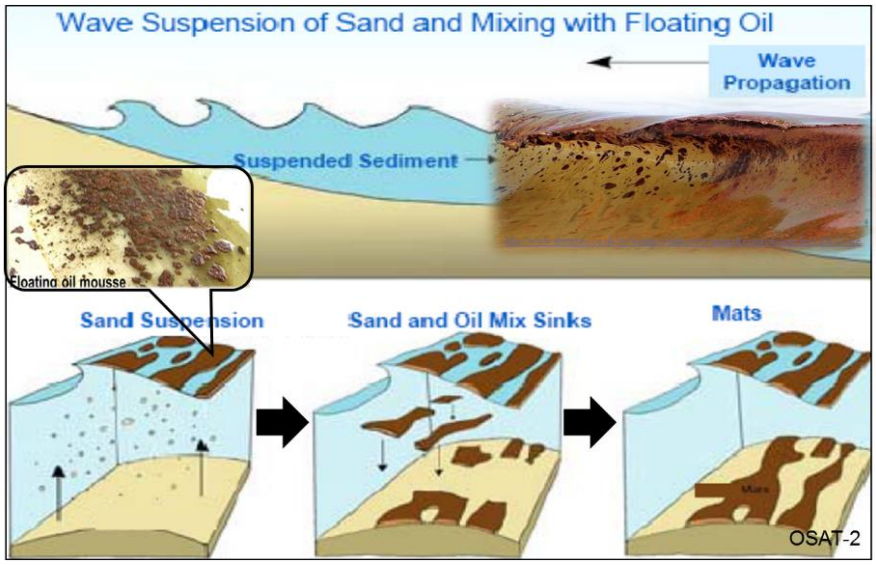

Figure 1.3 Mechanism of the formation of submerged oil mats (SOMs) and surface residual balls (SRBs) (modified after OSAT-2 report)

1.5 Scope and objectives of this research effort

Different types of oil spill residues washing onto sandy beaches is a common worldwide environmental problem. The focus of this dissertation is to characterize the oil spill residues that have been deposited along the Alabama shoreline since June 2010, when the first wave of DWH oil arrived along this shoreline. This dissertation is organized into four key chapters, with each chapter focusing of specific objectives and tasks, as discussed below:

The object of the first chapter (the current chapter) is to provide an overall summary of oil spill contamination problem and its impacts.

The objective of the second chapter is to analyze the distribution of biomarkers in DWH oil spill samples collected from Alabama beaches and confirm their origin, and evaluate the overall oil weathering levels.

The objective of the third chapter is to investigate the temporal and spatial variations of polycyclic aromatic hydrocarbons (PAHs) in DWH oil spill samples collected from Alabama shoreline from June 2010 to August 2014. The data are used to develop a better understanding of overall PAH weathering patterns and the impacts of various offshore and nearshore processes on net weathering rates.

The objective of the fourth chapter is to compare DWH oil spill with another recent oil spill that occurred in Galveston Bay, Texas (March 2014 oil spill). Samples from both spills are analyzed and the results are compared to understand the similarities and differences between these two GOM oil spill events.

The final chapter provides a summary of the key findings of this dissertation and also points out some possible future research directions.

Chapter 2

Chemical fingerprinting of petroleum biomarkers in Deepwater Horizon oil spill samples collected from Alabama shoreline

2.1 Introduction

Understanding the fate and transport of spilled crude oil in marine environments is an important environmental management problem. From June 2010 to the present, several DWH oil-related samples such as emulsions, surface slicks and tar balls, were deposited on Alabama's beaches (Hayworth and Clement, 2011; Hayworth et al., 2011). Our team has been monitoring the tar ball activity along Alabama's beaches and other oil-related contamination issues for the past five years (Hayworth et al., 2015). The continuous deposition of tar balls is a major concern for residents living along GOM beaches, and therefore a fundamental understanding of the origin of these tar balls, and also how the concentrations of various oil components are evolving with time in these tar ball samples is needed to better evaluate its long term impacts on GOM ecosystems. The primarily objective of this study is to analyze the biomarker fingerprints of various types of suspected DWH-related weathered oil spill residues recovered from Alabama's beaches.

Advanced analytical instruments such as gas chromatography/flame ionization detector (GC/FID) and gas chromatography/mass spectrometry (GC/MS) have been routinely used to analyze biomarkers in crude and weathered oil samples (Barakat et al., 1999; Hauser et al., 1999; Mostafa et al., 2009; Pauzi Zakaria et al., 2001; Stout, 2003; muWang et al., 2004; Wang et al., 1994a; Wang et al., 1994b; Wang et al., 2001; Wang et al., 1999; Wang and Fingas, 2003; Yim et al., 2011). In this work, we used a GC/MS method, run in selected ion monitoring (SIM) mode, for biomarker fingerprinting and quantification. Field samples were processed using a rapid cleanup procedure and were analyzed for hopanes and steranes. An Agilent GC/MS system was used to fingerprint and quantify hopanes in DWH source oil, emulsified mousse (which first arrived on Alabama's beaches in June 2010), and seven different tar balls and tar-mat fragments collected from Alabama beaches between September 2011 to February 2012. In addition, steranes profiles in DWH source oil and several field samples were also fingerprinted. Parts of this effort are published in the Marine Pollution Bulletin journal article titled: chemical fingerprinting of petroleum biomarkers in Deepwater Horizon oil spill samples collected from Alabama shoreline (Mulabagal, Yin et al., 2013).

2.2 Materials and methods

2.2.1. Materials

All of the organic solvents used in this study were of analytical or higher grade and were purchased from VWR International (Suwanee, GA). Polytetrafluoroethylene

membrane filters (PTFE, 0.45 and 0.2 µm) were purchased from VWR International (Suwanee, GA). Hopane standards were purchased from Chiron, Trondwheim, Norway. Anhydrous sodium sulfate (>99.0%, granular) and silica gel (60-200 µm) were purchased from Sigma-Aldrich (Allentown, PA). Chem Tube-hydromatrix was purchased from Agilent Technologies (Wilmington, DE). Deactivated GC liners (splitless tapered glass wool), GC capillary columns (J&W DB-EUPAH, p/n 121-9627, 340 ℃, 20 m x 180 µm x 0.14 µm; HP-5, p/n 19091J-436, 60 m x 250 µm x 0.25 µm; fused silica, p/n 160-7625, 450 ℃, 0.7 m x 150 µm x 0 µm) were purchased from Agilent Technologies (Wilmington, DE).

2.2.2 Sample details

Chemical fingerprinting of hopanes in seven different tar ball samples was completed. A sample of MC252 source oil, obtained from British Petroleum (BP), is designated as "DWH oil" in this study. The emulsified form of DWH oil (orange-colored mousse) collected from Orange Beach, Alabama, on June 11th, 2010, is designated as "Mousse." The small volume of original source crude oil (11.3 mL) was transferred in to an open 4-oz jar and was evaporated for six months under fume hood (Mott Manufacturing Limited, Ontario, Canada) at a face velocity of 200 fpm. The weathering process was completed at room temperature (22 ℃) and the resulting evaporated crude was designated as: "Evaporated DWH oil" (EDWH). Our research team has collected and archived several hundred tar balls and tar mat fragments over the past five years; details of these sampling trips are summarized in Hayworth et al. (2015). For this study, we randomly selected seven distinct tar balls collected between September 2011 to

February 2012 over the 22-mile long study region shown in Figure 2.1, and these samples are designated as: TB1, TB2, TB3, TB4, TB5, TB6 and TB7. The sampling locations of these tar balls are shown in Figure 2.1, and their GPS coordinates and other details are summarized in Table 2.1. In addition to the above samples, we also analyzed three standard reference crude oil samples: Arabian crude (AC), Bazra crude (BC) and Venezuelan heavy crude (VHC) which were purchased from ONTA Inc., Toronto, Canada.

Figure 2.1 Tar ball sampling locations along Alabama shoreline from Perdido Pass to Fort Morgan [Scale: from TB1 (Orange Beach point) to TB6 (Morgan Town Blvd.) is about 22 miles].

2.2.3 Estimation of oil percentage in tar ball samples

To determine the amount of residual oil fraction remaining in the tar ball samples, about 1 g of each tar ball was weighed and was extracted with 10 mL of dichloromethane four times. The dissolved oil fraction was decanted and the remaining solid (sand)

fraction was dried and weighted. The sand fraction in these tar-ball samples varied from 76% to 89% and these results are summarized in Table 2.1.

Table 2.1 Details of tar ball samples collected from various Alabama beaches

Sample	Latitude/N	Longitude/W	Sample Date	Location details of the	Sand
TB1	30°16'14.98"	87°34'1.46"	9/6/2011	Orange beach opposite to St. Thomas church	84%
TB2	30°14'28.65"	87°44'3.28"	9/8/2011	Lagoon Pass	83%
TB3	30°14'12.43"	87°45'46.94"	9/24/2011	2432 West Beach Blvd. (near Lee's landing marker)	89%
TB4	30°13'44.90"	87°49'41.26"	11/12/2011	Mobile Street (Bon Secour National Wildlife Refuge)	86%
TB5	30°14'47.76"	87°41'27.32"	1/25/2012	Gulf Shores public beach near Hangout Point	85%
TB6	30°13'50.38"	87°54'33.69"	2/18/2012	Morgan town Blvd.	88%
TB7	30°14'30.23"	87°43'41.90"	2/19/2012	Lagoon Pass	76%

2.2.4. Sample preparation procedure

About 25 mg of DWH, EDWH, mousse, and other crude oil samples (AC, BC, and VHC) were placed into 40 mL clear vials. To these pure oil samples we added 10 ml of hexane to maintain an effective oil concentration of 25 mg of oil phase per 10 ml of hexane. We then added 0.5 g of Chem-Tube-Hydromatrix and the samples were vortexed for five minutes, and the solutions were then allowed to settle at room temperature for 4 hours. The supernatant in each vial was then filtered through 0.45 μm

PTFE membrane filter and 4 mL of the extract was transferred to a vial containing 0.5 g of cleanup mixture consisting of 0.25 g of silica gel 60 (60-100μm) and 0.25 g of anhydrous sodium sulfate. The mixture was vortexed for 2 minutes, allowed to settle for 2 minutes, and then filtered through 0.2 μm PTFE membrane.

As shown in Table 2.1, our initial oil extraction data indicated that the tar balls contained considerable amount of sand ranging from 76% to 89%. Based on these data, we extracted the tar ball samples with appropriate amounts of hexane to maintain a concentration of 25 mg weathered oil per 10 ml of solvent. The extract was then subject to all the cleanup procedures discussed above. The final samples were spiked with the internal standard C_{30}ββ-hopane (IS, 17β(*H*),21β(*H*)-hopane, 100 ng/mL) prior to analysis. All samples were extracted and prepared in triplicate and each sample was analyzed in duplicate. To quantify extraction and cleanup recoveries, field samples were spiked with a known amount of C_{30}αβ-hopane (17α(*H*),21β(*H*)-hopane) and analyzed using GC/MS. The cleanup steps used for sterane analysis also followed a similar procedure.

2.2.5 Calibration curve

The calibration curve used to quantify hopane concentration levels was generated using a commercially available C_{30}αβ-hopane (17α(*H*), 21β(*H*)) standard (purchased from Chiron). Various dilutions ranging from 50-400 ng/mL of 17α(*H*), 21β(*H*)-hopane, spiked with the internal standard C_{30}ββ-hopane (17β(*H*),21β(*H*)-hopane of 100 ng/mL), were prepared to develop the calibration curve.

2.2.6 GC/MS analysis of hopanes and steranes in crude and weathered tar ball samples

Hopane analysis was performed using an Agilent Technologies triple quadrupole (7000B) GC/MS/MS system run in the GC/MS SIM mode. Chromatographic separation for hopanes was achieved using a DB-EUPAH (J&W Agilent Technologies) column (20 m x 180 µm x 0.14 µm) in constant pressure mode. The initial GC oven temperature (50 ℃ maintained for initial 2 min) was ramped to 310 ℃ (for 1 min) at 6 ℃/min and held for 15 min resulting in a 60.3 minute total run time. A post-run step was completed using a back-flush column, a novel technology available in our Agilent GC. The back-flush post-run step allowed reverse flushing of residual compounds retained within the column. The back-flush run was performed for 4 min at 310 ℃. The ion source temperature was maintained at 280 ℃ and the quad temperatures were set at 180 ℃. Helium was used as carrier gas, and the helium flow rate was set at 1 mL/min. The inlet pressure was 24.7 psi and inlet temperature was set at 280 ºC; sample injection (1 µL) was performed in the pulsed splitless mode. Target hopane analysis (in crude, weathered oil, and tar ball samples) was performed using a characteristic precursor ion at *m/z* 191 in SIM mode. Method extraction and cleanup recovery studies were performed by spiking samples with a known concentration of $C_{30}\alpha\beta$-hopane; recoveries were in the range of 86% to 91%.

Steranes fingerprints were developed using a longer Agilent GC column (19091J-436, 60 m x 250 µm x 0.25 µm) in the SIM mode. The oven temperature was kept at 50 ℃ during injection (for 1 min) then the temperature was increased at a rate of 70 ℃ /min to 150 ℃. After 2 min, the temperature was raised to 310 ℃ at a rate of 5 ℃ /min and

was fixed at 310 ℃ for 15 min; the total run time for the method was 51.4 min. The inlet and source temperatures were maintained at 300 ℃. SIM chromatograms for steranes were developed using the standard *m/z* 217 ion (Rosenbauer et al., 2010). All the qualitative and quantitative datasets were acquired using an Agilent data acquisition system and were analyzed using Agilent Technologies Mass Hunter Workstation Qualitative (B4.0) and Quantitative Analysis (B 5.0) software.

2.3 Results and discussion

2.3.1. Comparison of hopane and sterane fingerprints

Hopane fingerprints for DWH, EDWH oil, mousse and tar-ball (TB1-TB7) samples are shown in Figures 2.2 and 2.3. The structural assignments of various hopanes were achieved by pattern recognition of mass spectra, comparison of GC-retention time data with reference standards, and through available literature data for hopane fingerprints (Peters and Moldowan, 1993; Wang et al., 1997). The chromatographic profiles show that hopane distributions in DWH oil, mousse and tar ball samples are dominated by C_{27} to C_{35} pentacyclic hopanes, with high levels of C30 αβ-hopane (see Figures 2.2 and 2.3). The concentrations of T_s, T_m and C_{31}-C_{35} 22S/22R homohopane epimers in these samples are relatively low compared to C30 αβ-hopane levels. The figures show that hopane distribution in DWH crude oil, mousse and weathered-tar-ball samples have similar-looking fingerprints.

Although the above results have shown that the DWH oil and its related tar balls contained C_{30} αβ-hopane as the major biomarker, crude oils can vary in their hopane content from C_{27} to C_{35} and have a unique source-specific finger print. To demonstrate source-specific hopane distribution patterns, three crude oil samples of different geological origin (AC, BC, and VHC samples) were analyzed and their hopane fingerprints were compared with those of DWH oil in Figure 2.4. These data show that the intensity of C_{27}, C_{29} and C_{30} hopanes are distinctly different in all four crude oils, thus demonstrating the source-specific nature of hopane fingerprints.

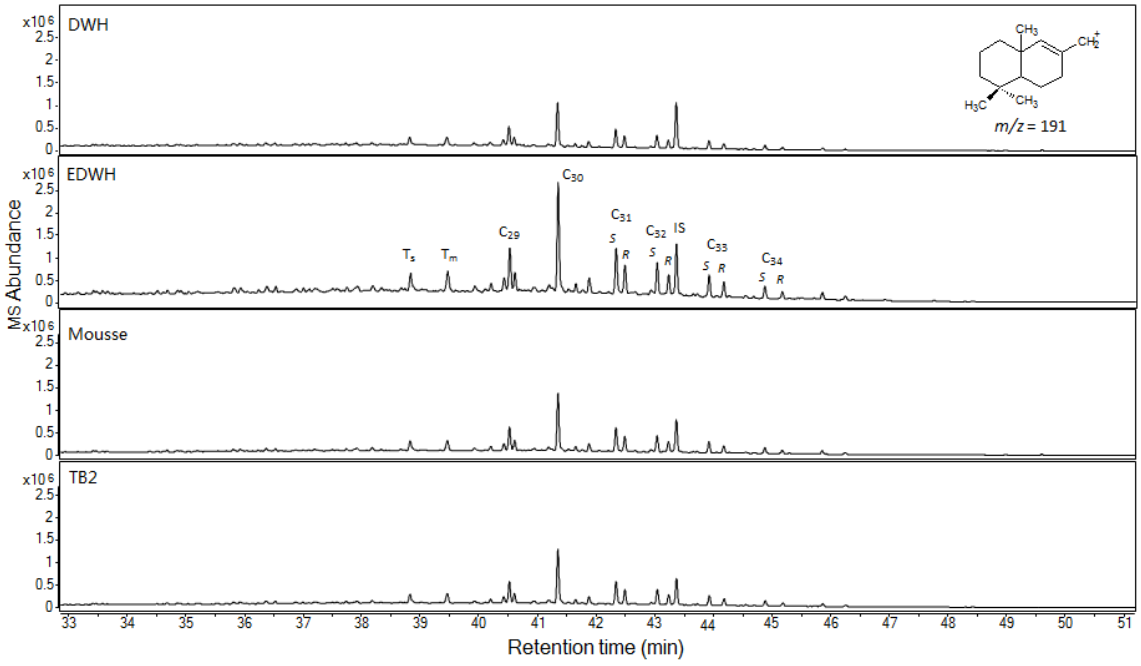

Figure 2.2 Comparison of hopane distribution in Deepwater Horizon (DWH) oil, evaporated Deepwater Horizon (EDWH) oil, mousse and tar ball samples. T_s: 18α(H)-22,29,30-trisnorneohopane; T_m: 17α(H)-22,29,30-trisnorhopane; C29: 17α(H),21β(H)-30-norhopane; C30: 17α(H),21β(H)-hopane; C31: 17α(H),21β(H)-31-homohopane-22S/22R;

C32:17α(H),21β(H)-32-bishomohopane-22S/22R; C33: 17α(H),21β(H)-33-trishomohopane-22S/22R; C33: 17α(H),21β(H)-33-tetrakishomohopane-22S/22R; IS) internal standard (17β(H),21β(H)-hopane).

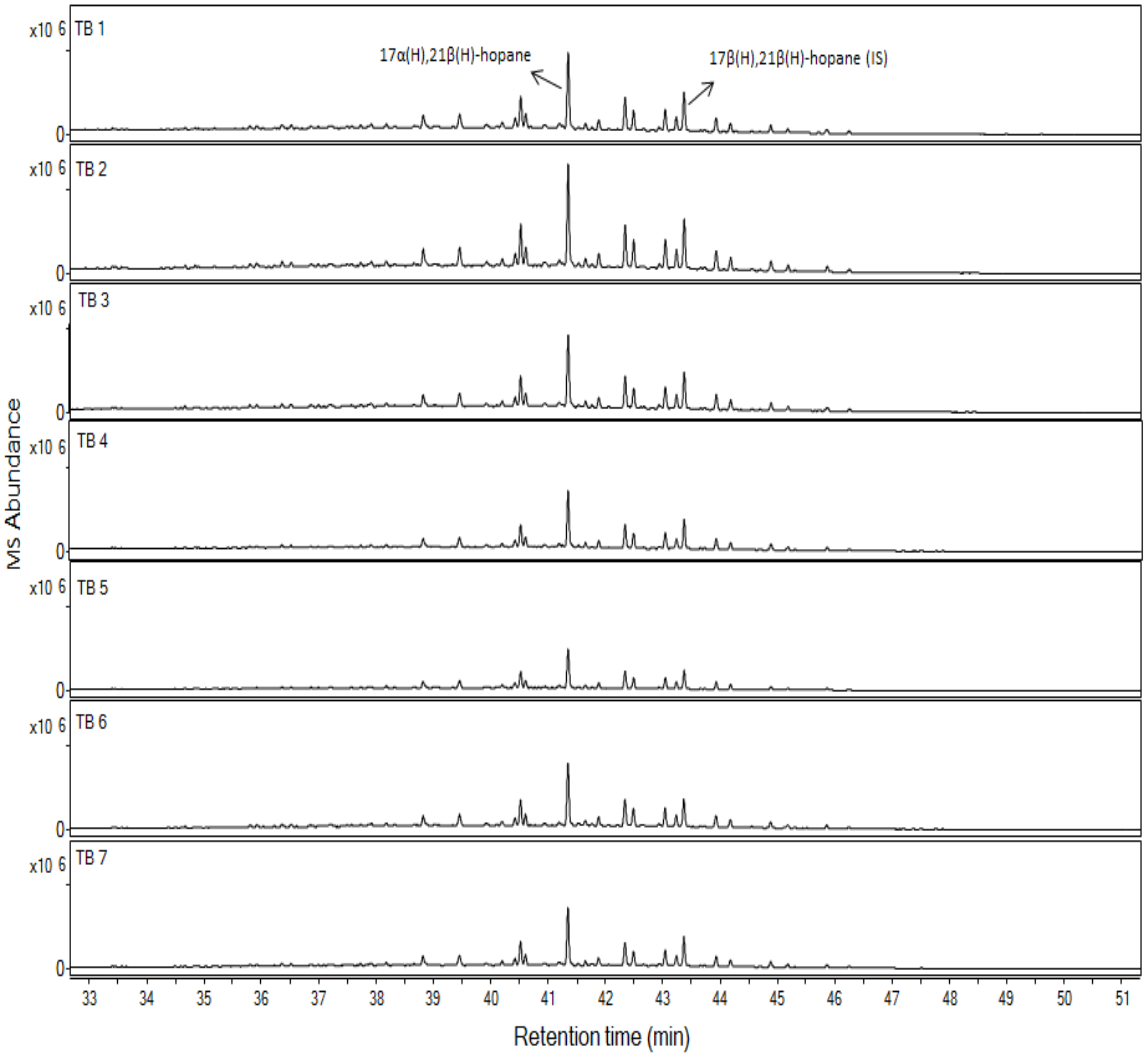

Figure 2.3 Hopane patterns in seven tar ball samples collected from Alabama beaches.

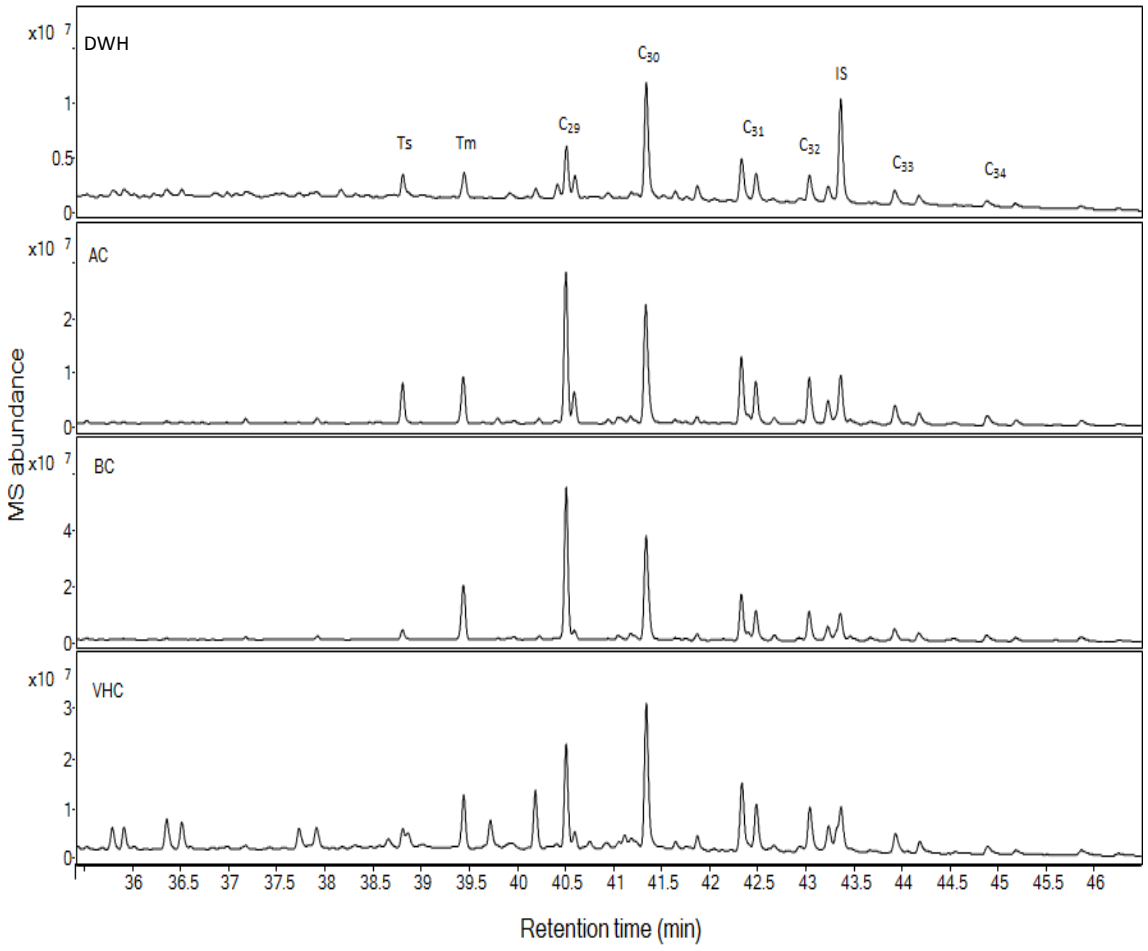

Figure 2.4 Distribution of hopanes in Deepwater Horizon oil (DWH), Arabian Crude (AC), Bazra Crude (BC), and Venezuelan Heavy Crude (VHC).

The chromatographic fingerprints of steranes in DWH oil, mousse and tar balls (TB2 and TB7) were also developed using a GC/MS method acquired in SIM mode (*m/z* of 217). Comparisons of chromatographic profiles of steranes in DWH oil, mousse and tar balls are shown in Figure 2.5. The results show that C_{27}, C_{28} and C_{29} steranes were abundant in DWH oil, which is known to be the characteristic signature of DWH source crude (Rosenbauer et al., 2010). Chromatographic signatures of steranes in mousse

sample are similar to DWH oil (see Figure 2.5). Similarly, the relative distribution of various sterane peaks in mousse and tar ball samples are almost identical indicating that these samples must have originated from the same source.

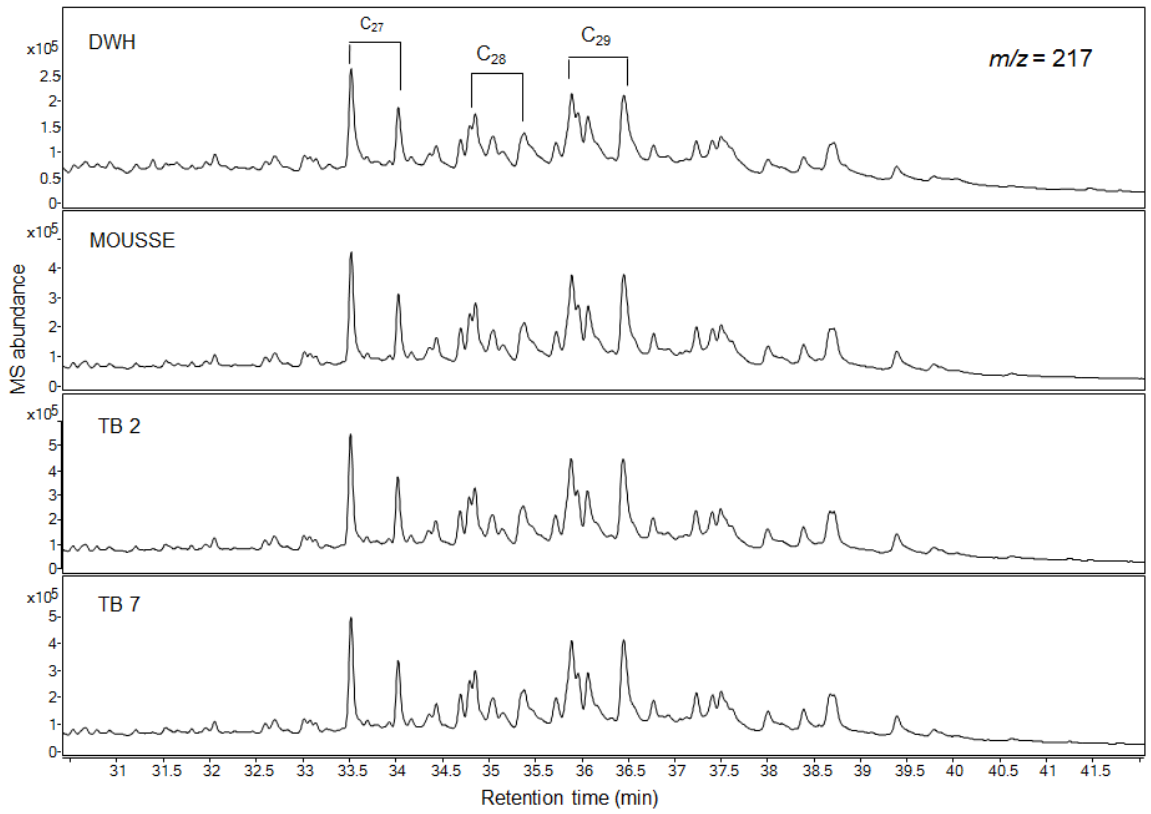

Figure 2.5 Chromatographic signatures of steranes (m/z 217) in DWH oil, mousse collected on June 2010, tar ball collected on September 2011 (TB2), and tar ball collected on February 2012 (TB7).

2.3.2 Diagnostic ratios of source-specific hopanes

The relative ratios of source-specific hopanes often differ from oil to oil. This variation depends on source rock, depositional environment, and maturity of the oil. Wang et al. (2004) reported that the diagnostic ratios of hopane biomarkers commonly used for oil spill fingerprinting include: T_s/T_m, $T_s/(T_s+T_m)$, C_{29}/C_{30}, and homohopane. The ratios of T_s/T_m, $T_s/(T_s+T_m)$ and C_{29}/C_{30} were also reported as characteristic markers and can be used for source identification (Wang et al., 2011; Wang et al., 1994c). We computed the following hopane characteristic ratios: T_s/T_m, $C_{29}\alpha\beta/C_{30}\alpha\beta$, $C_{31}(S)/C_{31}(S+R)$, $C_{32}(S)/C_{32}(S+R)$, $C_{33}(S)/C_{33}(S+R)$, $C_{34}(S)/C_{34}(S+R)$, and $C_{35}(S)/C_{35}(S+R)$. The ratios were calculated for all the field samples (mousse and seven tar ball samples) and were compared against the values estimated for the DWH source crude oil and the results are summarized in Table 2.2. These estimates were derived from the estimated values of peak areas of different characteristic hopanes. The computed values for T_s/T_m for DWH oil and mousse samples were 0.91 and 0.92, respectively; the values of C_{29}/C_{30} for DWH oil and mousse samples were 0.38 and 0.37, respectively. The ratios of T_s/T_m for tar ball samples ranged from 0.92 to 0.95, and the values of C_{29}/C_{30} ranged from 0.38 to 0.37 (see Table 2.2). The agreement of diagnostic hopane ratios for the tar ball samples and their match with those values estimated for the DWH source oil provide compelling evidence that all these tar balls originated from the DWH oil spill. The data show that the characteristic hopane pair ratios in DWH related oil and tar ball samples, especially T_s/T_m and C_{29}/C_{30}, were relatively unaffected by weathering; similar results have been shown by others (Shen, 1984). Shen (1984) also pointed out that samples that differ in their T_s/T_m ratios by over 20% most likely originated from

different sources. We compared the diagnostic hopane ratios of the three reference crude oils (AC, BC, and VHC) with DWH oil. The ratios of T_s/T_m in AC, BC, VHC, and DWH oils are 0.82, 0.19, 0.35 and 0.91; and C_{29}/C_{30} ratios are 1.04, 1.19 and 0.63 and 0.38 respectively (Table 2.2). As expected, the diagnostic ratios of both T_s/T_m and C_{29}/C_{30} measured in AC, BC, and VHC oils are considerably different from the values measured in DWH oil indicating that all four oil samples originated from distinctly different reservoirs.

Table 2.2 Diagnostic ratios of characteristic hopanes in crude oil, mousse, and tar ball samples

Sample	**Diagnostic ratios of Hopanes**						
	T_s/T_m	**$T_s/(T_s+T_m)$**	**C_{29}/C_{30}**	**$C_{31}S/(S+R)$**	**$C_{32}S/(S+R)$**	**$C_{33}S/(S+R)$**	**$C_{34}S/(S+R)$**
DWH oil	0.91 ±0.06	0.47 ±0.02	0.38 ±0.02	0.61 ±0.01	0.65 ±0.01	0.60 ±0.02	0.67 ±0.04
EDWH oil	0.91 ±0.04	0.47 ±0.01	0.37 ±0.02	0.63 ±0.02	0.62 ±0.01	0.63 ±0.01	0.63 ±0.01
Mousse	0.92 ±0.05	0.48 ±0.01	0.37 ±0.01	0.63 ±0.01	0.65 ±0.01	0.61 ±0.01	0.63 ±0.01
TB 1	0.92 ±0.06	0.48 ±0.02	0.38 ±0.01	0.63 ±0.03	0.64 ±0.02	0.63 ±0.03	0.65 ±0.03
TB 2	0.93 ±0.03	0.49 ±0.01	0.37 ±0.01	0.64 ±0.01	0.64 ±0.01	0.61 ±0.02	0.59 ±0.01
TB 3	0.95 ±0.03	0.49 ±0.01	0.38 ±0.01	0.64 ±0.03	0.63 ±0.01	0.60 ±0.03	0.62 ±0.01
TB 4	0.94 ±0.03	0.48 ±0.02	0.37 ±0.02	0.62 ±0.01	0.63 ±0.01	0.65 ±0.01	0.63 ±0.02
TB 5	0.93 ±0.06	0.48 ±0.02	0.37 ±0.02	0.61 ±0.01	0.64 ±0.02	0.63 ±0.02	0.63 ±0.01
TB 6	0.93 ±0.03	0.48 ±0.01	0.37 ±0.02	0.62 ±0.00	0.63 ±0.02	0.63 ±0.03	0.65 ±0.02
TB 7	0.93 ±0.03	0.49 ±0.01	0.37 ±0.02	0.62 ±0.00	0.63 ±0.00	0.63 ±0.01	0.66 ±0.01
AC	0.82 ±0.01	0.45 ±0.01	1.04 ±0.05	0.62 ±0.02	0.64 ±0.01	0.59 ±0.01	0.62 ±0.03
BC	0.19 ±0.01	0.16 ±0.01	1.19 ±0.00	0.60 ±0.00	0.65 ±0.02	0.55 ±0.06	0.61 ±0.01
VHC	0.35 ±0.03	0.26 ±0.01	0.63 ±0.02	0.60 ±0.00	0.63 ±0.00	0.60 ±0.03	0.58 ±0.04

2.3.3 Quantitation of primary hopane ($C_{30}\alpha\beta$-hopane) in crude and weathered oil samples

The concentration of $C_{30}\alpha\beta$-hopane (the primary hopane compound) was quantified in all crude-oil and tar-ball samples. A calibration curve was first developed using Chiron $C_{30}\alpha\beta$-hopane standard (> 98% by GC/MS) with concentrations ranging from 50-400 ng/mL and spiked with an internal standard ($C_{30}\beta\beta$-hopane, 100 ng/mL, > 98% by GC/MS). The calibration response was linear across the selected analytical range, yielding a correlation coefficient (r^2) value of 0.999. Quantitative results indicate that DWH oil contained 53 ± 3 mg/kg of $C_{30}\alpha\beta$-hopane, which is consistent with the values of 44 ± 21 mg/kg reported in a multi-laboratory study completed by National Institute of Standards and Technology (NIST) (Schantz and Kucklick, 2011). The average values of $C_{30}\alpha\beta$-hopane in EDWH and mousse samples were 103 and 91 mg/kg, respectively. The amount of $C_{30}\alpha\beta$-hopane in the tar ball samples TB1, TB2, TB3, TB4, TB5, TB6 and TB7 were 102, 104, 111, 123, 103, 120 and 119 mg/kg oil, respectively. The amount of $C_{30}\alpha\beta$-hopane in AC, BC, and VHC crude oil samples was 94, 131 and 85 mg/kg, respectively.

2.3.4 Assessment of weathering levels using $C_{30}\alpha\beta$-hopane concentrations

We used $C_{30}\alpha\beta$-hopane as an internal conservative biomarker to estimate the degree of weathering of EDWH, mousse and the seven tar ball samples using the following equation (Wang et al., 2001):

$$P(\%) = \left(1 - \frac{C_s}{C_w}\right) \times 100,$$

where *P* is the percentage weathering level with respect to the source crude, and *Cs* and *Cw* are the concentrations of C_{30}αβ-hopane in the source oil (DWH) and weathered sample, respectively. The weathering levels of EDWH and mousse samples were found to be 49% and 42%, respectively. The level of weathering estimated for the tar ball samples TB1 to TB7 were: 48%, 49%, 52%, 57%, 48%, 56%, and 55%, respectively. The EDWH sample was prepared by evaporating a known amount DWH source crude oil for about six month. The sample was periodically weighed and gravimetric analysis of the data indicated that the crude oil evaporated by 25% within a day, 30% within 2 days, 40% within a month, and about 47% in six months. The hopane-based procedure estimated that the 6-month old EDWH sample should have weathered by 49%, which compares well with the gravimetric-measurement based weathering level of 47%. This data indicates that the accumulation level of C_{30}αβ-hopane in weathered samples can be used to track the overall weathering level.

Figure 2.6 summarizes all the C_{30}αβ-hopane data and the estimated values of percentage weathering levels for all the field samples. The data points shown in Figure 2.6 are organized based on the approximate time (in days) taken by the sample to weather in the environment, with zero indicating the beginning of the accident (note the data for the fresh oil collected at the well head was plotted at this point). Floating mousse material was collected from Alabama beaches on June 11th, 2010 (assumed to have weathered about 50 days over the ocean). The hopane concentration levels show that due to various ocean-scale transport processes, including evaporation and dissolution, the oil in the form of mousse that arrived along the beaches was already weathered by about 42%. However, it is interesting to note that the average weathering level of the tar ball

samples collected after about 2 years was about 50%. This data indicates that very little weathering has occurred once the oil was buried in Alabama's nearshore environment.

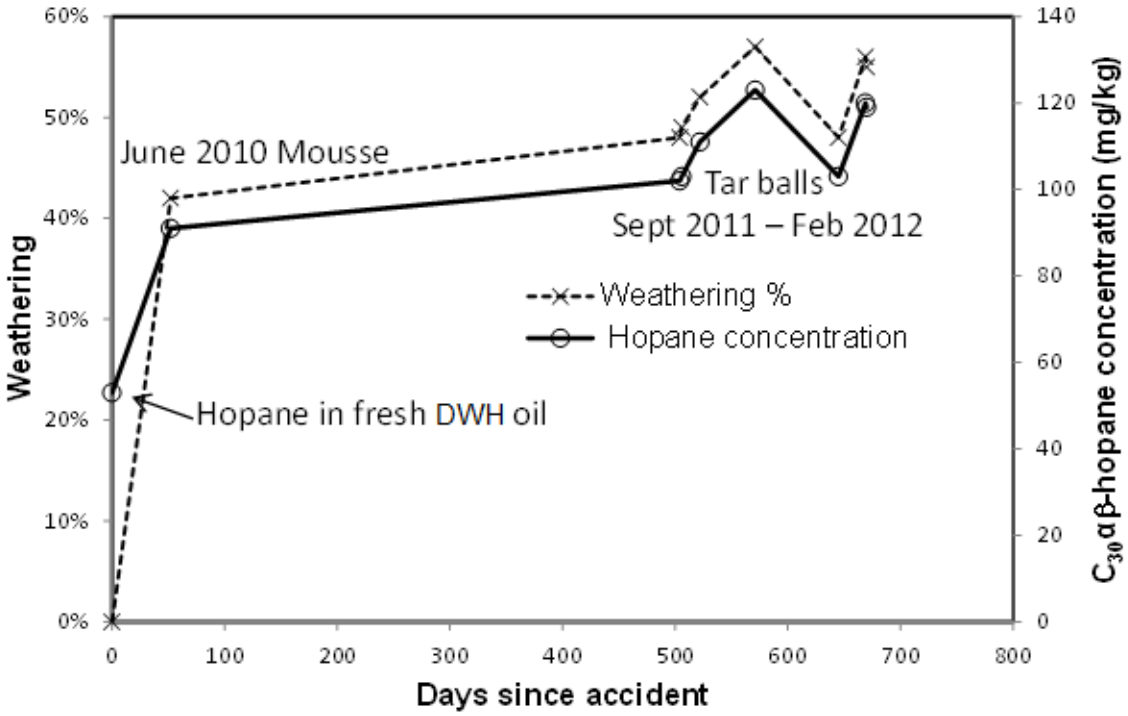

Figure 2.6 Changes in $C_{30}\alpha\beta$-hopane concentration and percentage weathering level (data for DWH oil, mousse and tar-ball are arranged based the time they were exposed to environmental weathering processes).

2.4 Conclusions

We used a GC/MS method for fingerprinting hopanes and steranes in source crude oil and weathered tar ball samples. The method uses simplified extraction and cleanup protocols that are relatively easy to implement. This study is the first to quantify

hopane chemical profiles of multiple DWH oil spill related tar balls collected along the Alabama shoreline. In this work we have presented hopane fingerprints, diagnostic ratios of characteristic hopane pairs, and $C_{30}\alpha\beta$-hopane concentration levels for DWH source crude oil, three other reference crude oils, emulsified mousse collected on Alabama's beaches in June 2010, and seven different tar balls collected from Alabama's beaches from September 2011 to February 2012. We have also provided the sterane fingerprints of several field samples and compared them against DWH oil fingerprints. The $C_{30}\alpha\beta$-hopane was found to be the most abundant hopane in DWH oil and $C_{30}\alpha\beta$-hopane concentration was found to be 53 ± 3 mg/kg, which is well within the range of 44 ± 21 mg/kg reported in a multi-laboratory study completed by NIST. Based on measured $C_{30}\alpha\beta$-hopane concentrations, the average weathering level of the tar ball samples collected after about two years (between September 2010 to February 2012) is 50%, which is quite close to the weathering level of 42% estimated for the first-arrival mousse collected in June 2010. This result indicates that the oil submerged along the Alabama coastline has not weathered significantly over the past two years. The lab-synthesized weathered oil sample (EDWH sample) showed that evaporation alone can weather DWH oil sample by about 40% within a month; therefore, evaporation during transport across the GOM (from the MC252 well head to Alabama's shoreline) was likely the most important weathering process. Comparison of hopane fingerprints, selective sterane fingerprints, and characteristic hopane ratios, especially the ratios of T_s/T_m and C_{29}/C_{30}, show that mousse and the tar ball samples analyzed in this study originated from DWH oil. According to our field observation, the MC252-related tar balls are fragile, soft, sticky brownish material containing considerable amount of sand and have a noticeable

petroleum odor. In contrast, the highly weathered non-MC252 tar balls hard, dark and have a very weak petroleum odor (and often no odor). In this regard, both chemical and physical characteristics approved the studied tar balls were from DWH oil spill.

Chapter 3

Long-term monitoring data to describe the fate of polycyclic aromatic hydrocarbons in Deepwater Horizon oil submerged off Alabama's beaches

3.1 Background

Figure 3.1 shows typical Deepwater Horizon submerged oil mat (SOM) and surface residual balls (SRBs) or tar balls found near Alabama's beaches. The SOM shown in the figure is a piece of oil mat fragmented from a larger SOM. Both SOMs and SRBs contain various hazardous chemicals including polycyclic aromatic hydrocarbons (PAHs) which can be toxic to human and ecological systems (Liu et al., 2012; Urbano et al., 2013). For example, Dubansky et al. (2013) found up-regulation of cytochrome P4501A protein in the gills, liver, intestines and kidneys of killifish (an abundant, non-migratory baitfish) when they were exposed to BP oil spill contaminated sediments. Also, laboratory exposures of killifish embryos to oil contaminated sediments resulted in developmental abnormalities. Their study concluded that these data are predictive of potential population-level impacts when killifish are exposed to oiled sediment present along the northern GOM coast.

Figure 3.1 Typical mousse, SOM, and SRB samples recovered from Alabama's beaches

Since the first arrival of ocean-weathered oil on Alabama's beaches in June, 2010, our research team has continuously monitored the ~50 km long sandy beaches located from the Alabama-Florida border to Mobile Bay (see Figure 3.2). Our interests have principally been to observe and document the physical and chemical evolution of oil buried (in the form of SOMs and SRBs) near this beach system. Hayworth et al. (2015) described our field sampling approaches and the temporal evolution of the physical characteristics of SOMs and SRBs present in the system. Here we present the results of a 4-year chemical characterization study to examine the temporal trends in PAH levels measured in oil spill samples collected from Alabama's beaches from June 2010 to August 2014. These data are used to develop a framework for describing the fate of PAHs trapped in SOMs and SRBs buried near DWH-oil-spill impacted GOM beaches. Parts of this effort are published in the Science of the Total Environment journal article

titled: long-term monitoring data to describe the fate of polycyclic aromatic hydrocarbons in Deepwater Horizon oil submerged off Alabama's beaches (Yin et al., 2015b).

Figure 3.2 Field sampling locations (modified from map data ©2013 Google). FM represents Fort Morgan, BS represents Bon Secour National Wildlife Refuge, LP represents Lagoon Pass and OB represents Orange Beach.

3.2 Material and methods

3.2.1 Sample collection

MC252 reference crude oil (or DWH oil) was supplied by British Petroleum (BP) and is referred to as MC252 oil. A number of ocean-weathered, first arrival oil spill samples were collected from various beaches in Alabama. We used a floating mousse sample recovered near Orange Beach (see Figure 3.2) on June 11, 2010, as the reference ocean-weathered oil spill (OWO) sample. Details of SRB sampling locations used in this study are shown in Figure 3.2 and the GPS coordinates are given in Table 3.1. Temporal

variations in target PAHs were assessed by sampling SRBs at a fixed location, Lagoon Pass (LP), 6 different times: September 08, 2011 (LP1), February 19, 2012 (LP2), September 02, 2012 (LP3), February 15, 2013 (LP4), June 14, 2013 (LP5), and August 01, 2014 (LP6). Lagoon Pass was selected for temporal sampling since this location consistently had very high level of SRB activity. To assess spatial variations in PAH levels, we used the SRBs collected from four different locations: Orange Beach (OB), September 2012 Lagoon Pass sample (LP3), Bon Secour National Wildlife Refuge (BS), and Fort Morgan (FM). All these samples were collected on September 2, 2012.

Table 3.1 Details of field samples

Sample	**Latitude/N**	**Longitude/W**	**Location**
LP 1 to 6	30°14’25.55”	87°44’16.58”	Gulf Shores near Lagoon Pass
OB	30°16’14.98”	87°34’1.46”	Orange Beach
BS	30°13’44.90”	87°49’41.26”	Bon Secour Wildlife Refuge
FM	30°13’50.38”	87°54’33.69”	Fort Morgan

During each sampling event, representative field samples with SRB sizes ranging from 1-10 cm were collected; total weight of samples recovered from various locations ranged from 0.5 kg to several kilograms. Each SRB sample collected at a particular location was stored in a plastic bag, sealed and labelled. The bag was then stored on ice in a cooler and then transferred to the laboratory. A homogenized subsample (weight

ranging from 100 to 500 g from each field sample) was prepared in the laboratory by breaking the SRBs into smaller fragments and removing inorganic and organic debris (shells, stones, sticks etc.). To avoid cross contamination, these homogenized field samples were prepared separately and stored in different containers. Additionally, we also prepared a laboratory-weathered reference oil sample by evaporating a small quantity (triplicated samples weighing 0.79, 0.80, and 0.80 grams of oil) of MC252 reference crude oil in a dark fume hood for a period of six days. The resulting laboratory-weathered MC252 oil sample is identified as LWO.

3.2.2 Materials

The organic solvents used in this study were of analytical grade or higher. The solvents, silica gel (60-200 μm), and anhydrous sodium sulfate (ACS grade) were purchased from VWR International (Suwanee, GA). C_{30}ββ-hopane (17β(*H*),21β(*H*)-hopane) standard was purchased from Chiron, Trondeim, Norway. PAH standard mixtures consisting of twenty-seven PAHs (naphthalene, 1-methylnaphthalene, 2-methylnaphthalene, 2,6-dimethylnaphthalene, 2,3,5-trimethylnaphthalene, biphenyl, acenaphthylene, acenaphthene, fluorene, phenanthrene, 1-methylphenanthrene, anthracene, dibenzothiophene, fluoranthene, pyrene, benzo(*a*)anthracene, chrysene, benzo(*b*)fluoranthene, benzo(*j*)fluoranthene, benzo(*k*)fluoranthene, benzo(*e*)pyrene, benzo(*a*)pyrene, perylene, dibenz(*a,c*)anthracene, dibenz(*a,h*)anthracene, indeno(1,2,3,-*cd*)pyrene and benzo(*ghi*)perylene) were purchased from Agilent Technologies, Wilmington, DE. A mixture of four surrogate standards (SS) including naphthalene-d_8, acenaphthene-d_{10}, phenanthrene-d_{10} and benzo(*a*)pyrene-d_{12} were purchased from Ultra

Scientific Analytical Solutions (North Kingstown, RI). Internal standard (IS) *p*-terphenyl-d_{14} (purity 98.5%) was purchased from AccuStandard (New Haven, CT, USA). Chromatographic separation of various PAH compounds was achieved using a J&W DB-EUPAH (Agilent Technologies) column (20 m x 180 µm x 0.14 µm). The back flush setup used Agilent Technologies inert fused silica column (0.7 m x 150 µm x 0 µm; 450 ℃).

Prior to use, activated silica gel was prepared according to an established protocol (Wang et al., 1994b). Silica gel was serially rinsed three times with 250 ml acetone, hexane and dichloromethane and then left to dry for 12 hours in a fume hood. After drying, silica gel was heated in an oven at 40-50 ℃ for 8 hours and then activated at 180 ℃ for 20 hours. Anhydrous sodium sulfate was purified by heating at 400 ℃ for 4 hours and then cooled and stored in tightly sealed glass containers.

3.2.3 Estimation of oil percentage levels

About 1 gram of the homogenized sample was extracted using 10 ml of dichloromethane. The extraction step was repeated four times and the remaining solid residues in the vial was dried and weighed. The average values of oil content determined are: 17%, 24%, 22%, 15%, 17%, and 16% for LP1 to LP6 samples, and 12%, 12% and 12% for OB, BS and FM samples, respectively. The average standard deviation of these estimates was 0.9%.

3.2.4 Analytical and quantitation methods

3.2.4.1 Column fractionation

Column chromatographic fractionation was performed using an approach modified from a published method (Wang et al., 1994b). A glass column (250 mm × 10 mm) was plugged with glass wool at the bottom, and then packed with 3 g of activated silica gel and topped with 1g of anhydrous sodium sulfate. The chromatographic column was charged with 20 ml of hexane and the eluent was discarded. About 12 mg of oil or 25 mg of mousse sample was weighed in a vial, spiked with four surrogate standards and mixed with 1 ml of hexane. Entire mixture was transferred to the column, and the vial was sequentially washed with 2 ml of hexane (with 1 ml in each step); contents from sequential washing were also transferred to the column. For SRB samples, about 25 mg oil of equivalent sample was used, and the weight was adjusted based on oil content (for example, 147 mg of LP1, having 17 % oil content yields 25 mg of oil). About 12 ml of hexane was added to the column to elute aliphatic hydrocarbon fractions, and this hexane fraction was labeled as F1. Then 15 ml of solvent containing a mixture of 50% hexane and 50% dichloromethane was used to elute the aromatic hydrocarbon fraction, and this fraction was labeled as F2. The F1 and F2 fractions were concentrated under a gentle stream of nitrogen and required amount of solvent was added to adjust the final sample volume to 10 ml. 1 ml of the adjusted F1 and F2 samples were spiked with C_{30}ββ-hopane (17β(*H*),21β(*H*)-hopane) and *p*-terphenyl-d_{14}, respectively, prior to chemical analysis. All the samples were prepared in duplicate and analyzed in triplicate.

3.2.4.2. Determination of PAHs depletion levels

Organic compounds in crude oil will weather concurrently; therefore, it is important to use a conservative marker to normalize the concentration of contaminants measured in environmental samples (Douglas et al., 1996). We used C_{30}αβ-hopane as the conservative marker for normalization. Hopane response in the original crude oil source sample was quantified by first computing a ratio H_{oil}, which is the peak area of C_{30}αβ-hopane in crude oil (normalized to the oil weight) to the peak area of the internal standard C_{30}ββ-hopane. We also estimated another hopane ratio $H_{weathered}$, which is the peak area of C_{30}αβ-hopane in a weathered oil spill sample (normalized to oil weights) to the peak area of the internal standard C_{30}ββ-hopane. These ratios were used to compute the hopane normalizing factor, $H_{oil}/H_{weathered}$, which was then used to estimate the degree of weathering for a target PAH using the following formula (Douglas et al., 1996; Radovic et al., 2014):

$$\text{Actual \% depletion of PAH} = \left(1 - \frac{\text{PAH in weatherd sample}}{\text{PAH in reference oil}} \times \frac{H_{oil}}{H_{weathered}}\right) \times 100 \qquad (1)$$

Concentrations of PAHs and the responses of biomarker compounds were quantified using an Agilent 7890 gas chromatograph coupled with an Agilent 7000B triple quadrupole (QqQ) mass spectrometer, fitted with an electron ionization (EI) source and a collision cell.

3.2.4.3 GC conditions and MS parameters

Hopane content was analyzed using a GC/MS procedure performed in the single ion monitoring (SIM) mode. The electron ionization (EI) source temperature was set at

280 ℃. The initial GC oven temperature of 50 ℃ (0.5 min hold) was ramped to 310 ℃ for 15 min at 6 ℃/min, resulting in total run time of 58.8 min.

A subset of seventeen PAHs including acenaphthylene, acenaphthene, biphenyl, anthracene, fluoranthene, pyrene, benzo(*a*)anthracene, benzo(*b*)fluoranthene, benzo(*j*)fluoranthene, benzo(*k*)fluoranthene, benzo(*a*)pyrene, benzo(*e*)pyrene, perylene, dibenz(*a,c*)anthracene, dibenz(*a,h*)anthracene, indeno(1,2,3,-*cd*)pyrene, and benzo(*ghi*)perylene were analyzed using a multiple reaction monitoring (MRM) method. The MRM transitions used to quantify each of the above seventeen PAHs, along with the details of surrogate and internal standards are summarized in the Appendix (see Table A1). Six time segments were used in the MRM method for enhancing the method sensitivity. The initial GC oven temperature of 50 ℃ (0.8 min hold) was ramped to 180 ℃ at 70 ℃ /min (0 minutes hold); 7 ℃ /min to 230 ℃ (1 min hold); 40 ℃/min to 280 ℃ (1 min hold); 330 ℃ at 25 ℃ /min (5 min hold); resulting in a total run time of 20.05 min. Post-run back flush was performed for 4 min at 330 ℃. Helium was used as a carrier gas at a flow rate of 0.9 ml/min. Inlet temperature was set at 300 ℃, and sample injection (1 µl) was performed in the pulsed splitless mode. The temperature of the EI source was maintained at 350 ℃, and the quadruple temperatures (for both quad 1 and quad 2) were set at 180 ℃. To facilitate collision-induced dissociation in the collision cell, high purity nitrogen was delivered at a flow rate of 1.5 ml/min, and helium was delivered at a flow rate of 2.3 ml/min to quench the reactions.

For analyzing various alkylated PAHs and their respective parent PAHs, a SIM (GC/MS) method was used. We measured 5 parent PAHs (naphthalene, phenanthrene,

dibenzothiophene, fluorene, chrysene) and their 18 alkylated PAH homologs. The initial GC oven temperature (50 ℃, 1 min hold) was ramped to 300 ℃ at 5 ℃ /min (12 min hold), resulting in a total run time of 63 min. Post-run back flush was performed for 4 min at 325 ℃. The target ions monitored during the SIM analysis and standards use are summarized in the table given in the appendix (see Table A2).

3.2.4.4 Quantitation method

The parent PAHs were quantified by employing Agilent Technologies MassHunter MS/MS quantitation software. The PAH standard solution was used to build a GC/MS/MS calibration curve with eight calibration points at concentration levels 1, 2, 5, 10, 20, 50, 100 and 200 ng/ml. Average response from three injections was used to compute these calibration points. For quantitation, a minimum of five calibration points were used to obtain a linearity level > 0.99. Furthermore, the calibration points were inverse concentration weighted to minimize bias from low concentration calibration points.

Alkylated PAHs were quantified using Agilent Technologies MassHunter MS quantitation software. Calibration curves were developed for the following compounds: naphthalene, 2-methylnaphthalene, 2,6-dimethylnaphthalene, 2,3,5-trimethylnaphthalene, fluorene, phenanthrene, 1-methylphenanthrene, dibenzothiophene and chrysene. The concentration levels used for calibration curves were: 1, 2, 5, 10, 20, 50, 100, 200, 500 and 1000 ng/ml. The linearity of each calibration curve was at least 0.997, and an inverse concentration weighting method was used to minimize bias from low concentration calibration points. Since commercial standards for all forms of alkylated PAHs are not

available, we used a semi-quantitative method that employed a relative response factor (RRF) approach to estimate alkylated PAHs concentrations (Wang et al., 1994b; Wang and Fingas, 2003). Table A2 summarizes the reference standards used in the RRF approach to quantify various alkylated homologs.

3.2.5 Quality assurance and quality Control

Each sample was spiked with an internal standard *p*-terphenyl-d_{14}, prior to analysis to compensate for instrumental variations. In addition, all the samples were spiked with a surrogate standard mixture containing naphthalene-d_8, acenaphthene-d_{10}, phenanthrene-d_{10} and benzo(*a*)pyrene-d_{12} to monitor net recovery levels before the sample preparation step. The measured recovery levels ranged from 65-92%, 68-91%, 72-107%, 95-153% for the four surrogate standards, respectively. Limit of detection (LOD) and limit of quantitation (LOQ) for the method was determined by measuring a series of blanks (MacDougall and Crummett, 1980). The blank mean value and the standard deviation (SD) were calculated. LOD for the method was estimated as the mean blank value plus 3 times SD, and LOQ was estimated as the mean blank value plus 10 times SD (MacDougall and Crummett, 1980; Mottier et al., 2000). The range of LOD and LOQ for various PAHs and their homologs were 0.20 to 3.65 ng/ml and 0.24 to 4.32 ng/ml, respectively.

3.3 Results and discussion

3.3.1 Source identification

Field samples were analyzed first to confirm their origin. In terms of physical characteristics, all the samples matched MC252 residual oil characteristics described in previous studies (OSAT-2, 2011) and Chapter 2, they were all brownish, sticky material with considerable amount of sand, and had a strong petroleum odor. To compare their chemical fingerprints, we first analyzed hopane and sterane compounds in these samples using the analytical approaches described in Chapter 2. In environmental forensic analysis of oil spills, source-specific diagnostic ratios of certain group of hopanes will vary from one oil to another (Chandru et al., 2008; Wang et al., 1999; Wang and Fingas, 2003). In Chapter 2, we established that fresh and weathered MC252 oil can be distinguished from other oils by two source-specific hopane ratios, namely: T_s/T_m and C_{29}/C_{30}. Figure 3.3 shows the T_s/T_m and C_{29}/C_{30} hopane ratios of various oil spill samples collected from June 2010 to August 2014, and compares them with the ratios measured for the MC252 reference oil. The data show T_s/T_m and C_{29}/C_{30} values vary from 0.92 to 0.98 and 0.36 to 0.40, respectively. The profiles of various samples match the profile of MC252 reference oil (see Figure 4.3).

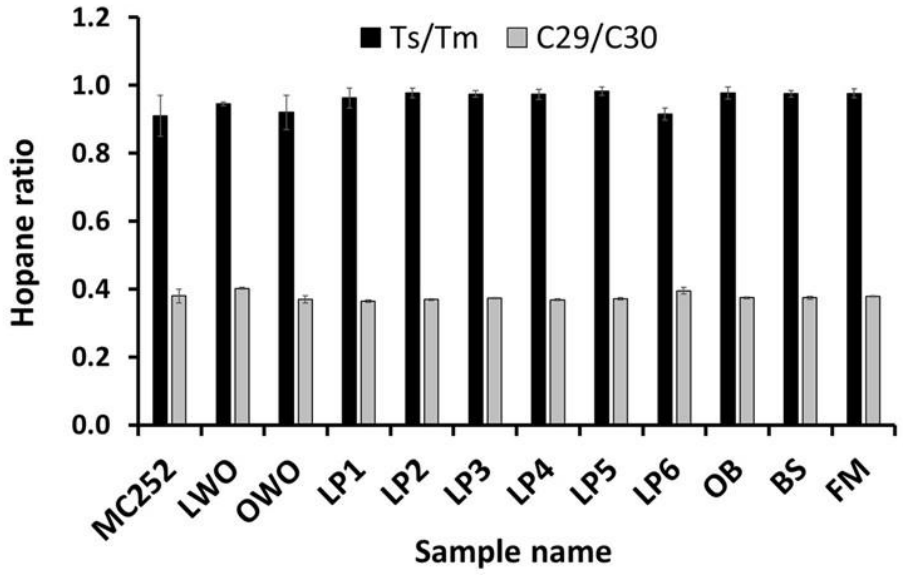

Figure 3.3 Identification of the origin of field samples based on hopane diagnostic ratios

3.3.2 Comparison of PAHs measured in MC252 oil, laboratory weathered MC252 oil (LWO), and ocean-weathered MC252 oil (OWO)

To quantify the effects of open water weathering processes including evaporation, dissolution, photo-oxidation and biochemical reactions, we compared PAH levels measured in the source oil with PAHs in LWO and OWO samples. MC252 source oil contains high levels of volatile hydrocarbons, hence we postulated that evaporation should have removed a considerable amount of PAHs and other organics while the oil was in the open ocean (Liu et al., 2012). To estimate the effects of evaporation on weathering, we monitored the changes in the weight of the LWO sample for 6 days, and these results are summarized in Figure 3.4. The data show that within 5 hours about 33% of the oil mass was volatilized, and within a day about 39% of the oil mass was removed.

The rate of evaporation declined considerably after about 12 hours; and after 6 days of evaporation about 44% of the total oil mass was removed from the system. The average standard deviation of these weathering data was 0.7%.

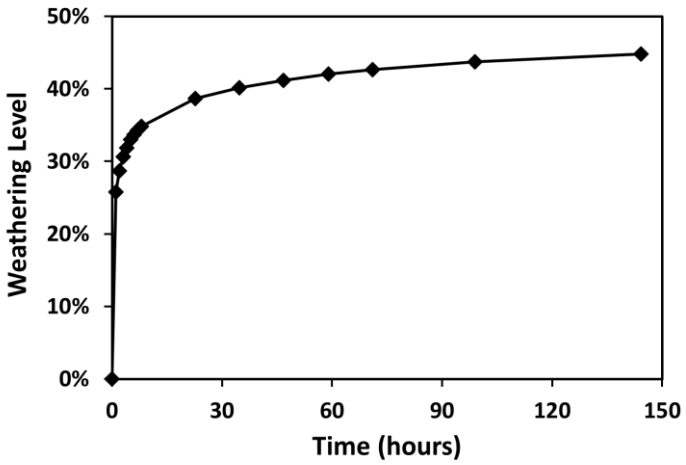

Figure 3.4 Changes in MC252 mass due to evaporation

The concentrations of 22 parent PAHs and 18 alkylated PAH homologs measured in the original MC252 source oil are summarized in Table 3.2. The total amount of target PAHs measured was 16,115 mg/kg oil. PAHs in the source oil were predominantly low molecular weight compounds (2 and 3 ring), mostly naphthalene and its alkylated homologs, which accounted for about 68% of the total PAH mass. Phenanthrene and its alkylated homologs contributed 18%, followed by fluorene and its alkylated homologs which contributed another 8%. High molecular weight (4 to 6 ring) PAHs accounted for only 0.5% of the total target PAHs in the source oil. Although their relative percentage is low, several of these high molecular weight PAHs (such as benzo(*a*)pyrene, chrysene and alkylated chrysene homologs) are known to be highly toxic compounds (Boese et al.,

1998; Hoffman and Gay, 1981; Machala et al., 2008; Nisbet and Lagoy, 1992). Table 3.2 also shows the concentrations of various parent PAHs and their alkylated homologs measured in the LWO sample. The total amount of PAHs measured was 12,718 mg/kg-oil. Since the original amount of PAHs in MC252 oil was 16,115 mg/kg-oil, the apparent percentage loss of PAH mass was 21%. However, as discussed in the methods section, to quantify the true percentage depletion level (or net weathering level), the measured concentrations must be normalized to a conservative species (Douglas et al., 1996). In this study we used hopane responses and estimated the value of the hopane normalization factor ($H_{oil}/H_{weathered}$) for LWO as 0.53. Using equation (1), the true loss of PAHs in the LWO sample after 6 days of evaporation was 58%. These results indicate that evaporation must have removed a considerable amount of PAHs when the spill oil was transported over the open ocean. The percentage depletion levels of individual PAHs in the LWO sample are summarized in Table 4.2. The data show that light PAHs (such as naphthalene and its alkylated homologs) will be rapidly removed by the evaporation processes; however, high molecular weight PAHs (3 or more rings) will be fully conserved. For example, the 2-ring parent naphthalene level dropped from 712 mg/kg-oil to below detection limit, while the 4-ring parent chrysene concentration increased in the weathered sample from 49 mg/kg-oil to 95 mg/kg-oil. The concentrating effect observed here is due to changes in the overall oil mass. When chrysene concentrations were normalized using the hopane normalization factor for the sample (i.e., $H_{oil}/H_{weathered}$ value of 0.53), the actual percentage depletion was zero; chrysene was unaffected by evaporation. Overall, the data shown in Table 3.2 indicate that the evaporation process

Table 3.2 Concentration (average ± SD) of parent PAHs and alkylated PAHs (mg/kg-oil) in MC252, LWO and OWO samples (depletion levels were computed using Eqn. 1)

Compound	MC252	LWO	Depletion of PAHs in LWO	OWO	Depletion of PAHs in OWO
C_0-Naphthalene	712 ±3	DL	100%	DL	100%
C_1-Naphthalenes	2405 ±3	1.3 ±0.3	100%	DL	100%
C_2-Naphthalenes	3335 ±5	89 ±2	99%	0.70 ±0.09	100%
C_3-Naphthalenes	2445 ±6	1293 ±9	72%	8 ±1	100%
C_4-Naphthalenes	2031 ±8	2358 ±29	39%	37 ±5	99%
C_0-Phenanthrene	297 ±1	474 ±8	16%	28 ±3	94%
C_1-Phenanthrenes	849 ±4	1561 ±6	3%	285 ±8	80%
C_2-Phenanthrenes	853 ±6	1687 ±4	0%	437 ±3	70%
C_3-Phenanthrenes	601 ±3	1166 ±3	0%	281 ±1	73%
C_4-Phenanthrenes	330 ±1	649 ±7	0%	152 ±9	73%
C_0-Dibenzothiophene	45 ±1	65 ±1	23%	2.7 ±0.3	96%
C_1-Dibenzothiophenes	70 ±1	125 ±1	6%	16 ±2	87%
C_2-Dibenzothiophenes	101 ±1	187 ±1	3%	43 ±4	75%
C_3-Dibenzothiophenes	69 ±1	132 ±1	0%	36 ±3	69%
C_0-Fluorene	123 ±1	77 ±0.4	67%	0.58 ±0.03	100%
C_1-Fluorenes	384 ±7	514 ±8	29%	17 ±2	97%
C_2-Fluorenes	409 ±5	709 ±5	9%	42 ±3	94%
C_3-Fluorenes	368 ±3	675 ±9	3%	72 ±8	89%
C_0-Chrysene	49 ±1	95 ±1	0%	46 ±4	45%
C_1-Chrysenes	92 ±4	182 ±1	0%	63 ±4	60%
C_2-Chrysenes	105 ±1	220 ±2	0%	44 ±2	76%
C_3-Chrysenes	72 ±1	157 ±3	0%	17.3 ±0.8	86%
C_4-Chrysenes	36 ±1	83 ±2	0%	7.7 ±0.5	88%
Biphenyl	175 ±2	DL	100%	DL	100%
Acenaphthylene	5.2 ±0.7	1.4 ±0.1	86%	DL	100%
Acenaphthene	58 ±2	33 ±1	71%	DL	100%
Anthracene	5.4 ±0.4	11 ±1	0%	1.0 ±0.1	89%
Fluoranthene	6.2 ±0.4	13 ±1	0%	3.9 ±0.7	63%
Pyrene	17 ±2	35 ±2	0%	6.8 ±0.6	77%
Benzo(*a*)anthracene	9.7 ±0.9	19 ±1	0%	0.35 ±0.05	98%
Benzo(*b*)fluoranthene	8 ±1	20 ±1	0%	6.4 ±0.7	55%
Benzo(*k*)fluoranthene	2.8 ±0.6	6.1 ±0.1	0%	1.5 ±0.3	68%
Benzo(*j*)fluoranthene	2.5 ±0.1	4.9 ±0.3	0%	0.90 ±0.07	79%
Benzo(*e*)pyrene	13 ±1	27 ±1	0%	8 ±1	64%
Benzo(*a*)pyrene	2.3 ±0.2	3.9 ±0.4	11%	0.36 ±0.05	91%
Perylene	1.5 ±0.2	2.5 ±0.2	9%	0.26 ±0.02	90%
Dibenz(*a*,*c*)anthracene	6 ±1	13 ±1	0%	0.5 ±0.1	95%
Dibenz(*a*,*h*)anthracene	3.0 ±0.8	5.8 ±0.4	0%	0.8 ±0.3	84%
Indeno(1,2,3,-*cd*)pyrene	1.4 ±0.5	2.7 ±0.6	3%	0.6 ±0.2	75%
Benzo(*ghi*)perylene	5 ±1	9.8 ±0.7	1%	1.9 ±0.5	78%
Total PAHs	16115	12718	58%	1714	94%

DL-Below detection limit

should have preferentially removed several light PAHs including naphthalenes, parent fluorene, biphenyl, acenaphthylene, and acenaphthene; also, evaporation should have concentrated various heavy PAHs.

The ocean-weathered MC252 oil, which arrived along the Alabama shoreline on June 11, 2010, travelled over 120 miles weathering over open GOM water. In addition to evaporation, the OWO sample would have been influenced by other natural weathering processes such as chemical dissolution, photo-degradation and biodegradation. In this study, we used the OWO sample to quantify the combined effects of all natural open water weathering processes. Table 3.2 shows the concentrations of parent PAHs and alkylated PAHs measured in the OWO sample. The total amount of PAHs measured was 1,714 mg/kg-oil. The true percentage depletion level, computed after hopane normalization (using the estimated value of $H_{oil}/H_{weathered}$ = 0.58), was 94%. This depletion level was substantially higher than the net weathering level estimated for the LWO sample, which was only 58%. The OWO sample data show that both light PAHs as well as some heavy PAHs were weathered in the open water environment. As expected, light parent naphthalene and its alkylated homologs decreased to nearly zero. Interestingly, heavy PAHs did not show the concentration effects observed in the LWO sample. For example, the 4-ring parent chrysene concentration decreased from 49 mg/kg-oil in the source oil to 46 mg/kg-oil in the OWO sample; after hopane normalization, the true percentage depletion level for chrysene was estimated to be 45%. This depletion level was distinctly different from the conservative concentration effect for chrysene (i.e., 0% depletion) observed in the LWO sample. These results indicate that in addition to evaporation, other ocean-scale weathering processes played an important role in

transforming chrysene (and also other PAHs) while MC252 oil was transported over the open ocean from the well head to Alabama's beaches.

3.3.3 Temporal distribution of target PAHs in SRBs

As pointed out in OSAT2 (2011), in the vicinity of the shoreline, a portion of ocean-weathered oil interacted with sediment particles and were buried as SOMs. These SOMs are later fragmented by nearshore forces to form SRBs. Both SOMs and SRBs are discontinuously buried and uncovered as they evolve; and they can be conceptually viewed as oil spill residues buried in a partially-closed sediment system (as compared to the open ocean system discussed above). To understand the temporal evolution of various PAHs in this partially-closed system, we compared the PAH depletion levels in six different SRB samples collected at a location near Lagoon Pass in Gulf Shores, Alabama, over a 4-year period. The PAH concentrations reported here are measured in the residual oil extracted from the SRBs. The measured concentration data are summarized in Table 3.3. The data show that the total PAHs measured in the six SRB samples are: 2,382, 2,047, 1,892, 2,206, 2,013 and 1533 mg/kg-oil for LP1, LP2, LP3, LP4, LP5 and LP6, respectively. The hopane normalization factors for various samples are estimated to be: 0.48 for LP1, 0.53 for LP2, 0.59 for LP3, 0.40 for LP4, 0.44 for LP5 and 0.52 for LP6. Using these factors, the true percentage depletion levels of PAHs were estimated to be: 93% for LP1, 93% for LP2, 93% for LP3, 95% for LP4, 95% for LP5 and 95% for LP6. These data indicate that once open ocean weathered oil was trapped within the partially-closed sediment system (SOMs or SRBs), PAH weathering rates slowed down considerably. In the section below we provide additional data to explore

Table 3.3 Concentration (average ± SD) of parent PAHs and alkylated PAHs measured in SRB samples (mg/kg-oil)

Compound	Temporal Samples						Spatial Samples		
	LP1	**LP2**	**LP3**	**LP4**	**LP5**	**LP6**	**OB**	**BS**	**FM**
C_0-Naphthalene	DL	DL	DL	DL	DL	DL	DL	DL	DL
C_1-Naphthalenes	DL	DL	DL	DL	DL	DL	DL	DL	DL
C_2-Naphthalenes	0.88 ±0.06	0.59 ±0.03	0.58 ±0.07	1.1 ±0.1	1.05 ±0.08	0.85 ±0.06	1.06 ±0.06	1.7 ±0.2	0.58 ±0.06
C_3-Naphthalenes	9 ±1	4.0 ±0.6	5.5 ±0.3	12.0 ±0.3	13.7 ±0.7	10.1 ±0.2	16.2 ±0.4	32 ±6	1.2 ±0.1
C_4-Naphthalenes	47 ±7	25 ±4	32 ±2	61 ±2	64 ±1	59 ±2	77 ±1	148 ±3	8 ±1
C_0-Phenanthrene	32.6 ±0.3	23.6 ±0.4	24.5 ±0.8	10.2 ±0.3	9.1 ±0.8	3.0 ±0.2	13 ±1	16.6 ±0.1	1.65 ±0.06
C_1-Phenanthrenes	346 ±4	292 ±5	276 ±9	183 ±7	131 ±2	32 ±3	192 ±2	247 ±2	42 ±1
C_2-Phenanthrenes	601 ±8	521 ±5	472 ±12	517 ±4	445 ±2	286 ±13	495 ±3	605 ±2	164 ±6
C_3-Phenanthrenes	403 ±54	353 ±5	318 ±10	412 ±4	390 ±2	339 ±12	406 ±2	482 ±3	170 ±10
C_4-Phenanthrenes	233 ±2	207 ±4	185 ±6	253 ±9	232 ±1	215 ±7	247 ±8	282 ±7	124 ±8
C_0-Dibenzothiophene	2.8 ±0.4	2.4 ±0.3	2.7 ±0.2	4.7 ±0.2	7.7 ±0.1	2.4 ±0.5	4.0 ±0.2	4.5 ±0.2	0.14 ±0.01
C_1-Dibenzothiophenes	19 ±2	16 ±2	16 ±1	15.2 ±0.4	15.8 ±0.3	6.3 ±0.5	17.0 ±0.7	19 ±2	2.5 ±0.1
C_2-Dibenzothiophenes	57 ±7	51 ±6	48 ±3	62 ±2	62 ±1	40 ±1	63 ±2	69 ±5	17.7 ±0.7
C_3-Dibenzothiophenes	51 ±7	46 ±5	43 ±3	59 ±2	57 ±2	45 ±1	60 ±2	64 ±3	24 ±1
C_0-Fluorene	0.60 ±0.05	0.41 ±0.04	0.50 ±0.03	0.66 ±0.03	1.27 ±0.04	0.45 ±0.05	0.71 ±0.02	0.91 ±0.08	DL
C_1-Fluorenes	23 ±3	18 ±2	21 ±2	23.7 ±0.8	25 ±1	15 ±2	26 ±1	35 ±4	4.2 ±0.3
C_2-Fluorenes	62 ±9	59 ±7	62 ±5	80 ±3	85 ±3	53 ±4	80 ±1	106 ±11	12 ±1
C_3-Fluorenes	105 ±12	101 ±12	99 ±8	141 ±5	141 ±2	117 ±7	140 ±1	171 ±12	31 ±2
C_0-Chrysene	65 ±8	59 ±6	53 ±4	75 ±2	67 ±1	60 ±2	75 ±3	73 ±1	48 ±2
C_1-Chrysenes	90 ±12	82 ±8	74 ±6	109 ±4	96 ±1	90 ±2	110 ±4	111 ±2	70 ±4
C_2-Chrysenes	67 ±9	61 ±6	55 ±5	82 ±3	72 ±1	69 ±1	86 ±3	90 ±2	51 ±3
C_3-Chrysenes	28 ±4	25 ±3	24 ±3	35 ±2	33 ±2	30 ±1	39 ±2	42.4 ±0.7	21 ±2
C_4-Chrysenes	13 ±2	11 ±1	10 ±1	16.0 ±0.7	15 ±1	13.0 ±0.5	18 ±1	19.1 ±0.1	10.1 ±0.6
Biphenyl	DL	DL	DL	DL	DL	DL	DL	DL	DL
Acenaphthylene	DL	DL	DL	DL	DL	DL	DL	DL	DL
Acenaphthene	DL	DL	DL	DL	DL	DL	0.58 ±0.06	1.2 ±0.3	DL
Anthracene	1.4 ±0.2	1.2 ±0.2	1.3 ±0.1	1.57 ±0.08	1.72 ±0.09	1.18 ±0.04	1.6 ±0.2	2.1 ±0.2	0.35 ±0.03
Fluoranthene	5.3 ±0.6	4.5 ±0.5	4.1 ±0.4	5.7 ±0.2	5.4 ±0.5	4.5 ±0.2	5.3 ±0.4	5.8 ±0.4	2.0 ±0.2
Pyrene	10 ±1	9 ±1	8.0 ±0.7	11.3 ±0.3	11.1 ±0.1	9.5 ±0.5	11.6 ±0.4	12.2 ±0.8	4.4 ±0.3
Benzo(*a*)anthracene	0.58 ±0.07	0.50 ±0.05	0.46 ±0.05	0.64 ±0.03	0.60 ±0.04	0.67 ±0.05	0.78 ±0.03	1.2 ±0.1	0.30 ±0.01
Benzo(*b*)fluoranthene	9 ±1	8.3 ±0.9	7.6 ±0.7	11.1 ±0.2	9.75 ±0.01	8.8 ±0.1	11.6 ±0.5	11.3 ±0.6	7.0 ±0.4
Benzo(*k*)fluoranthene	2.2 ±0.3	1.9 ±0.3	1.7 ±0.2	2.37 ±0.08	2.16 ±0.04	2.0 ±0.1	2.5 ±0.2	2.6 ±0.2	1.62 ±0.07
Benzo(*j*)fluoranthene	1.3 ±0.2	1.1 ±0.2	1.01 ±0.07	1.5 ±0.1	1.4 ±0.1	1.2 ±0.1	1.6 ±0.1	1.67 ±0.09	1.0 ±0.1
Benzo(*e*)pyrene	11 ±1	10 ±1	9.4 ±0.9	13.6 ±0.3	12.0 ±0.1	11.4 ±0.2	14.6 ±0.7	15.5 ±0.5	8.4 ±0.5
Benzo(*a*)pyrene	0.44 ±0.02	0.38 ±0.02	0.39 ±0.04	0.44 ±0.05	0.46 ±0.06	0.48 ±0.04	0.53 ±0.05	0.68 ±0.07	0.38 ±0.03
Perylene	0.34 ±0.03	0.28 ±0.02	0.27 ±0.02	0.34 ±0.03	0.34 ±0.01	0.28 ±0.02	0.37 ±0.02	0.42 ±0.03	0.25 ±0.02
Dibenz(*a*,*c*)anthracene	0.73 ±0.06	0.57 ±0.07	0.54 ±0.07	0.71 ±0.06	0.69 ±0.04	0.84 ±0.07	1.0 ±0.1	1.37 ±0.08	0.37 ±0.05
Dibenz(*a*,*h*)anthracene	1.2 ±0.2	1.0 ±0.3	0.9 ±0.1	1.10 ±0.08	1.04 ±0.06	0.8 ±0.2	1.1 ±0.2	1.4 ±0.2	0.63 ±0.09
Indeno(1,2,3,-	0.9 ±0.1	0.7 ±0.1	0.59 ±0.08	0.8 ±0.2	0.71 ±0.08	0.6 ±0.1	0.9 ±0.2	0.9 ±0.2	0.51 ±0.08
Benzo(*ghi*)perylene	2.9 ±0.4	2.5 ±0.3	2.3 ±0.2	3.3 ±0.1	2.89 ±0.05	2.9 ±0.1	3.5 ±0.5	3.9 ±0.3	1.7 ±0.1
Total PAHs	2382	2047	1892	2206	2013	1533	2206	2727	832

DL- Below detection limit

how individual PAH concentrations in SRBs have evolved over the past four years. The percentage depletion levels for selected parent PAHs and alkylated PAHs in temporal LP samples were computed and the results are summarized in Figure 3.5. We have organized the PAHs data into six distinct groups based on their structural properties. Group-1 includes C_0 to C_4 alkylated phenanthrenes, Group-2 includes C_0 to C_3 alkylated dibenzothiophenes, Group-3 includes C_0 to C_3 alkylated fluorenes, Group-4 includes C_0 to C_4 alkylated chrysenes, Group-5 includes various benzo- compounds (benzo(*a*)anthracene, benzo(*b*)fluoranthene, benzo(*k*)fluoranthene, benzo(*j*)fluoranthene, benzo(*e*)pyrene, benzo(*a*)pyrene and benzo(*ghi*)perylene), and Group-6 includes all other compounds (anthracene, fluoranthene, pyrene, perylene, dibenz(*a,c*)anthracene, dibenz(*a,h*)anthracene and indeno(1,2,3,-*cd*)pyrene). Note naphthalene and its alkylated homologs, biphenyl, acenaphthylene, and acenaphthene were not considered since these compounds were predominantly removed by ocean-scale weathering processes and hence were low or undetectable (refer to first arrival OWO sample data in Table 4.2).

Figure 3.5 shows the temporal changes in all six groups of PAHs measured in the SRB samples recovered from Lagoon Pass. Figure 3.5(a) presents temporal variations in the depletion levels of C_0 to C_4 alkylated phenanthrenes. The percentage depletion levels for C_0-phenanthrene measured in various SRBs collected over four years ranged from 95% to 99%. These results, compared to results reported for the OWO sample (see Table 3.2) indicate that the C_0-phenanthrene weathering rate decreased once the oil was trapped within SOMs/SRBs. Figure 3.5(a) also shows that similar to parent phenanthrene, rates of degradation of C_1, C_2, C_3 and C_4 alkylated phenanthrenes in SRBs have also slowed down. The C_1 depletion levels ranged from 80% to 98% and C_2 levels ranged from 66%

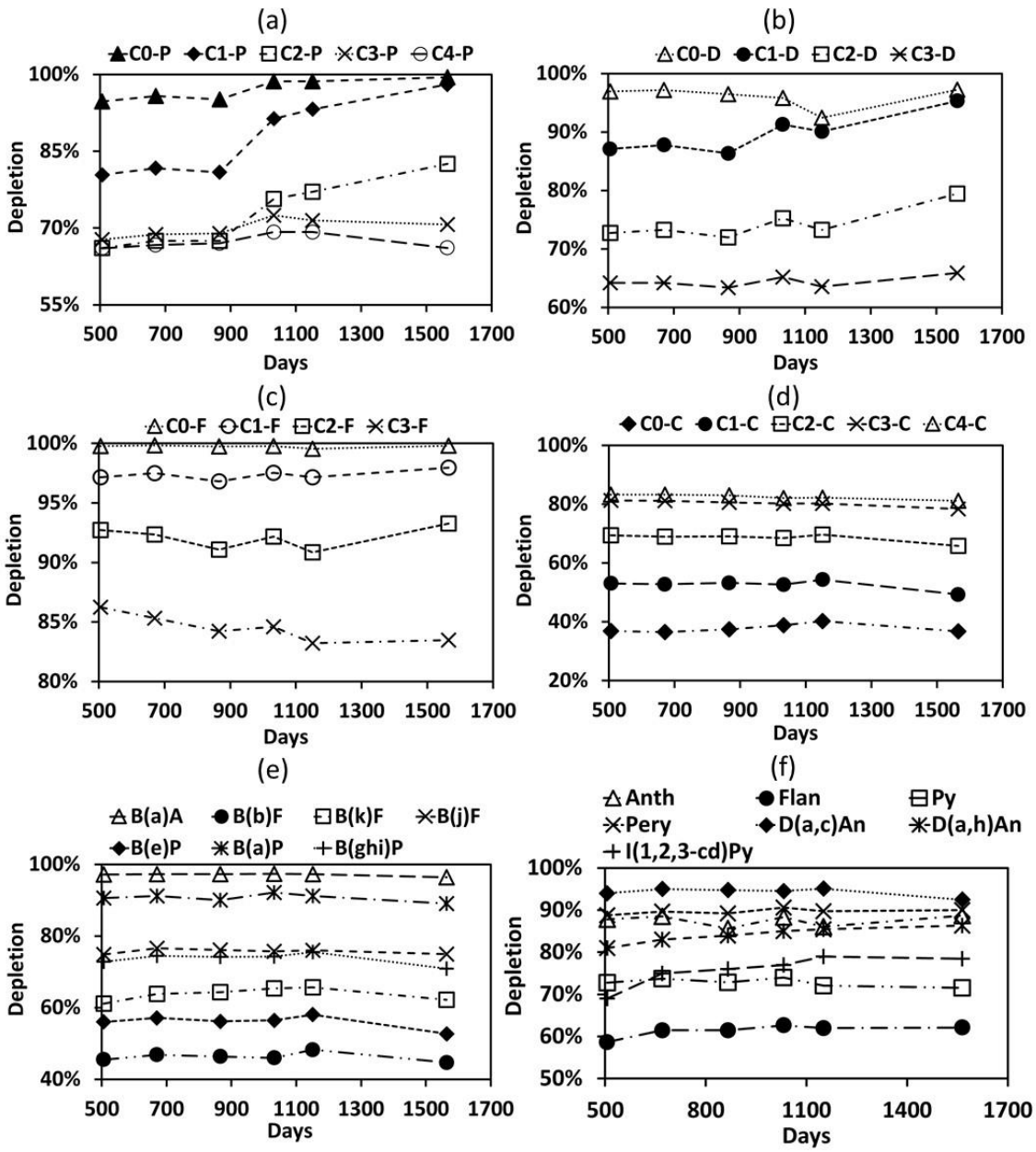

Figure 3.5 Temporal variations (days from the DWH oil spill accident) in the percentage depletion level of six groups of parent PAHs and alkylated PAHs

to 83% over the past four years and they continue to degrade at a reduced rate. The C_3 depletion levels ranged from 68% to 72% and C_4 levels ranged from 66% to 69%, and

these levels appear to be fairly stable. Furthermore, the net loss of various phenanthrenes appears to decrease with the level of alkylation, indicating a trend where the net depletion for $C_0 > C_1 > C_2 > C_3 > C_4$.

The temporal evolution of C_0 to C_3 alkylated dibenzothiophenes are shown in Figure 3.5(b), and the temporal changes in C_0 to C_3 alkylated fluorenes are shown in Figure 3.5(c). In both cases, the level of weathering is high for parent PAHs when compared to their alkylated homologs. For C_0-dibenzothiophene, the removal levels ranged from 92% to 97%; this removal level was higher than those observed for C_1-dibenzothiophenes (86% to 95%), followed by C_2-dibenzothiophenes (72% to 79%) and C_3-dibenzothiophenes (63% to 66%). For fluorenes, C_0-fluorene weathered by almost 100%, followed by C_1-fluorenes (97% to 98%), C_2-fluorenes (91% to 93%), and C_3-fluorenes (83% to 86%). Weathering rates for both dibenzothiophenes and fluorenes appear to have slowed once the oil was trapped in SRBs. For both dibenzothiophene and fluorene compounds, the overall loss appears to decrease with alkylation levels with a trend of $C_0 > C_1 > C_2 > C_3$, which is identical to the trend observed for phenanthrenes.

The temporal evolution of C_0 to C_4 alkylated chrysenes are shown in Figure 3.5(d). Interestingly, the overall removal trend for chrysene homologs is: $C_4 > C_3 > C_2 > C_1 > C_0$, which is opposite the trend observed for phenanthrenes, dibenzothiophenes and fluorenes. The highly alkylated C_4-chrysenes were the most weathered species (81% to 83%), followed by C_3-chrysenes (78% to 81%), C_2-chrysenes (66% to 70%), and C_1-chrysenes (49% to 54%). The least degraded compound in this group is the C_0-chrysene, which was degraded only by about 37% to 40%. Weathering of chrysene and its alkylated homologs

appears to have essentially stopped once the oil was trapped in SRBs. Previous laboratory-scale experiments have shown that the rate of photo-degradation of chrysenes in crude oil increases with increased alkylation when the oil is exposed to ultraviolet light (Garrett et al., 1998). This could explain why higher alkylated chrysene homologs are degraded more (than the lower alkylated chrysenes) in OWO and SRB samples. These data also suggest that chrysene weathering was predominantly due to physicochemical processes rather than biological degradation processes.

The temporal evolution of various benzo- compounds in Group-5 are shown in Figure 3.5(e). These data show that benzo(*a*)anthracene weathered by about 96% to 97%, benzo(*a*)pyrene by about 89% to 92%, benzo(*j*)fluoranthene by about 75% to 77%, benzo(*ghi*)perylene by about 71% to 76%, benzo(*k*)fluoranthene by about 61% to 66%, benzo(*e*)pyrene by about 53% to 58%, and benzo(*b*)fluoranthene by about 45% to 48%. The trend lines shown in Figure 3.5(e) are almost horizontal, indicating that little weathering has occurred over the past 4 years.

The temporal evolution of Group-6 PAHs are shown in Figure 3.5(f). The data show that dibenz(*a,c*)anthracene weathered by about 92% to 95%, perylene by about 89% to 91%, anthracene by about 86% to 89%, dibenz(*a,h*)anthracene by about 81% to 86%, indeno(1,2,3,-*cd*)pyrene by about 69% to 79%, pyrene by about 72% to 74%, and fluoranthene by about 59% to 63%. Again, the trend lines are almost horizontal indicating little or no additional weathering has occurred over the past four years.

3.3.4 Spatial distribution of target PAHs in SRBs

To assess spatial variations in PAH levels along Alabama's beaches, we also measured target PAHs in SRB samples collected from the four sampling locations (see Figure 3.2) on September 2, 2012. The measured concentration levels of various PAHs are summarized in Table 3.3. The percentage depletion levels, computed after hopane normalization, are given in Table 3.4. No spatial trends are apparent in the PAH percentage depletion levels, indicating that all SRBs found along Alabama's beaches have undergone similar type of weathering processes.

Table 3.4 Percentage depletion of parent PAHs and alkylated PAHs in SRB samples collected from various locations (Hopane normalization factors: 0.36 for OB, 0.59 for LP3, 0.41 for BS, and 0.42 for FM, depletion levels were computed using Eqn. 1)

Compound	**Spatial locations**			
	OB	**LP3**	**BS**	**FM**
C_0-Phenanthrene	98%	95%	98%	100%
C_1-Phenanthrenes	92%	81%	88%	98%
C_2-Phenanthrenes	79%	67%	71%	92%
C_3-Phenanthrenes	75%	69%	67%	88%
C_4-Phenanthrenes	73%	67%	65%	84%
C_0-Dibenzothiophene	97%	96%	96%	100%
C_1-Dibenzothiophenes	91%	86%	89%	98%
C_2-Dibenzothiophenes	77%	72%	72%	93%
C_3-Dibenzothiophenes	68%	63%	61%	85%
C_0-Fluorene	100%	100%	100%	100%
C_1-Fluorenes	98%	97%	96%	100%
C_2-Fluorenes	93%	91%	89%	99%
C_3-Fluorenes	86%	84%	81%	96%
C_0-Chrysene	45%	37%	38%	59%
C_1-Chrysenes	57%	53%	50%	68%
C_2-Chrysenes	70%	69%	64%	80%
C_3-Chrysenes	80%	81%	76%	88%
C_4-Chrysenes	82%	83%	78%	88%
Benzo(*a*)anthracene	97%	97%	95%	99%
Benzo(*b*)fluoranthene	49%	46%	43%	64%
Benzo(*k*)fluoranthene	66%	64%	61%	75%
Benzo(*j*)fluoranthene	76%	76%	72%	84%
Benzo(*e*)pyrene	58%	56%	50%	72%
Benzo(*a*)pyrene	91%	90%	88%	93%
Benzo(*ghi*)perylene	75%	74%	69%	86%
Anthracene	89%	86%	84%	97%
Fluoranthene	69%	61%	61%	86%
Pyrene	76%	73%	71%	89%
Perylene	91%	89%	88%	93%
Dibenz(*a*,*c*)anthracene	94%	95%	90%	97%
Dibenz(*a*,*h*)anthracene	87%	84%	80%	91%
Indeno(1,2,3,-*cd*)pyrene	78%	76%	74%	85%
Total PAHs	95%	93%	93%	98%

3.4 Conclusions

We have presented the results of a long-term monitoring study that has quantified 22 parent PAHs and 18 alkylated PAH homologs in oil spill samples recovered from Alabama's beaches from June 2010 to August 2014. In this study, we have analyzed four types of oil spill samples which include: the original MC252 crude oil, a week-old laboratory weathered oil, about a month-old ocean weathered oil, and several shoreline-weathered oil spill samples (SRB samples) collected from Alabama beaches over the past four years. Our results show that low molecular weight PAHs were the dominant group of PAHs in the source crude. When the oil was allowed to evaporate under laboratory conditions, about 58% of PAH compounds were removed within 6 days, and most of the evaporated PAHs were low molecular weight volatile compounds. Several high molecular weight PAHs (e.g., parent chrysene) concentrated like a conservative biomarker in the laboratory evaporated sample. The PAH levels measured in the ocean-weathered sample, on the other hand, indicated that both light as well as several of the heavy PAHs have weathered in the open ocean environment. The depletion levels of all light PAHs and their alkylated homologs were close to 100%. The percentage depletion level for the 4-ring parent chrysene, for example, in the ocean-weathered sample was 45%, which was substantially higher than the close to 0% depletion level for chrysene observed in the laboratory-evaporated sample. Similar trends were also observed for several other heavy PAHs. These results indicate that in addition to evaporation, other physico-chemical weathering processes, such as photo-oxidation, dissolution and biochemical reactions should have played an important role in removing PAHs when the oil was floating over the open ocean. Interestingly, all these weathering processes have

slowed down significantly (or even ceased in some cases, e.g., chrysene) once the oil was buried within the partially closed nearshore beach environment. This dataset, when combined with the conceptual framework for physical evolution of MC252 residual oil and their potential toxic effects discussed in other recent published studies (Dubansky et al., 2013; Hayworth et al., 2015; Plant et al., 2013), suggest the likelihood that non-recoverable MC252 oil, present in the form of SOMs and SRBs that are not amenable to physical removal, have the potential to pose long-term ecological risks to GOM beaches for several years.

Chapter 4

A Tale of Two Recent Spills - Comparison of 2014 Galveston Bay and 2010 Deepwater Horizon Oil Spill Residues

4.1 Introduction

On March 22, 2014, on the weekend of the 25th anniversary of the catastrophic Exxon Valdez oil spill in Alaska, the bulk carrier M/V Summer Wind collided with the oil barge Kirby, near Texas City, about 50 km southeast of Houston, Texas. The accident released approximately 168,000 gallons of marine fuel oil (known as RMG-380, highly viscous, sticky, heavy black oil) into Galveston Bay (GB). After the accident, oil residues began washing up on several beaches along GB. The oil spill also spread into the Gulf of Mexico (GOM) and within a week the spill was rapidly transported by shoreline currents to the Matagorda Island Wildlife Management Area located about 200 km south of GB. By the end of March, overflight observers noted beached oil being rapidly buried under clean sand on Matagorda Island (NOAA, 2014b). Unfortunately, oil spill incidents like these occur in GB on a regular basis: according to the Texas General Land Office, 3954 oil spills occurred in GB between 1998 and 2010 (TGLO, 2010).

Oil spill residues washing onto shores is a common problem for many northern GOM beach systems. In 2010, the Deepwater Horizon (DWH) accident released about

210 million gallons of Louisiana light sweet crude oil into the GOM, impacting over 1,600 miles of shoreline, and depositing oil on Florida, Alabama, Mississippi, Louisiana and Texas beaches. The negative environmental, ecological, social, and economic consequences of this event continue today (Fisher et al., 2014; Hayworth et al., 2015; Hayworth et al., 2011; Mason et al., 2014; McCrea-Strub et al., 2011; White et al., 2012). Impacted beaches and dunes, estuaries, and tidal brackish and freshwater wetlands and the numerous species inhabiting them were, and remain, at risk of long-term detrimental effects as a result the spill (Fisher et al., 2014; Hayworth et al., 2011; Martinez et al., 2012; Mason et al., 2014; McCrea-Strub et al., 2011; White et al., 2012).

The amount of oil released during the GB accident was relatively small compared to the DWH accident. The physicochemical characteristics of these two oils are also different. The fuel oil released during GB spill was a heavy, viscous, refined oil containing low levels of volatile hydrocarbons, while the oil released during the DWH accident (MC252 crude oil) was an unrefined, low viscosity, sweet crude enriched in light, volatile hydrocarbons. Another major difference between the two events is that the GB spill was a surface release discharged about a kilometer away from the nearest shoreline; while the DWH event occurred about 75 km from the nearest shoreline, about 1.5 km under water. Also, large volumes of chemical dispersants were injected subsurface during the DWH spill response, which was unique. Owing to its proximity to the shoreline, GB oil weathered in marine waters for only a few hours to days before being deposited on nearby beaches. DWH oil, on the other hand, was weathered by ocean-scale processes such as volatilization, dissolution, emulsification, photo-degradation and/or biodegradation for 3 or more weeks before being deposited on

northern GOM shorelines. The GB spill occurred close to several sensitive wildlife areas, during breeding season for several migratory birds and marine species. Table 4.1 summarizes some of the key features of these two oil spills.

Table 4.1 Comparisons of Galveston Bay and Deepwater Horizon oil spills

	Galveston Bay Oil Spill	**Deepwater Horizon Oil Spill**
API at 15 ℃	~ 11 (Vermeire, 2012)	~ 35 (Atlas and Hazen, 2011)
Viscosity (cSt)	~ 380 at 50 ℃ (Vermeire, 2012)	~5 at 40 ℃ (Somasundaran et al., 2014)
Volume of the spill	~168,000 gallons	~210 million gallons
Type of oil	Refined marine fuel oil	Unrefined Louisiana sweet crude oil
Type of accident	Vessels collision	Explosion of oil rig
Type of spill	Tanker release	Well head release
Point of release	Surface oil spill	Subsurface oil spill, ~1.5 km below sea
Spill location	~ 1 km away from beaches	~70 km away from beaches
Weathering patterns	Fate of remnant oil is yet to be studied	Fate of remnant oil has been studied for ~5 years (Aeppli et al., 2012; Aeppli et al., 2014; Hayworth et al., 2015; Hayworth et al., 2011; Liu et al., 2012; OSAT-3, 2014; Radovic et al., 2014; Xia et al., 2012)

The objective of this work is to compare observational and chemical characterization data of first-arrival samples collected from GB and DWH oil spill impacted beaches. Chemical characterization efforts included the measurement of concentrations of n-alkanes, several biomarkers, five groups of alkylated polycyclic aromatic hydrocarbons (PAHs) and other seventeen PAHs. Biomarker data for the GB oil presented in this study are important since they can be used for identifying and

differentiating GB residues from other residues; they are also useful for understanding weathering levels. PAH data are useful for comparing and quantifying potential long-term environmental impacts of GB and DWH oil spill residues. Parts of this effort are published in the Plos One journal article titled: a tale of two recent spills-comparison of 2014 Galveston Bay and 2010 Deepwater Horizon oil spill residues (Yin et al., 2015a).

4.2 Materials and methods

Organic solvents used in this study were of analytical or higher grade and were purchased from VWR International (Suwanee, GA). Silica gel (60-200 μm) and anhydrous sodium sulfate (ACS grade) were also purchased from VWR International (Suwanee, GA). Prior to use, silica gel was activated using well-established procedures (Wang et al., 1994a). C_8-C_{40} alkanes, pristane and phytane mixtures and hexadecane-d_{34} were purchased from Sigma-Aldrich. Biomarkers namely C_{30}αβ-hopane (17α(*H*),21β(*H*)-hopane), C_{27}ααα(R)-sterane (5α,14α,17α(*H*) cholestane 20R), and C_{30}ββ-hopane (17β(*H*),21β(*H*)-hopane) were purchased form Chiron, Norway. PAH reference mixture consisting of 27 different PAHs (naphthalene, 1-methylnaphthalene, 2-methylnaphthalene, 2,6-dimethylnaphthalene, 2,3,5-trimethylnaphthalene, biphenyl, acenaphthylene, acenaphthene, fluorene, phenanthrene, 1-methylphenanthrene, anthracene, dibenzothiophene, fluoranthene, pyrene, benz[*a*]anthracene, chrysene, benzo[*b*]fluoranthene, benzo[*j*]fluoranthene, benzo[*k*]fluoranthene, benzo[*e*]pyrene, benzo[*a*]pyrene, perylene, dibenz[*a,c*]anthracene, dibenz[*a,h*]anthracene, indeno[1,2,3,-*cd*]pyrene and benzo[*ghi*]perylene) was purchased from Agilent (Wilmington, DE). The

reference solution for *p*-terphenyl-d_{14} was purchased from AccuStandard (New Haven, CT).

The oil spill samples recovered from GB beaches contained sand and other inorganics: organic fraction in the sample was 65% (*w*/*w*), estimated by a standard solvent extraction method using dichloromethane. The DWH oil spill sample was free of sand and other residues and it fully dissolved in dichloromethane. For biomarker and PAH quantitative assessments, about 20 mg of GB or DWH sample was dissolved in hexane and prepared using the column chromatographic fractionation method in Chapter 3. The hexane eluted fraction (F1) was used for n-alkanes and biomarkers analysis, and the hexane: dichloromethane (50%, v/v) mixture eluted fraction (F2) was used for PAH analysis. Each sample was prepared in duplicate and analyzed three times.

Both F1 and F2 elutes were analyzed using an Agilent 7890 GC equipped with an Agilent 7000B QqQ mass spectrometer detector. Single ion monitoring (SIM) mode was used for F1 analysis with a m/z value of 57 for n-alkanes (Smith and Strickland, 2007), m/z of 78 for hexadecane-d_{34}, m/z of 191 for hopanes and m/z of 217 for steranes (in Chapter 2). The five groups of alkylated-PAH homologs and seventeen other PAHs in the F2 fraction were analyzed using SIM and multiple reaction monitoring (MRM) methods, respectively, using the established analytical approaches in Chapter 3.

Quantification of n-alkanes was achieved by integrating all major chromatographic peaks of n-alkanes observed at the target ion m/z of 57. Hexadecane-d_{34} was used as the internal standard. The total concentrations of hopanes and steranes were quantified by integrating appropriate peak areas of chromatograms observed at m/z

191 (retention time from 37 to 46 minutes) and m/z 217 (retention time from 32 to 40 minutes), respectively. The reference standards used for quantification were: $C_{30}\alpha\beta$-hopane for hopanes, and $C_{27}\alpha\alpha\alpha$(R)-sterane for steranes. $C_{30}\beta\beta$-hopane was used as an internal standard to normalize the response factors used for estimating total hopanes and steranes. Based on available alkylated PAH standards, five groups of alkylated PAHs were quantified in this study using previously developed methods (Wang et al., 1994a). The analytical standards used for quantifying various PAHs within these five groups were as follows: in Group-1: naphthalene for quantifying C_0-naphthalene, 2-methylnaphthalene for C_1-naphthalenes, 2,6-dimethylnaphthalene for C_2-naphthalenes, 2,3,5-trimethylnaphthalene for C_3- and C_4-naphthalenes; in Group-2: phenanthrene for C_0-phenanthrene and 1-methylphenanthrene for C_1- to C_4-phenanthrenes; in Group-3: dibenzothiophene for C_0- to C_3-dibenzothiophenes; in Group-4: fluorene for C_0- to C_3-fluorenes; and in Group-5: chrysene for C_0- to C_4-chrysenes. Seventeen other PAHs were also quantified in this study, which include: biphenyl, acenaphthylene, acenaphthene, anthracene, fluoranthene, pyrene, benzo[*a*]anthracene, benzo[*b*]fluoranthene, benzo[*j*]fluoranthene, benzo[*k*]fluoranthene, benzo[*e*]pyrene, benzo[*a*]pyrene, perylene, dibenz[*a,c*]anthracene, dibenz[*a,h*]anthracene, indeno[1,2,3,-*cd*]pyrene and benzo[*ghi*]perylene; these compounds were quantified using the 27-PAH Agilent standard mixture and previously published analytical procedures (Xia et al., 2012). The internal standard *p*-terphenyl-d_{14} was used to normalize all PAH response factors.

4.3 Field observations and samples collection

Figure 4.1 shows the GB and DWH oil spill sites and our sampling locations. No specific permissions were required for sampling at these locations. Also, the field studies did not involve endangered or protected species. The GPS coordinates for our DWH field site in Alabama are: 30°16'42.8"N 87°33'17.1"W, and the GPS coordinates for our GB field site in Texas are: 29°22'22.6"N 94°49'48.6"W. GB oil began washing on GB beaches within few hours after the spill on March 22, 2014. The GB samples analyzed in this study were collected on March 29, 2014, from an amenity beach located along the Texas City Dike road, about 2 km away from the spill location. The DWH oil first arrived on Alabama's beaches in early June, 2010, over a month after the accident. The DWH samples considered in this study were collected on June 11, 2010 from Orange Beach, Alabama, located about 175 km from oil release location. Further details on the DWH field site, observed contamination patterns, and field sampling methods are discussed in Hayworth et al. (2015).

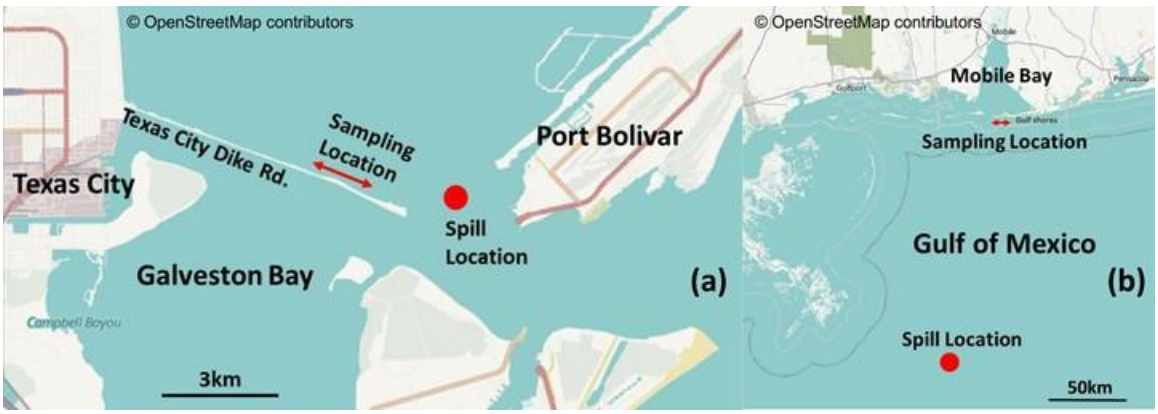

Figure 4.1 Locations of the two oil spills and sampling points: a) Galveston Bay spill; and b) Deepwater Horizon spill (maps from OpenStreetMap)

Figure 4.2 shows typical first-arrival oil deposition patterns observed at these two field sites. Although the overall deposition patterns appear similar, the physical characteristics of oil residues were distinctly different. Deposited GB first-arrival oil was black/grayish, highly viscous material, while the DWH first-arrival oil was a brownish, low viscosity emulsion. On the day of sampling (June 11, 2010), DWH oil was actively washing ashore along most of Alabama's 50 km sandy beach system, and public access to these contaminated beaches was unrestricted. In contrast, on the day of GB oil sampling (March 29, 2014), oil was actively washing ashore along a limited stretch of GB shoreline and public access to these active deposition areas was restricted. Therefore, our GB oil spill sampling efforts were completed near a sparsely contaminated area, located about 2 km from the spill site, which had been previously cleaned and re-opened to the public.

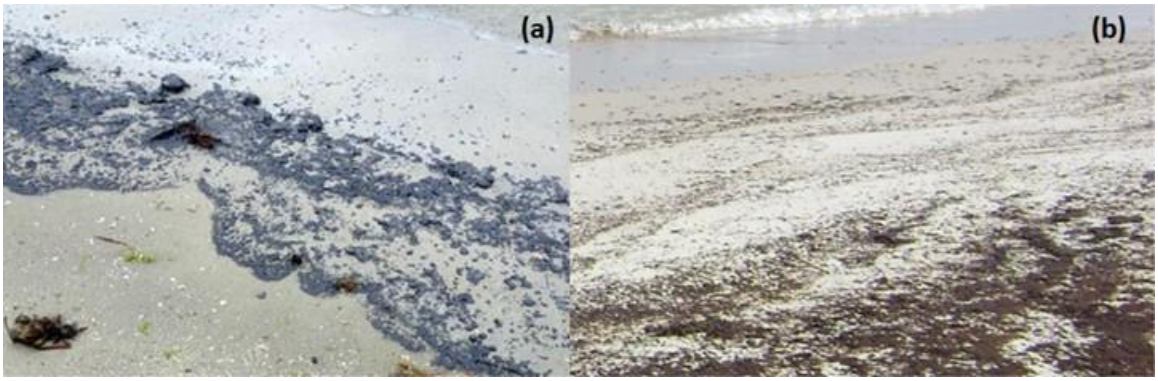

Figure 4.2 Comparison of Galveston Bay and Deepwater Horizon oil spill deposition patterns: a) blackish oily material deposited on a sandy beach in Galveston Bay, Texas (Photo taken on March 23rd, 2014, by NOAA's Office of Response and Restoration); b)

brownish emulsified oil deposited on a sandy beach in Orange Beach, Alabama (Photo taken on June 11th, 2010, by Auburn University team)

Figure 4.3 shows some of the field observations made at this site. Despite the clean-up efforts, the shoreline water along these "cleaned areas" had a strong petroleum odor and the nearshore waters at several locations had patches of floating oil sheen (see Figure 4.3 a). We also observed oil sticking to rocks, beached objects and vegetation (Figure 4.3 b & c). Furthermore, small blobs of oil (about 2 cm diameter; see Figure 4.3 d) were randomly scattered in the intertidal zone. During our sampling effort, we collected oil adhered to rocks and beached objects, and also collected several beached oil

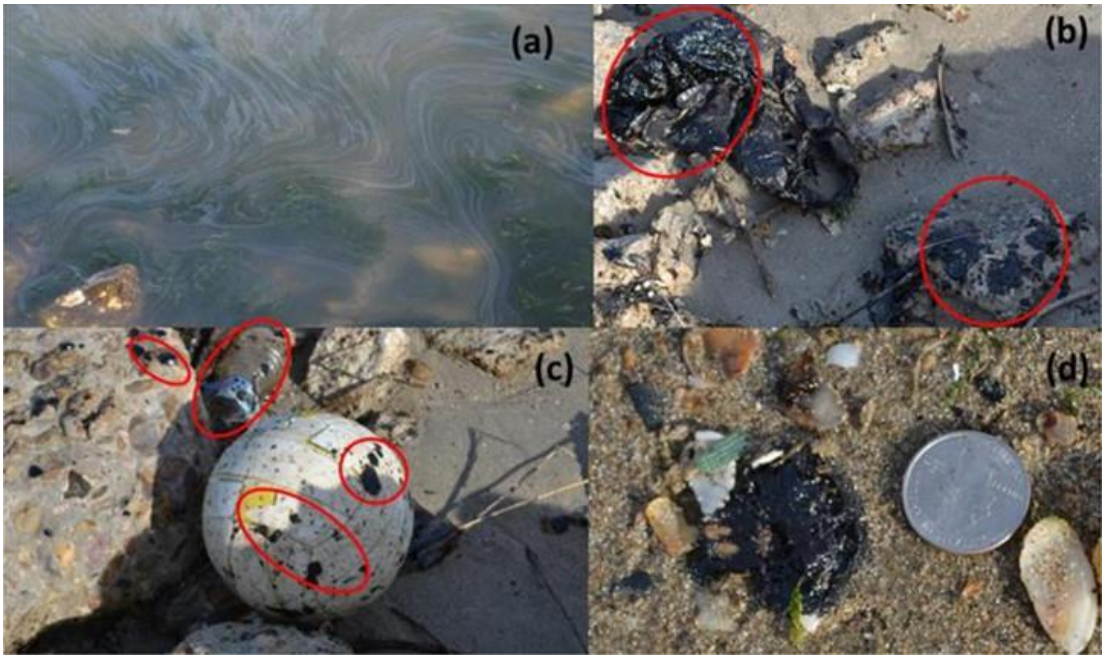

Figure 4.3 Field observations made at the Texas Dike road (Photographs taken on March 29th 2014, by Auburn University team): a) oil sheen observed in nearshore water; b) oil on a plastic sheet and rocks; c) oil on rocks and on a beached soccer ball and other objects; and d) beached oil blobs observed close to the waterline

blobs from the intertidal zone. These samples were shipped to our laboratory for chemical analysis.

4.4 Results and discussion

4.4.1 Chemical characterization data for n-Alkanes

Figure 4.4 shows the n-alkane chromatograms (m/z 57) of GB and DWH oil spill residues. The chromatogram for GB residues indicates the presence of n-alkane compounds ranging from C_{13} to C_{29}. In comparison, n-alkanes profile for DWH oil residue was relatively narrow indicating the presence of compounds ranging from C_{16} to C_{30}, and the lighter alkanes were absent in this sample. From literature data we know that unweathered DWH crude oil contained a wide range of n-alkanes starting from C_9 (Liu et al., 2012). Therefore, the absence of light n-alkanes (i.e., compounds below C_{16}) in the DWH first-arrival sample is due to ocean-scale weathering effects. The DWH samples were recovered from Alabama beaches about 50 days after the accident. During this period, the DWH oil traveled over 175 km in marine waters with ocean-scale weathering processes selectively depleting most of the lighter n-alkanes. In contrast, the GB samples were recovered seven days post-accident; the oil traveled only about 2-3 km in marine waters and experienced very little natural weathering; hence, the relative distribution of light n-alkanes are expected to be high in these samples. Also, both oil residues were sampled at the same seasonal time period (spring) in the northern GOM, with similar water temperatures. Thus, the residence time in marine environment is likely the primary driver for oil evaporation, with temperature playing a minor role (Fingas, 1997).

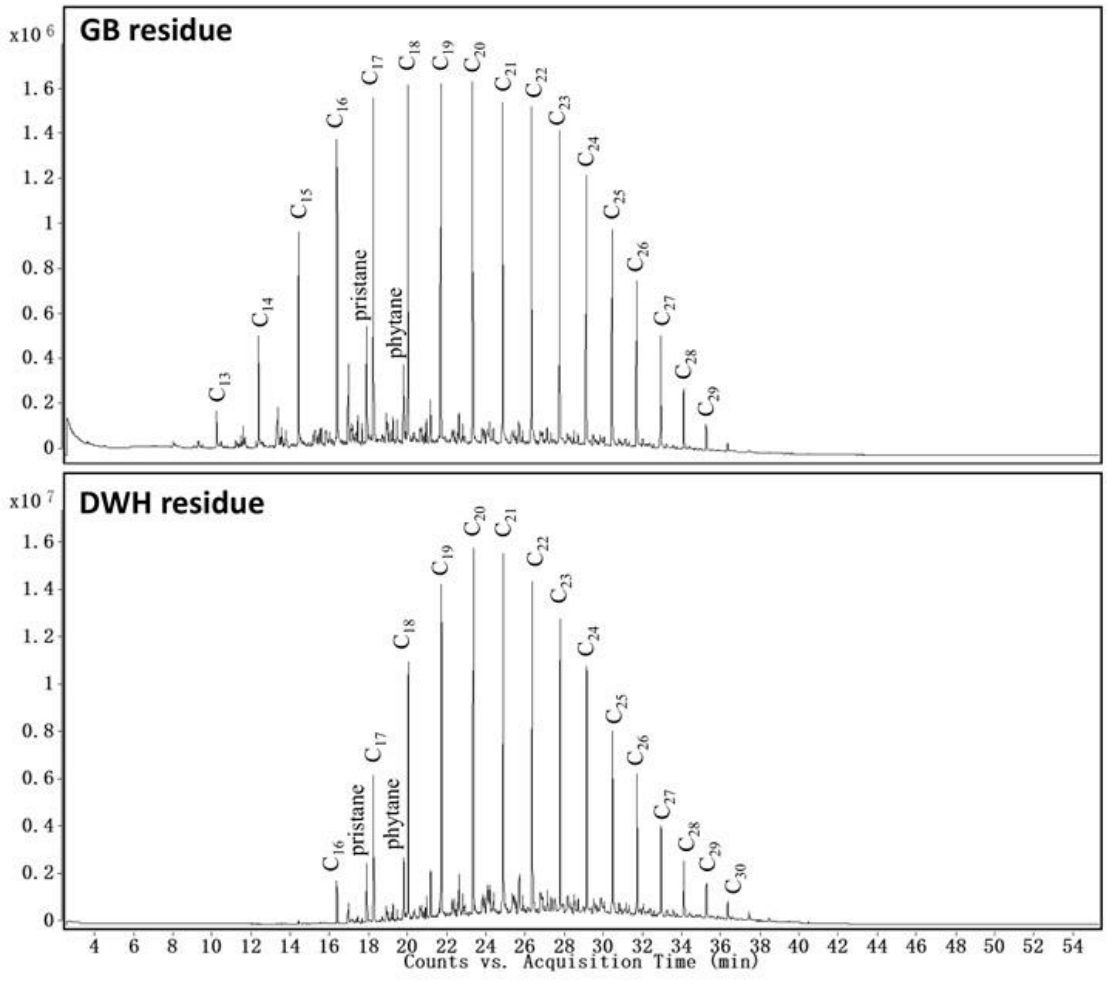

Figure 4.4 Comparison of extracted ion chromatograms of n-alkanes (m/z of 57) for Galveston Bay and Deepwater Horizon oil spill residues

We also quantified n-alkane concentrations by integrating all major peaks for m/z 57, and the concentration levels for various n-alkanes ranging from C_{13} to C_{30} are presented in Figure 4.5. Using the data shown in Figure 4.5, the total amount (values reported as mean ± SD) of n-alkanes in GB and DWH samples are estimated to be 9 ± 1 and 37 ± 2 mg/g of oil, respectively. The total concentration of n-alkanes in GB residues is low since it is a highly refined fuel oil. The ratios of pristane/phytane, C_{17}/pristane,

and C_{18}/phytane are often used for oil source identification (Wang et al., 1999). Based on peak responses, the ratios of pristane/phytane, C_{17}/pristane and C_{18}/phytane were calculated as: 1.48 ± 0.04, 2.13 ± 0.04, and 3.21 ± 0.08 for GB sample and 0.91 ± 0.01, 1.73 ± 0.01, and 2.84 ± 0.02 for DWH sample. These ratios are indicative of differences in the chemical characteristics of these two oils.

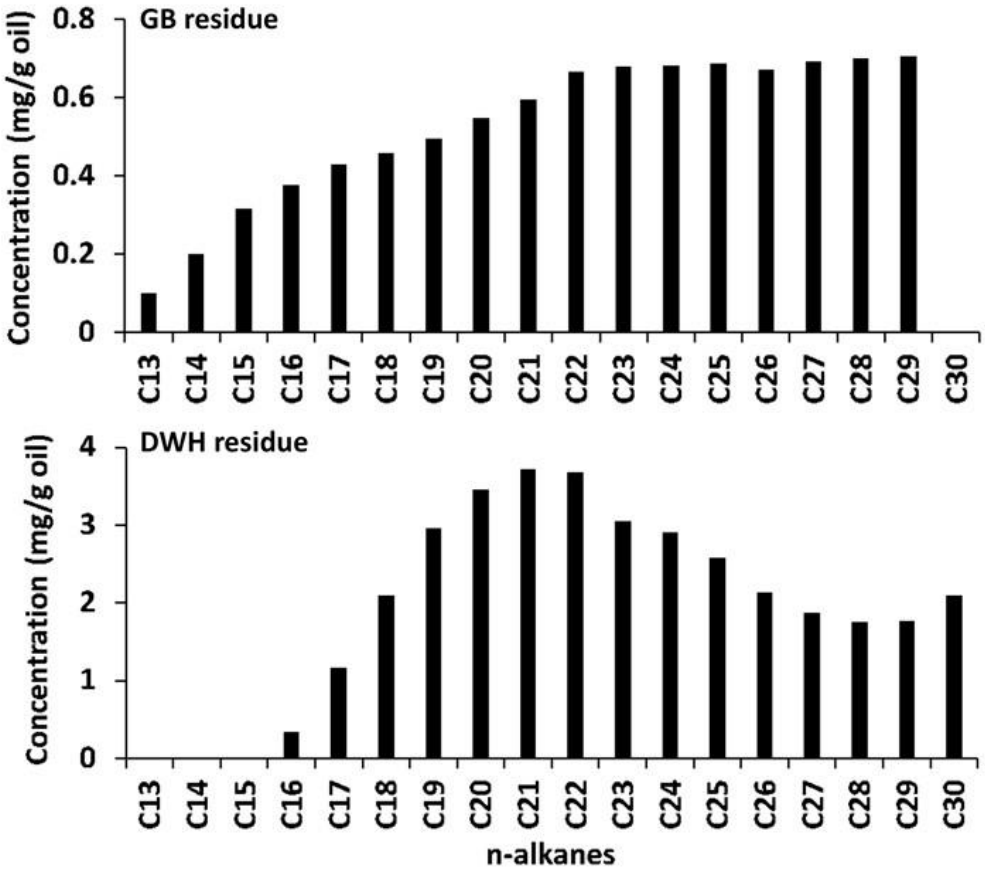

Figure 4.5 Concentration levels of various n-alkanes (ranging from C_{13} to C_{30}) measured in Galveston Bay and Deepwater Horizon oil spill residues

4.4.2 Chemical characterization data for biomarker compounds

In this study, we focused on the biomarker fingerprints of hopanes and steranes, which are the most widely used compounds for fingerprinting oil spill accidents (Wang et al., 1999; Wang and Fingas, 2003). Recently, Aeppli et al. (2014) compared the fate of biomarkers in DWH oil spill residues and concluded that hopanes and steranes, quantified at m/z values of 191 and 217, respectively, are the most reliable signatures for fingerprinting DWH oil spill residues. Figure 4.6 shows GC/MS chromatograms of hopanes (at m/z 191) present in GB and DWH residues. The total amount of hopanes in GB and DWH samples were estimated to be 380±33 mg/kg oil and 439±16 mg/kg oil, respectively. Analysis of hopane chromatograms show that in the DWH sample the hopane distribution ranged from C_{27} to C_{35} with $C_{30}\alpha\beta$-hopane being the most abundant compound. The GB chromatogram, on the other hand, shows higher abundance of $C_{29}\alpha\beta$ and $C_{30}\alpha\beta$ hopanes; also, the response levels are higher for several other possible tricyclic or tetracyclic terpanes, yielding a wider fingerprint (see Figure 4.6). It is well established that $C_{30}\alpha\beta$-hopane is highly resistant to environmental weathering (Aeppli et al., 2014; Douglas et al., 1996; Wang et al., 1999); thus, the amount of $C_{30}\alpha\beta$-hopane will increase over time, and this effect can be used to estimate the degree of weathering. Furthermore, $C_{30}\alpha\beta$-hopane can also be used as a recalcitrant internal biomarker for quantifying the degradation rates of other chemical compounds (Douglas et al., 1996). In this study, we estimated the concentrations of $C_{30}\alpha\beta$-hopane in the GB residue as 81±6 mg/kg oil. The concentration of $C_{30}\alpha\beta$-hopane in the DWH residue has already been reported in Chapter 2 as 91±6 mg/kg oil. These concentration levels can be used as a starting point for understanding future weathering patterns of these oil residues.

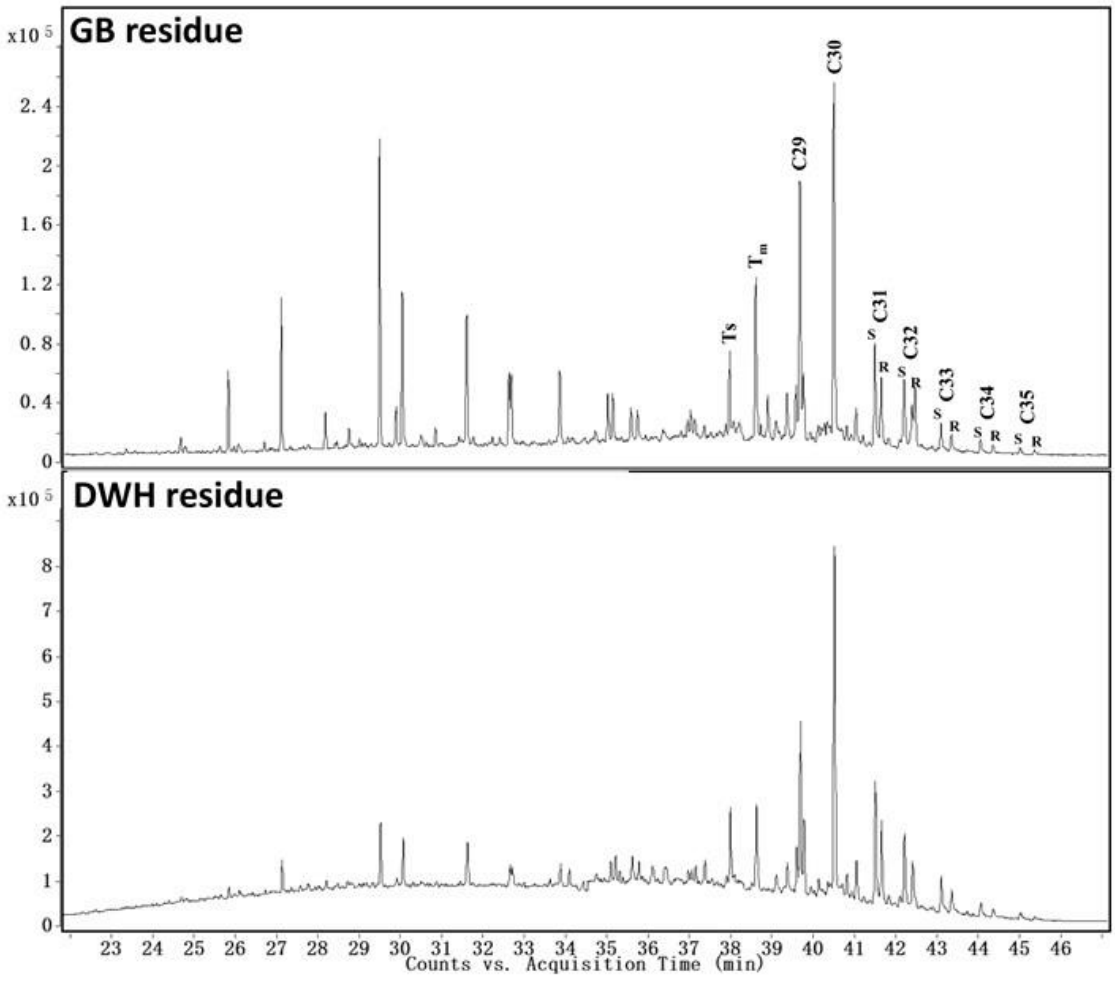

Figure 4.6 Comparison of extracted ion chromatograms of hopanes (m/z of 191) for Galveston Bay and Deepwater Horizon oil spill residues

The diagnostic ratios of different types of hopanes can be used to identify and differentiate oil spill sources (Wang et al., 1999; Wang and Fingas, 2003; Yim et al., 2011). Various ratios including those of T_s/T_m, C_{29}/C_{30}, $C_{31}(S)/C_{31}(S+R)$, $C_{32}(S)/C_{32}(S+R)$, $C_{33}(S)/C_{33}(S+R)$, $C_{34}(S)/C_{34}(S+R)$ and $C_{35}(S)/C_{35}(S+R)$ in GB and DWH residues are summarized in Table 4.2 (part of hopane data for DWH oil are from

Chapter 2). These data are also presented as radar plots in Figure 4.7; the figures reveal that unique fingerprint patterns exist for these two oils, and these patterns can be used to differentiate these two spills from other past or future oil spills.

Table 4.2 Hopane and sterane diagnostic ratios (mean ± SD) estimated for Galveston Bay and Deepwater Horizon oil spill residues

Diagnostic ratio	**GB residue**	**DWH residue**
Hopane ratio		
T_s/T_m	0.41 ±0.02	0.92 ±0.05
C_{29}/C_{30}	0.67 ±0.03	0.37 ±0.01
$C_{31}(S)/C_{31}(S+R)$	0.63 ±0.01	0.63 ±0.01
$C_{32}(S)/C_{32}(S+R)$	0.61 ±0.02	0.65 ±0.01
$C_{33}(S)/C_{33}(S+R)$	0.59 ±0.02	0.61 ±0.01
$C_{34}(S)/C_{34}(S+R)$	0.65 ±0.02	0.63 ±0.01
$C_{35}(S)/C_{35}(S+R)$	0.65 ±0.04	0.65 ±0.03
Sterane ratio		
$DiaC_{27}\beta\alpha(S)/ DiaC_{27}\beta\alpha(R)$	1.48 ±0.06	1.47 ±0.01
$C_{27}\alpha\beta\beta(R+S)/C_{29}\alpha\beta\beta(R+S)$	1.60 ±0.07	3.0 ±0.3
$C_{27}\alpha\beta\beta(R+S)/C_{27}(\alpha\beta\beta(R+S)+ \alpha\alpha\alpha(S+R))$	0.50 ±0.01	0.67 ±0.01
$C_{28}\alpha\beta\beta(R+S)/C_{28}(\alpha\beta\beta(R+S)+ \alpha\alpha\alpha(S+R))$	0.55 ±0.03	0.62 ±0.03
$C_{29}\alpha\beta\beta(R+S)/C_{29}(\alpha\beta\beta(R+S)+ \alpha\alpha\alpha(S+R))$	0.38 ±0.02	0.51 ±0.01

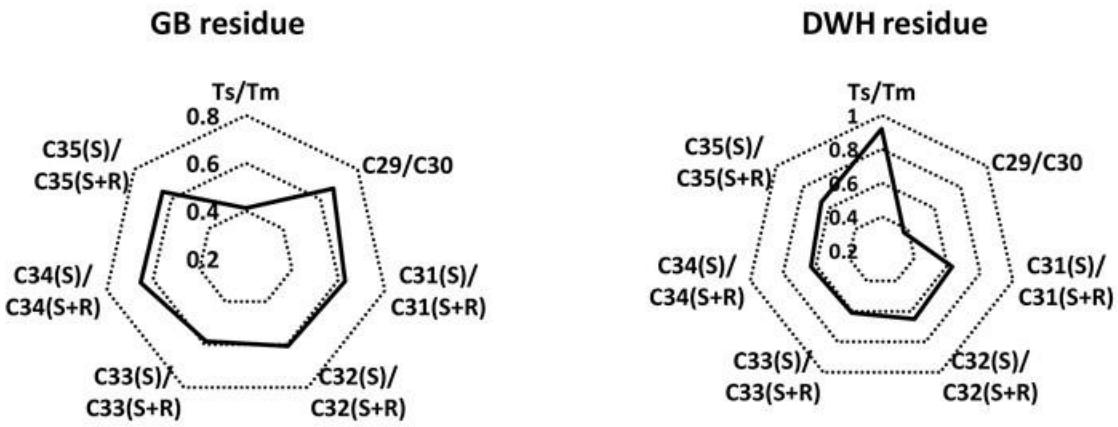

Figure 4.7 Radar plots of hopane diagnostic ratios of Galveston Bay and Deepwater Horizon oil spill residues

The total steranes in GB and DWH samples were found to be 221±5 and 720±30 mg/kg oil, respectively. Similar to hopane data, sterane data can also be used for source identification. Figure 4.8 shows the chromatograms of steranes (at m/z 217) for both GB and DWH residues. The data show that steranes in GB residue are dominated by several high molecular weight compounds (such as C_{29}-steranes). We have identified several sterane peaks based on published data (Peters et al., 2004; Rosenbauer et al., 2010) and used them to compute various diagnostic ratios that are suggested in the literature (Aeppli et al., 2014; Wang et al., 1999; Wang and Fingas, 2003); these results are summarized in Table 4.2. The sterane dataset provides an additional line of evidence for identifying and differentiating these two oil spills.

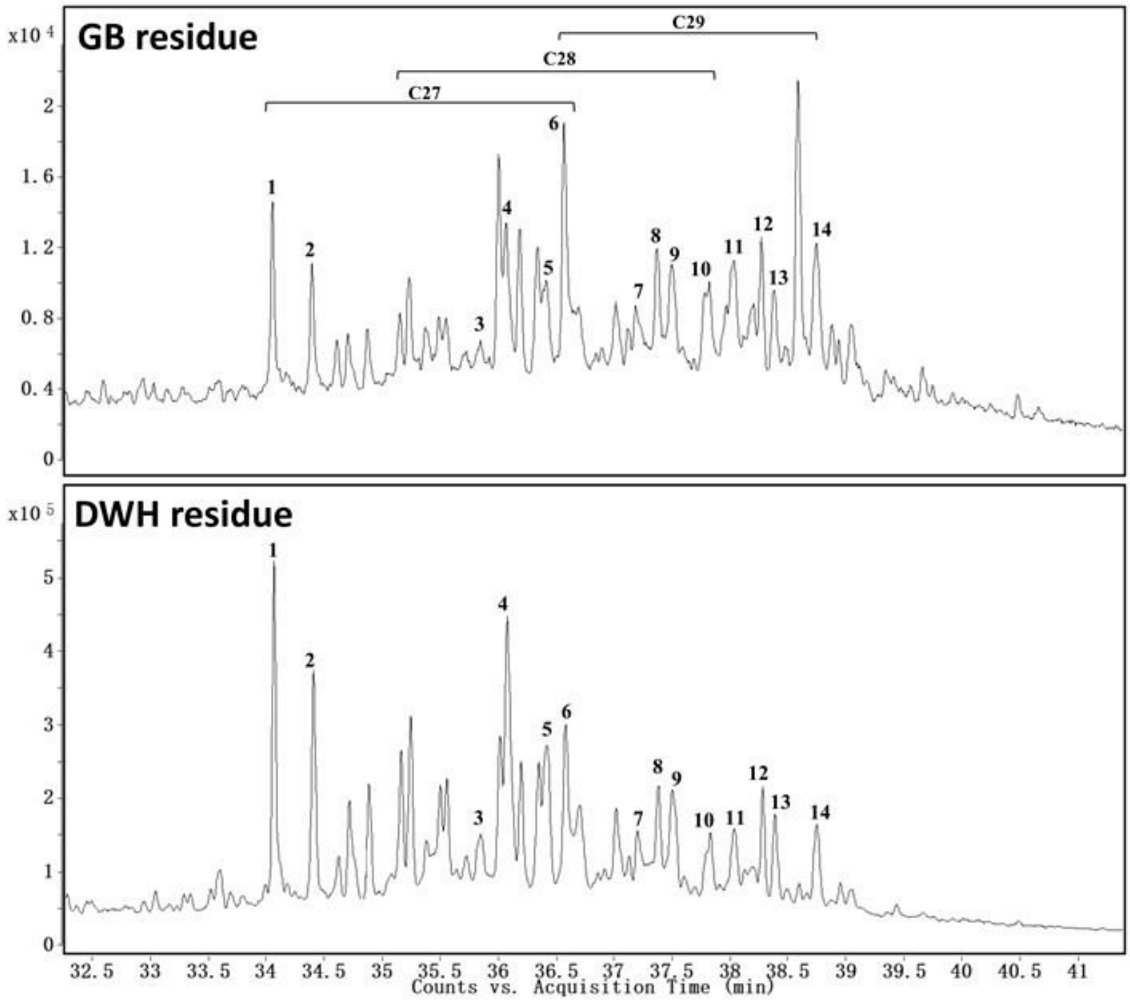

Figure 4.8 Comparison of extracted ion chromatograms of steranes (m/z of 217) for Galveston Bay and Deepwater Horizon oil spill residues [Peak 1: DiaC_{27}βα(S); Peak 2: DiaC_{27}βα(R); Peak 3: C_{27}ααα(S); Peak 4: C_{27}αββ(R); Peak 5: C_{27}αββ(S); Peak 6: C_{27}ααα(R); Peak 7: C_{28}ααα(S); Peak 8: C_{28}αββ(R); Peak 9: C_{28}αββ(S); Peak 10: C_{28}ααα(R); Peak 11: C_{29}ααα(S); Peak 12: C_{29}αββ(R); Peak 13: C_{29}αββ(S); Peak 14: C_{29}ααα(R)]

4.4.3 Chemical characterization data for PAH compounds

Figure 4.9 presents PAH concentration levels measured in DWH and GB residues. In Table 4.3 we summarize these concentrations in terms of five groups of alkylated PAHs (namely naphthalenes, phenanthrenes, dibenzothiophenes, fluorenes and chrysenes) with their parents, and seventeen other PAHs. The extracted ion chromatograms used for quantifying the alkylated PAHs in the GB residue are shown in supporting information (see S1 to S5). For the DWH sample, the total amount of PAHs was estimated to be 1,714 mg/kg oil. The data also show that the five groups of alkylated PAHs were the most dominant compounds and they accounted for about 95% of total PAHs. Among the five groups, phenanthrenes (Group-2) were the most abundant compounds in the DWH sample with a total concentration of 1,183 mg/kg oil (which is about 69% of total PAHs), followed by chrysenes (Group-5) with a total concentration of 178 mg/kg oil (which is 10% of total PAHs), fluorenes (Group-4) with a total concentration of 132 mg/kg oil (which is 8% of total PAHs), dibenzothiophenes (Group-3) with a total concentration of 98 mg/kg oil (which is 6% of total PAHs), and finally naphthalenes (Group-1) with a total concentration of 46 mg/kg oil (which is 3% of total PAHs). The total concentration of all other 3- to 6-ring parent PAHs was estimated to be 33 mg/kg oil, and biphenyl was not detected in the DWH sample.

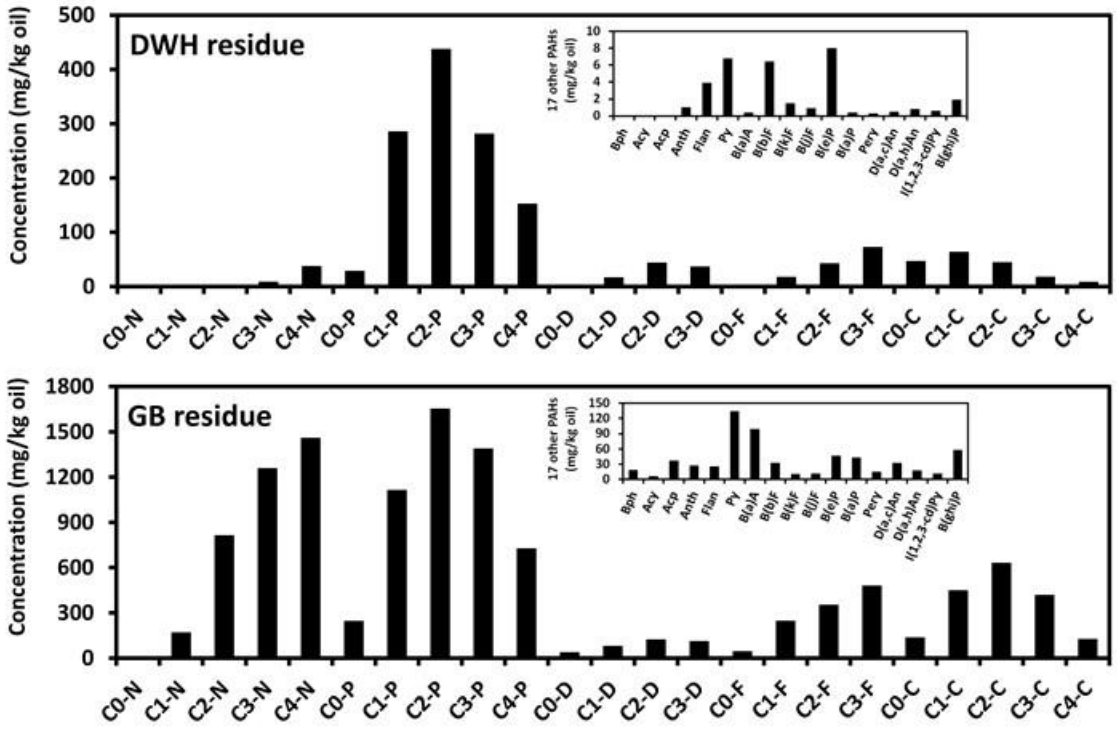

Figure 4.9 Concentration levels of various PAHs and alkylated PAH homologs measured in Deepwater Horizon and Galveston Bay oil spill residues

Table 4.3 Summary of average PAH concentration levels measured in Deepwater Horizon and Galveston Bay oil spill residues (unit: mg/kg oil)

Compound	DWH residue	GB residue
Five groups of alkylated PAHs and their parents		
Group-1: C_0- to C_4-naphthalenes	46	3,699
Group-2: C_0- to C_4-phenanthrenes	1,183	5,119
Group-3: C_0- to C_3-dibenzothiophenes	98	345
Group-4: C_0- to C_3-fluorenes	132	1,117
Group-5: C_0- to C_4-chrysenes	178	1,751
Sum of five groups of PAHs	1,636	12,031
Other seventeen PAHs		
Biphenyl (2-ring)	-	18
Sum of 3 to 6-ring PAHs	33	603
Total amount of PAHs	1,714	12,651

The total amount of PAHs measured in the GB sample was 12,651 mg/kg oil, which is about 7 times higher than the levels measured in the DWH sample (see Table 4.3). Similar to the DWH sample, PAHs in the GB sample were also dominated by the five groups of alkylated PAHs and accounted for about 95% of total PAHs. However, the relative distribution of various types of PAHs in the GB residue was different from the distribution observed for the DWH residue (see Figure 4.9). More importantly, individual concentration levels of almost all the PAHs measured in the GB sample were much higher than the levels measured in the DWH sample. Interestingly, phenanthrenes also are the most abundant group of PAHs in GB residue and the total concentration of phenanthrenes (Group-2) estimated was 5,119 mg/kg oil (which is about 40% of total PAHs). This concentration level is about 4 times higher than the level measured in the DWH sample. The second dominant group of compounds are naphthalenes (Group-1) with a total concentration of 3,699 mg/kg oil (which accounted for about 29% of total PAHs); this level is about 80 times higher than the level observed in the DWH sample. The next group is chrysenes (Group-5) with a total concentration of 1,751 mg/kg oil (which is about 14% of total PAHs); followed by fluorenes (Group-4) with a total concentration of 1,117 mg/kg oil (which is about 9% of total PAHs); and dibenzothiophenes (Group-3) with a total concentration of 345 mg/kg oil (which accounted for about 3% of total PAHs). The concentration of biphenyl and the sum of other 3- to 6-ring PAHs were estimated to be 18 mg/kg oil and 603 mg/kg oil, respectively. Since GB residues were collected a short time after the spill, the concentration levels of light molecular weight PAHs, such as naphthalenes and biphenyl

(which are highly volatile compounds that can easily evaporate during the early stage of a spill) were high, indicating the GB sample experienced very little weathering.

According to the Agency for Toxic Substances and Disease Registry (ATSDR, 1995), most heavy PAHs are either known or probable human carcinogens. For example, the 5-ring compound benzo[*a*]pyrene (BaP) has been shown to cause chromosomal replication errors and it can also affect human fertility levels. The concentration levels of BaP in GB and DWH samples were estimated to be 43 and 0.4 mg/kg oil, respectively. These data suggest that, in terms of BaP toxicity effects, the GB sample is about 100 times more toxic than the DWH sample. Furthermore, concentrations of several alkylated PAHs in the GB residue were relatively high. Previous studies have shown that alkylated phenanthrenes, for example, can induce various types of ecological toxic effects in marine organisms (Fallahtafti et al., 2012; Meador et al., 2008; Turcotte et al., 2011). Our data show that phenanthrene levels in the GB sample was approximately 4 times higher than the DWH sample, and these values were mostly dominated by alkylated phenanthrenes. These data indicate that GB residues might be more toxic than DWH residues. Also, recent studies have demonstrated that alkylated chrysenes in oil residues are likely to be recalcitrant for many years (Wang et al., 1994c). Emerging research has shown that although the measured aqueous solubility limits of individual alkylated chyrsenes are very low, these chemicals could still induce chronic toxic effects in certain sensitive species, e.g., Japanese medaka embryos (*Oryzias latipes*) (Lin et al., 2015). Additionally, studies have shown that the toxic effects of multiple PAHs present in oil spill residues will be additive (Barata et al., 2005). Therefore, based on total PAHs alone, the much higher concentrations present in GB residues are likely to cause far more

adverse effects to fishes and other marine species. However, since the toxicity of individual PAHs can vary significantly (Bellas et al., 2008; Di Toro et al., 2007; Incardona et al., 2014; Incardona et al., 2012), better understanding of overall detrimental ecological effects associated with GB and DWH spills warrants further studies.

4.5 Conclusions

This is the first study that reports field observations and chemical characterization data for the GB oil spill and compares the results against observations made during another major spill-the DWH oil spill. Our data document the differences in weathering patterns of GB and DWH oil spill residues. When compared to DWH first-arrival oil residue, GB first-arrival oil residue experienced much less weathering due to the proximity of the accident to the shoreline. Furthermore, the environmental transport characteristics of the heavy, highly refined GB fuel oil are much different than the raw light, sweet crude oil released during the DWH spill. For example, heavy fuel oil (like the GB oil) is expected to have a low evaporation rate (NOAA, 2014a). In comparison, previous studies have shown that the evaporation rate of DWH raw crude oil is very high and evaporation process alone can remove over 40% oil mass within a week from the DWH source oil (John et al., 2014).

The hopane fingerprinting data show that GB residue has a wider m/z 191 chromatogram and displays a distinctly different fingerprint compared to the DWH fingerprint. Interestingly, both GB and DWH residues had similar amounts of total

hopanes; however the relative ratios of various types of hopane were different, yielding distinctly different fingerprints. GB residue also showed distinctly different sterane fingerprints from the DWH residue; also, the total amount sterane measured in the GB residue was about three times lower than the DWH residue.

For the GB spill, early predictions indicated that the oil would be carried by northeasterly winds out into the GOM, and onshore winds would deposit oil onto various beaches (NOAA, 2014a). Later, overflight observations documented beached oil being rapidly buried under clean sand on Matagorda Island, located about 200 km away from the spill location (NOAA, 2014b). Based on both predicted and observed oil spill trajectories, and also based on the prior knowledge gained from studying the DWH accident, GB oil should have formed SRBs containing heavy fuel oil that are potentially distributed along various beaches located to the southwest of the GB. Since GB residues contain much higher levels of PAHs, these SRBs could pose long-term environmental risks. However, the amount of oil released from the GB spill is relatively low compared to the DWH spill and hence the spatial extent of these impacts will likely be relatively small. Managing oil spill impacts to beach systems is a significant environmental challenge, which is made more complex in systems that experience multiple spill events (such as the GB system). The biomarker and PAH datasets provided in this study are important baseline information for monitoring the long-term fate and the potential environmental impacts of the GB oil spill event.

Chapter 5

Conclusions and recommendations

5.1 Conclusions

Deepwater Horizon oil spill was one of the largest marine oil spill disasters in U.S. history which impacted the shorelines of Florida, Alabama, Mississippi and Louisiana. Amenity beaches located along Orange Beach, Gulf Shores and Fort Morgan regions in the State of Alabama were severely impacted by the spill. These beaches are priceless due to their economic and environmental values. The main focus of this study is to identify and fingerprint the source of the oil spill residues found along Alabama's beaches and to characterize the fate of petroleum chemicals trapped in these oil spill residues.

We first compared the chromatographic signatures of various petroleum biomarkers including hopanes and steranes present in Deepwater Horizon (DWH) source oil, three reference crude oils, and various types of oil spill residues collected along Alabama beaches. Characteristic hopane and sterane fingerprints show that all tested oil spill residues match the fingerprints of the DWH reference crude. Furthermore, measured concentration levels of an abundant hopane, C30αβ-hopane, show that most of the weathering observed in DWH-related tar balls found on Alabama's beaches is likely

the result of natural evaporation and dissolution processes that occurred when the oil was transported across the Gulf of Mexico. Based on the hopane and sterane datasets presented in this study and based on the fact that there is no past record of fragile, sticky tar ball deposition in our study region prior to the DWH oil spill, we conclude that virtually all fragile, sticky, brownish tar balls currently found on Alabama's beaches are from the Deepwater Horizon oil spill.

The four-year PAH dataset presented in this study show the temporal evolution of various PAHs and their alkylated homologs trapped in the oil spill samples collected near Lagoon Pass, Alabama. This dataset also shows that evaporation was a key weathering mechanism for PAH weathering. However, other weathering processes such as photo-degradation and dissolution have contributed to some additional PAH weathering, and also these weathering occurred during initial days when the oil was floating on offshore waters. The rate of PAH weathering appears to have decreased significantly once the oil was buried within nearshore environment, supporting a "slowing down" hypothesis. The heavy PAHs present in the submerged oil residues have the potential to cause various environmental impacts on Alabama's nearshore ecosystems; however the long-term consequences of these environmental exposures are currently unknown.

The experiences we have gained by analyzing DWH oil spill residues were enormous. The fingerprinting and PAHs characterization methods that were originally developed to the DWH oil spill residues were successfully applied to investigate another recent GOM oil spill accident, the 2014 Galveston Bay (GB) oil spill. Chemical characteristics of GB oil residues were characterized in terms of n-alkanes, hopanes and

steranes, and parent PAHs and their alkylated homologs. The similarities and differences between these two different GOM oil spills were identified. Our data show that although GB spill was relatively small but the GB residues were relatively more toxic than DWH residues. The chemical analysis and data interpretation methods used to investigate the two GOM oil spills provide a standard approach for investigating future oil spill accidents in this region.

This dissertation provides a comprehensive chemical characterization dataset for characterizing hydrocarbon pollution of the Gulf of Mexico, caused by DWH and GB oil spills. Also, this dissertation presents an initial understanding of rapid oil weathering patterns that occurred in open offshore environment, which is a two-phase oil-water system. Furthermore, our data show that the partially-closed nearshore environment, which is a three-phase oil-water-sediment system, could have much slower weathering rates. The data reported in this dissertation are expected to be valuable information for managing future GOM oil spill events.

5.2 Recommendations

This study investigated the chemical characteristics of several types of crude oils, and also estimated the temporal changes in the concentration levels of several toxic PAHs typically trapped in oil spill residues. There are still a number of scientific issues that require further investigations. Some possible future research directions are described below.

Advanced chemical characterization methods that can uniquely distinguish different types of GOM crude oils are needed. As of December 2009, about 21.20 billion barrels of oil and 190.2 trillion cubic feet of gas were estimated to be present in the Gulf of Mexico Outer Continental Shelf region (Maclay et al., 2013). Currently, over 4000 oil rigs exist in the northern GOM region and they are actively exploring and/or utilizing this huge oil reserve (Axtman, 2005). In this regard, the chance of having another large oil spill within this region is very high. Therefore, in order to better monitor future spills and differentiate their residues from historic old oil spill residues we need better methods for differentiating different types of GOM crudes. In addition to drilling operations, natural seeps are other possible sources of oil contamination in GOM. Therefore, advanced fingerprinting methods are also needed to differentiate anthropogenic releases from other natural seep inputs. The NRC (2003) study estimated that within GOM there are more than 600 natural oil seeps that have the potential to leak between one and five million barrels of oil every year. However, it is important to note that unlike the MC 252 well, a point source that released over 4.9 million barrels of oil at a very high rate within a relatively short period of 87 days, these natural seeps are distributed over a very large area and release oil at a much lower rate. Therefore, the relative environmental risks posed by a point release such as the DWH accident will be much higher than distributed natural seep releases.

Differentiating different types of petroleum residues and tar balls that wash along GOM shorelines is another important oil spill management issue. As concluded in this study, the MC252 oil spill related tar balls that remain near Alabama's beach environment can be uniquely differentiated from other traditional tar balls since they not

only have some unique chemical characteristics, but also they have several unique physical characteristics – sticky, brownish, petroleum smelling, high sand content etc. The SCCP study has reported that these physical characteristics are extremely unique to DWH oil spill residues (SCCP, 2011). These characteristics are the result of a large volume of emulsified oil (with density close to seawater density) washing towards the shoreline, and the emulsion having the opportunity to interact with suspended sand particles and subsequently sink to the bottom of the shoreline region. As far as we know, no one has recovered any non-DWH tar balls with such unique physical characteristics from Alabama's coastline. Further field studies are also needed to investigate other spill events that could have resulted in tar balls with these unique physical characteristics. Also, further laboratory studies are needed to investigate the future fate of PAHs trapped in these DWH tar balls.

References

Aeppli C, Carmichael CA, Nelson RK, Lemkau KL, Graham WM, Redmond MC, et al. Oil Weathering after the Deepwater Horizon Disaster Led to the Formation of Oxygenated Residues. Environmental Science & Technology 2012; 46: 8799-8807.

Aeppli C, Nelson RK, Radovic JR, Carmichael CA, Valentine DL, Reddy CM. Recalcitrance and Degradation of Petroleum Biomarkers upon Abiotic and Biotic Natural Weathering of Deepwater Horizon Oil. Environmental Science & Technology 2014; 48: 6726-6734.

Anderson CM, LaBelle RP. Update of comparative occurrence rates for offshore oil spills. Spill Science & Technology Bulletin 2000; 6: 303-321.

Atlas R, Bragg J. Bioremediation of marine oil spills: when and when not - the Exxon Valdez experience. Microbial Biotechnology 2009; 2: 213-221.

Atlas RM, Hazen TC. Oil Biodegradation and Bioremediation: A Tale of the Two Worst Spills in US History. Environmental Science & Technology 2011; 45: 6709-6715.

ATSDR. Chemical and physical information, in: Toxicological Profile for Polycyclic Aromatic Hydrocarbons (PAHs). Agency for Toxic Substances and Disease Registry, 1995.

Axtman K. Science of Oil Rigs: Surviving Gulf Storms. Christian Science Monitor, July 26, 2005. Internet document: http://www.csmonitor.com/2005/0726/p03s01-usgn.html 2005.

Barakat AO, Mostafa AR, Rullkotter J, Hegazi AR. Application of a multimolecular marker approach to fingerprint petroleum pollution in the marine environment. Marine Pollution Bulletin 1999; 38: 535-544.

Barata C, Calbet A, Saiz E, Ortiz L, Bayona JM. Predicting single and mixture toxicity of petrogenic polycyclic aromatic hydrocarbons to the copepod Oithona davisae. Environmental Toxicology and Chemistry 2005; 24: 2992-2999.

Bellas J, Saco-Alvarez L, Nieto O, Beiras R. Ecotoxicological evaluation of polycyclic aromatic hydrocarbons using marine invertebrate embryo-larval bioassays. Marine Pollution Bulletin 2008; 57: 493-502.

Boese BL, Lamberson JO, Swartz RC, Ozretich R, Cole F. Photoinduced Toxicity of PAHs and Alkylated PAHs to a Marine Infaunal Amphipod (Rhepoxynius abronius). Archives of Environmental Contamination and Toxicology 1998; 34: 235-240.

Bragg JR, Prince RC, Harner EJ, Atlas RM. Effectiveness of Bioremediation for the Exxon-Valdez Oil-Spill. Nature 1994; 368: 413-418.

Burgherr P. In-depth analysis of accidental oil spills from tankers in the context of global spill trends from all sources. Journal of Hazardous Materials 2007; 140: 245-256.

Canevari GP. The effect of crude oil composition on dispersant performance. International Oil Spill Conference Proceedings 1985; 1985: 441-444.

Carmichael CA, Arey JS, Graham WM, Linn LJ, Lemkau KL, Nelson RK, et al. Floating oil-covered debris from Deepwater Horizon: identification and application. Environmental Research Letters 2012; 7.

Chandru K, Zakaria MP, Anita S, Shahbazi A, Sakari M, Bahry PS, et al. Characterization of alkanes, hopanes, and polycyclic aromatic hydrocarbons (PAHs) in tax-balls collected from the East Coast of Peninsular Malaysia. Marine Pollution Bulletin 2008; 56: 950-962.

Das N, Chandran P. Microbial degradation of petroleum hydrocarbon contaminants: an overview. Biotechnol Res Int 2011; 2011: 941810.

Di Toro DM, McGrath JA, Stubblefield WA. Predicting the toxicity of neat and weathered crude oil: Toxic potential and the toxicity of saturated mixtures. Environmental Toxicology and Chemistry 2007; 26: 24-36.

Douglas GS, Bence AE, Prince RC, McMillen SJ, Butler EL. Environmental stability of selected petroleum hydrocarbon source and weathering ratios. Environmental Science & Technology 1996; 30: 2332-2339.

Dubansky B, Whitehead A, Miller JT, Rice CD, Galvez F. Multitissue molecular, genomic, and developmental effects of the Deepwater Horizon oil spill on resident Gulf killifish (Fundulus grandis). Environmental Science & Technology 2013; 47: 5074-82.

Fallahtafti S, Rantanen T, Brown RS, Snieckus V, Hodson PV. Toxicity of hydroxylated alkyl-phenanthrenes to the early life stages of Japanese medaka (Oryzias latipes). Aquatic Toxicology 2012; 106: 56-64.

Fathalla EM, Andersson JT. Products of Polycyclic Aromatic Sulfur Heterocycles in Oil Spill Photodegradation. Environmental Toxicology and Chemistry 2011; 30: 2004-2012.

Fingas M. The basics of oil spill cleanup: CRC Press, 2012a.

Fingas MF. Studies on the evaporation of crude oil and petroleum products: I. the relationship between evaporation rate and time. Journal of Hazardous Materials 1997; 56: 227-236.

Fingas MF. The Evaporation of Oil Spills: Development and Implementation of New Prediction Methodology. International Oil Spill Conference Proceedings 1999; 1999: 281-287.

Fingas MF. Studies on the Evaporation Regulation Mechanisms of Crude Oil and Petroleum Products. Advances in Chemical Engineering and Science 2012b; 2: 246.

Fingas MF. Modeling Oil and Petroleum Evaporation. Journal of Petroleum Science Research (JPSR) 2013; 2: 104-115.

Fisher CR, Hsing PY, Kaiser CL, Yoerger DR, Roberts HH, Shedd WW, et al. Footprint of Deepwater Horizon blowout impact to deep-water coral communities. Proceedings of the National Academy of Sciences of the United States of America 2014; 111: 11744-11749.

Garrett RM, Pickering IJ, Haith CE, Prince RC. Photooxidation of crude oils. Environmental Science & Technology 1998; 32: 3719-3723.

Harvey GR. Environmental Chemistry of PAHs, PAH and related compounds, in: Alasdair H. Neilson (Ed.), The Handbook of Environmental Chemistry Vol 3-I: Springer, Berlin, 1998.

Hauser A, Dashti H, Khan ZH. Identification of biomarker compounds in selected Kuwait crude oils. Fuel 1999; 78: 1483-1488.

Hayworth JS, Clement TP. BP's Operation Deep Clean-Could Dilution be the Solution to Beach Pollution? . Environmental Science & Technology 2011; 45: 4201-4202.

Hayworth JS, Clement TP, John GF, Yin F. Fate of Deepwater Horizon oil in Alabama's beach system: Understanding physical evolution processes based on observational data. Marine Pollution Bulletin 2015; 90: 95-105.

Hayworth JS, Clement TP, Valentine JF. Deepwater Horizon oil spill impacts on Alabama beaches. Hydrology and Earth System Sciences 2011; 15: 3639-3649.

Helmenstine AM. Chemical Composition of Petroleum. http://chemistry.about.com/od/geochemistry/a/Chemical-Composition-Of-Petroleum.htm, 2014.

Hoffman DJ, Gay ML. Embryotoxic effects of benzo[a]pyrene, chrysene, and 7,12-dimethylbenz[a]anthracene in petroleum hydrocarbon mixtures in mallard ducks. J Toxicol Environ Health 1981; 7: 775-87.

Hostettler FD, Lorenson TD, Bekins BA. Petroleum Fingerprinting with Organic Markers. Environmental Forensics 2013; 14: 262-277.

Idris HK, Salihu A, Abdulkadir I, Almustapha MN. Application of geochemical parameters for characterization of oil samples using GC-MS technique. International Journal of Physical Sciences 2008; 3: 152-155.

Incardona JP, Gardner LD, Linbo TL, Brown TL, Esbaugh AJ, Mager EM, et al. Deepwater Horizon crude oil impacts the developing hearts of large predatory pelagic fish. Proc Natl Acad Sci U S A 2014; 111: E1510-8.

Incardona JP, Vines CA, Linbo TL, Myers MS, Sloan CA, Anulacion BF, et al. Potent Phototoxicity of Marine Bunker Oil to Translucent Herring Embryos after Prolonged Weathering. Plos One 2012; 7.

ITOPF. OIL TANKER SPILL STATISTICS 2014. http://www.itopf.com/fileadmin/data/Documents/Company_Lit/Oil_Spill_Stats_2014FINALlowres.pdf, 2015.

John GF, Yin F, Mulabagal V, Hayworth JS, Clement TP. Development and application of an analytical method using gas chromatography/triple quadrupole mass spectrometry for characterizing alkylated chrysenes in crude oil samples. Rapid Commun Mass Spectrom 2014; 28: 948-56.

Lin H, Morandi GD, Brown RS, Snieckus V, Rantanen T, Jørgensen KB, et al. Quantitative structure-activity relationships for chronic toxicity of alkyl-chrysenes and alkyl-benz[a]anthracenes to Japanese medaka embryos (Oryzias latipes). Aquatic Toxicology 2015; In press.

Liu ZF, Liu JQ, Zhu QZ, Wu W. The weathering of oil after the Deepwater Horizon oil spill: insights from the chemical composition of the oil from the sea surface, salt marshes and sediments. Environmental Research Letters 2012; 7.

MacDougall D, Crummett WB. Guidelines for data acquisition and data quality evaluation in environmental chemistry. Analytical Chemistry 1980; 52: 2242-2249.

Machala M, Svihalkova-Sindlerova L, Pencikova K, Krcmar P, Topinka J, Milcova A, et al. Effects of methylated chrysenes on AhR-dependent and -independent toxic events in rat liver epithelial cells. Toxicology 2008; 247: 93-101.

Maclay DM, Shepard NK, Zeringue BA. Estimated Oil and Gas Reserves Gulf of Mexico OCS Region December 31, 2009, 2013.

Martinez ML, Feagin RA, Yeager KM, Day J, Costanza R, Harris JA, et al. Artificial modifications of the coast in response to the Deepwater Horizon oil spill: quick solutions or long-term liabilities? Frontiers in Ecology and the Environment 2012; 10: 44-49.

Mason OU, Scott NM, Gonzalez A, Robbins-Pianka A, Baelum J, Kimbrel J, et al. Metagenomics reveals sediment microbial community response to Deepwater Horizon oil spill. Isme Journal 2014; 8: 1464-1475.

McCrea-Strub A, Kleisner K, Sumaila UR, Swartz W, Watson R, Zeller D, et al. Potential Impact of the Deepwater Horizon Oil Spill on Commercial Fisheries in the Gulf of Mexico. Fisheries 2011; 36: 332-336.

McLean J, Spiecker PM, Sullivan A, Kilpatrick P. The Role of Petroleum Asphaltenes in the Stabilization of Water-in-Oil Emulsions. In: Mullins O, Sheu E, editors. Structures and Dynamics of Asphaltenes. Springer US, 1998, pp. 377-422.

Meador JP, Buzitis J, Bravo CF. Using fluorescent aromatic compounds in bile from juvenile salmonids to predict exposure to polycyclic aromatic hydrocarbons. Environmental Toxicology and Chemistry 2008; 27: 845-853.

Michel J, Owens EH, Zengel S, Graham A, Nixon Z, Allard T, et al. Extent and Degree of Shoreline Oiling: Deepwater Horizon Oil Spill, Gulf of Mexico, USA. Plos One 2013; 8.

Mostafa AR, Hegazi AH, El-Gayar MS, Andersson JT. Source characterization and the environmental impact of urban street dusts from Egypt based on hydrocarbon distributions. Fuel 2009; 88: 95-104.

Mottier P, Parisod V, Turesky RJ. Quantitative determination of polycyclic aromatic hydrocarbons in barbecued meat sausages by gas chromatography coupled to mass spectrometry. Journal of Agricultural and Food Chemistry 2000; 48: 1160-1166.

Mulabagal V, Yin F, John GF, Hayworth JS, Clement TP. Chemical fingerprinting of petroleum biomarkers in Deepwater Horizon oil spill samples collected from Alabama shoreline. Marine Pollution Bulletin 2013; 70: 147-154.

Mumtaz MM, George JD, Gold KW, Cibulas W, Derosa CT. ATSDR evaluation of health effects of chemicals .4. Polycyclic aromatic hydrocarbons (PAHs): Understanding a complex problem. Toxicology and Industrial Health 1996; 12: 742-971.

Neff JM. Polycyclic Aromatic Hydrocarbons in the Aquatic Environment: Sources, Fates and Biological Effects: Applied Science Publishers ltd., London, 1979.

Nisbet ICT, Lagoy PK. Toxic Equivalency Factors (Tefs) for Polycyclic Aromatic-Hydrocarbons (Pahs). Regulatory Toxicology and Pharmacology 1992; 16: 290-300.

NOAA. Kirby Barge Oil Spill, Houston/Texas City Ship Channel, Port Bolivar, Texas. http://response.restoration.noaa.gov/oil-and-chemical-spills/oil-spills/kirby-barge-oil-spill-houstontexas-city-ship-channel-port-bolivar, 2014a.

NOAA. Progress at the Texas City oil spill in Galveston Bay. http://usresponserestoration.wordpress.com/2014/03/28/progress-at-the-texas-city-y-oil-spill-in-galveston-bay/, 2014b.

NRC. Oil in the sea III: inputs, fates, and effects. National Research Council . Committee on Oil in the Sea Fates: national academies Press, 2003.

OSAT-2. Summary Report for Fate and Effects of Remant Oil Remaing in the Beach Environment. Operational Science Advisory Team (OSAT-2), Unified Area Command, 2011.

OSAT-3. Investigation of Recurring Residual Oil in Discrete Shoreline Areas in the Eastern Area of Responsibility Operational Science Advisory Team, Unified Area Command, 2014.

Pauzi Zakaria M, Okuda T, Takada H. Polycyclic Aromatic Hydrocarbon (PAHs) and Hopanes in Stranded Tar-balls on the Coasts of Peninsular Malaysia: Applications of Biomarkers for Identifying Sources of Oil Pollution. Marine Pollution Bulletin 2001; 42: 1357-1366.

Peters K, Walters C, Moldowan J. The biomarker guide: Volume 1, Biomarkers and isotopes in the environment and human history: Cambridge university press, UK, 2004.

Peters K, Walters C, Moldowan J. The biomarker guide, volume 2–Biomarkers and isotopes in petroleum exploration and earth history. Cambridge University Press, UK, 2005.

Peters KE, Moldowan JM. The biomarker guide: Interpreting molecular fossils in petroleum and ancient sediments, 1993.

Plant NG, Long JW, Dalyander PS, Thompson DM, Raabe EA. Application of a hydrodynamic and sediment transport model for guidance of response efforts related to the Deepwater Horizon oil spill in the Northern Gulf of Mexico along the coast of Alabama and Florida: U.S. Geological Survey Open-File Report 2012-1234, 46 p. 2013.

Pritchard PH, Mueller JG, Rogers JC, Kremer FV, Glaser JA. Oil spill bioremediation: experiences, lessons and results from the Exxon Valdez oil spill in Alaska. Biodegradation 1992; 3: 315-335.

Radovic JR, Aeppli C, Nelson RK, Jimenez N, Reddy CM, Bayona JM, et al. Assessment of photochemical processes in marine oil spill fingerprinting. Marine Pollution Bulletin 2014; 79: 268-77.

Rosenbauer, R.J. C, P.L. L, Angela, , Lorenson TD, Hostettler FD, Thomas B, et al. Reconnaissance of Macondo-1 well oil in sediment and tarballs from the northern Gulf of Mexico shoreline, Texas to Florida: U.S. Geological Survey Open-File Report 2010-1290, 22 p. 2010.

Ruddy BM, Huettel M, Kostka JE, Lobodin VV, Bythell BJ, McKenna AM, et al. Targeted Petroleomics: Analytical Investigation of Macondo Well Oil Oxidation Products from Pensacola Beach. Energy & Fuels 2014; 28: 4043-4050.

Sammarco PW, Kolian SR, Warby RAF, Bouldin JL, Subra WA, Porter SA. Distribution and concentrations of petroleum hydrocarbons associated with the BP/Deepwater Horizon Oil Spill, Gulf of Mexico. Marine Pollution Bulletin 2013; 73: 129-143.

SCCP. Shoreline clean up completing plan. Published by the Unified Command SCCP Core Group, November 2011.

Sebastião P, Guedes Soares C. Modeling the fate of oil spills at sea. Spill Science & Technology Bulletin 1995; 2: 121-131.

Shen J. Minimization of Interferences from Weathering Effects and Use of Biomarkers in Identification of Spilled Crude Oils by Gas-Chromatography Mass-Spectrometry. Analytical Chemistry 1984; 56: 214-217.

Smith LL, Strickland JR. Improved GC/MS method for quantitation of n-alkanes in plant and fecal material. Journal of Agricultural and Food Chemistry 2007; 55: 7301-7307.

Somasundaran P, Patra P, Farinato RS, Papadopoulos K. Oil Spill Remediation: Colloid Chemistry-based Principles and Solutions. pp.302, 2014.

Stout SA. Applications of petroleum fingerprinting in known and suspected pipeline releases—two case studies. Applied Geochemistry 2003; 18: 915-926.

TGLO. Galveston Bay status and trends. http://www.galvbaydata.org/WaterandSediment/OilSpills/tabid/218/Default.aspx. 2010.

Thibodeaux LJ, Valsaraj KT, John VT, Papadopoulos KD, Pratt LR, Pesika NS. Marine Oil Fate: Knowledge Gaps, Basic Research, and Development Needs; A Perspective Based on the Deepwater Horizon Spill. Environmental Engineering Science 2011; 28: 87-93.

Turcotte D, Akhtar P, Bowerman M, Kiparissis Y, Brown RS, Hodson PV. Measuring the Toxicity of Alkyl-Phenanthrenes to Early Life Stages of Medaka (Oryzias Latipes) Using Partition-Controlled Delivery. Environmental Toxicology and Chemistry 2011; 30: 487-495.

Urbano M, Elango V, Pardue JH. Biogeochemical characterization of MC252 oil:sand aggregates on a coastal headland beach. Marine Pollution Bulletin 2013; 77: 183-191.

USEPA. Appendix A to Part 423-126 Priority Pollutants. 47 FR 52304, Nov. 19, 1982. http://water.epa.gov/scitech/wastetech/guide/steam-electric/upload/Steam-Electric_Final-Rule_47-FR-52290_111982.pdf, 1982.

Vermeire MB. Everything You Need to Know About Marine Fuels. Published by Chevron Global Marine Products, 2012.

Wang HX, Xu JL, Zhao WK, Zhang JQ. Effects and Risk Evaluation of Oil Spillage in the Sea Areas of Changxing Island. International Journal of Environmental Research and Public Health 2014; 11: 8491-8507.

Wang Z, Yang C, Yang Z, Sun J, Hollebone B, Brown C, et al. Forensic fingerprinting and source identification of the 2009 Sarnia (Ontario) oil spill. Journal of Environmental Monitoring 2011; 13: 3004-3017.

Wang ZD, Fingas M, Lambert P, Zeng G, Yang C, Hollebone B. Characterization and identification of the Detroit River mystery oil spill (2002). Journal of Chromatography A 2004; 1038: 201-214.

Wang ZD, Fingas M, Landriault M, Sigouin L, Feng YP, Mullin J. Using systematic and comparative analytical data to identify the source of an unknown oil on contaminated birds. Journal of Chromatography A 1997; 775: 251-265.

Wang ZD, Fingas M, Li K. Fractionation of a Light Crude-Oil and Identification and Quantitation of Aliphatic, Aromatic, and Biomarker Compounds by Gc-Fid and Gc-Ms .1. Journal of Chromatographic Science 1994a; 32: 361-366.

Wang ZD, Fingas M, Li K. Fractionation of a Light Crude-Oil and Identification and Quantitation of Aliphatic, Aromatic, and Biomarker Compounds by Gc-Fid and Gc-Ms .2. Journal of Chromatographic Science 1994b; 32: 367-382.

Wang ZD, Fingas M, Owens EH, Sigouin L, Brown CE. Long-term fate and persistence of the spilled Metula oil in a marine salt marsh environment - Degradation of petroleum biomarkers. Journal of Chromatography A 2001; 926: 275-290.

Wang ZD, Fingas M, Page DS. Oil spill identification. Journal of Chromatography A 1999; 843: 369-411.

Wang ZD, Fingas M, Sergy G. Study of 22-Year-Old Arrow Oil Samples Using Biomarker Compounds by Gc/Ms. Environmental Science & Technology 1994c; 28: 1733-1746.

Wang ZD, Fingas MF. Development of oil hydrocarbon fingerprinting and identification techniques. Marine Pollution Bulletin 2003; 47: 423-452.

Wang ZD, Stout SA, Fingas M. Forensic fingerprinting of biomarkers for oil spill characterization and source identification. Environmental Forensics 2006; 7: 105-146.

White HK, Hsing PY, Cho W, Shank TM, Cordes EE, Quattrini AM, et al. Impact of the Deepwater Horizon oil spill on a deep-water coral community in the Gulf of Mexico. Proceedings of the National Academy of Sciences of the United States of America 2012; 109: 20303-20308.

Wolfe DA, Hameedi MJ, Galt JA, Watabayashi G, Short J, Oclaire C, et al. The Fate of the Oil Spilled from the Exxon-Valdez. Environmental Science & Technology 1994; 28: A560-A568.

Xia K, Hagood G, Childers C, Atkins J, Rogers B, Ware L, et al. Polycyclic Aromatic Hydrocarbons (PAHs) in Mississippi Seafood from Areas Affected by the Deepwater Horizon Oil Spill. Environmental Science & Technology 2012; 46: 5310-5318.

Yim UH, Ha SY, An JG, Won JH, Han GM, Hong SH, et al. Fingerprint and weathering characteristics of stranded oils after the Hebei Spirit oil spill. Journal of Hazardous Materials 2011; 197: 60-69.

Yin F, Hayworth JS, Clement TP. A Tale of Two Recent Spills-Comparison of 2014 Galveston Bay and 2010 Deepwater Horizon Oil Spill Residues. Plos One 2015a; 10.

Yin F, John GF, Hayworth JS, Clement TP. Long-term monitoring data to describe the fate of polycyclic aromatic hydrocarbons in Deepwater Horizon oil submerged off Alabama's beaches. Science of the Total Environment 2015; 508: 46-56.

Zakaria MP, Okuda T, Takada H. Polycyclic aromatic hydrocarbon (PAHs) and hopanes in stranded tar-balls on the coasts of Peninsular Malaysia: Applications of biomarkers for identifying sources of oil pollution. Marine Pollution Bulletin 2001; 42: 1357-1366.

Zuijdgeest A, Huettel M. Dispersants as Used in Response to the MC252-Spill Lead to Higher Mobility of Polycyclic Aromatic Hydrocarbons in Oil-Contaminated Gulf of Mexico Sand. Plos One 2012; 7.

Appendix

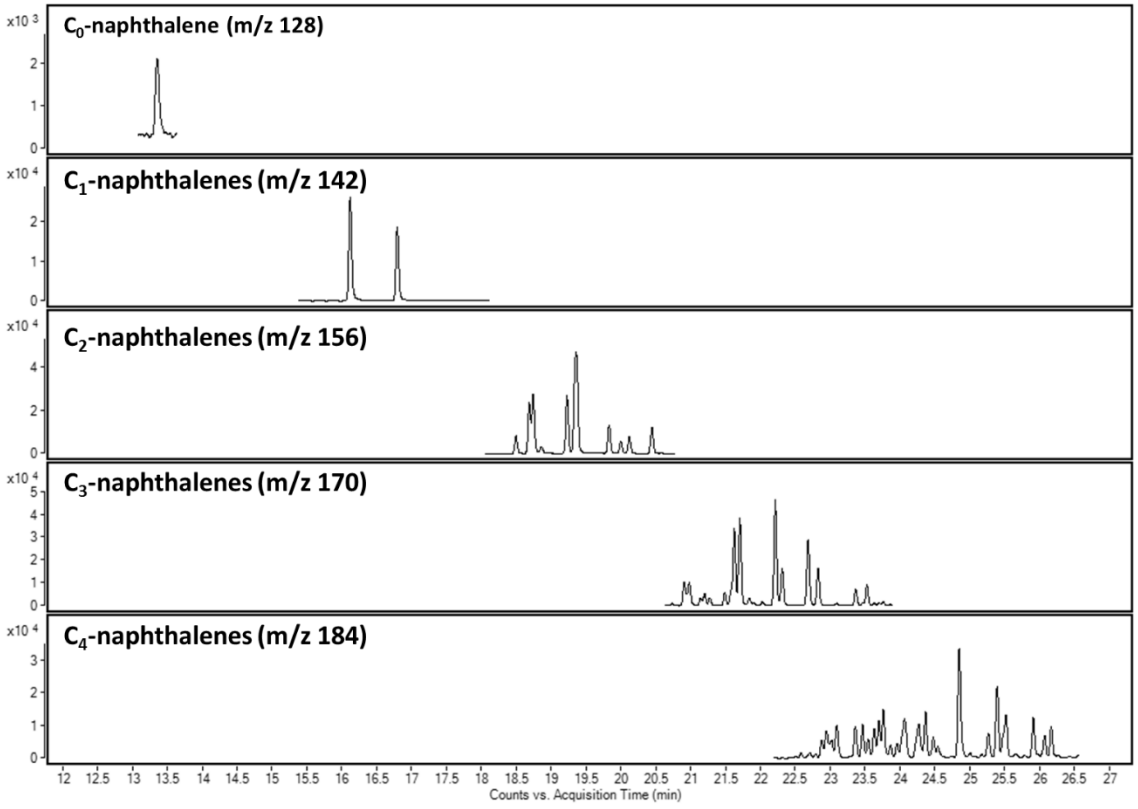

Figure A1 Extracted ion chromatograms of alkylated naphthalene homologs in GB sample

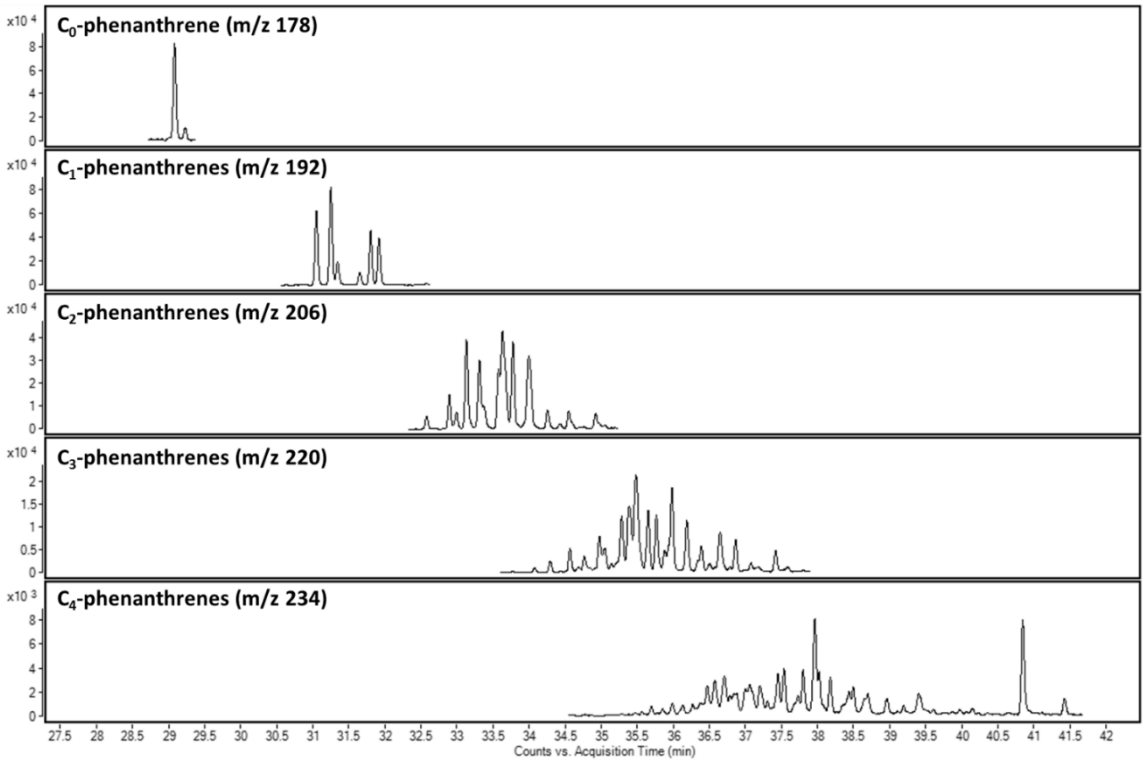

Figure A2 Extracted ion chromatogram of alkylated phenanthrene homologs in GB sample

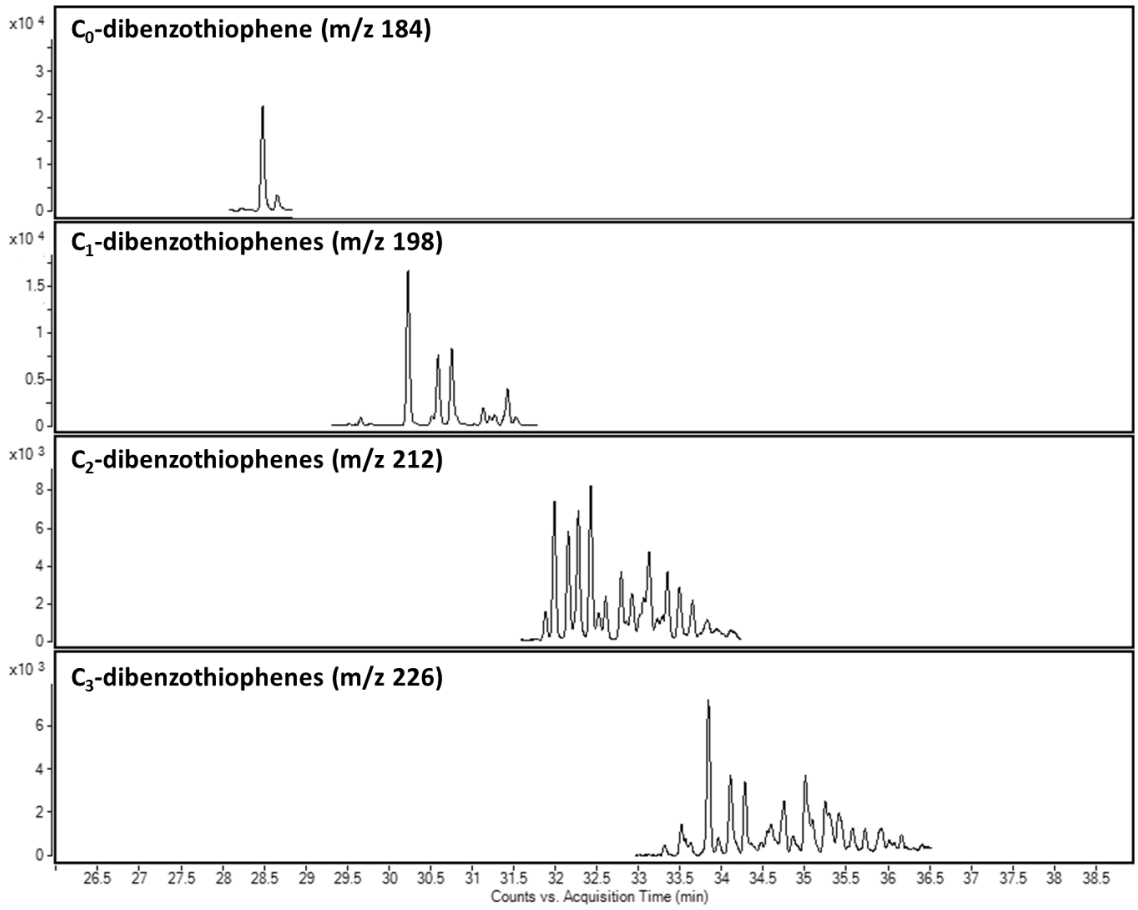

Figure A3 Extracted ion chromatogram of alkylated dibenzothiophene homologs in GB sample

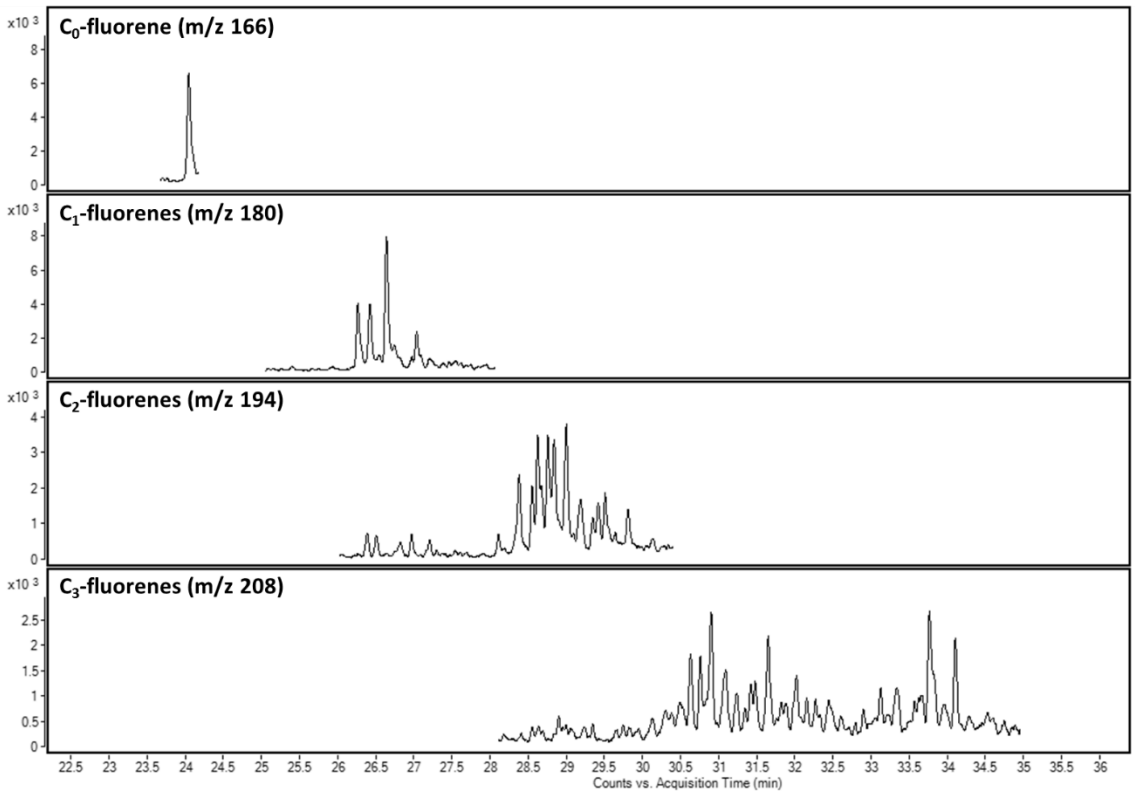

Figure A4 Extracted ion chromatogram of alkylated fluorene homologs in GB sample

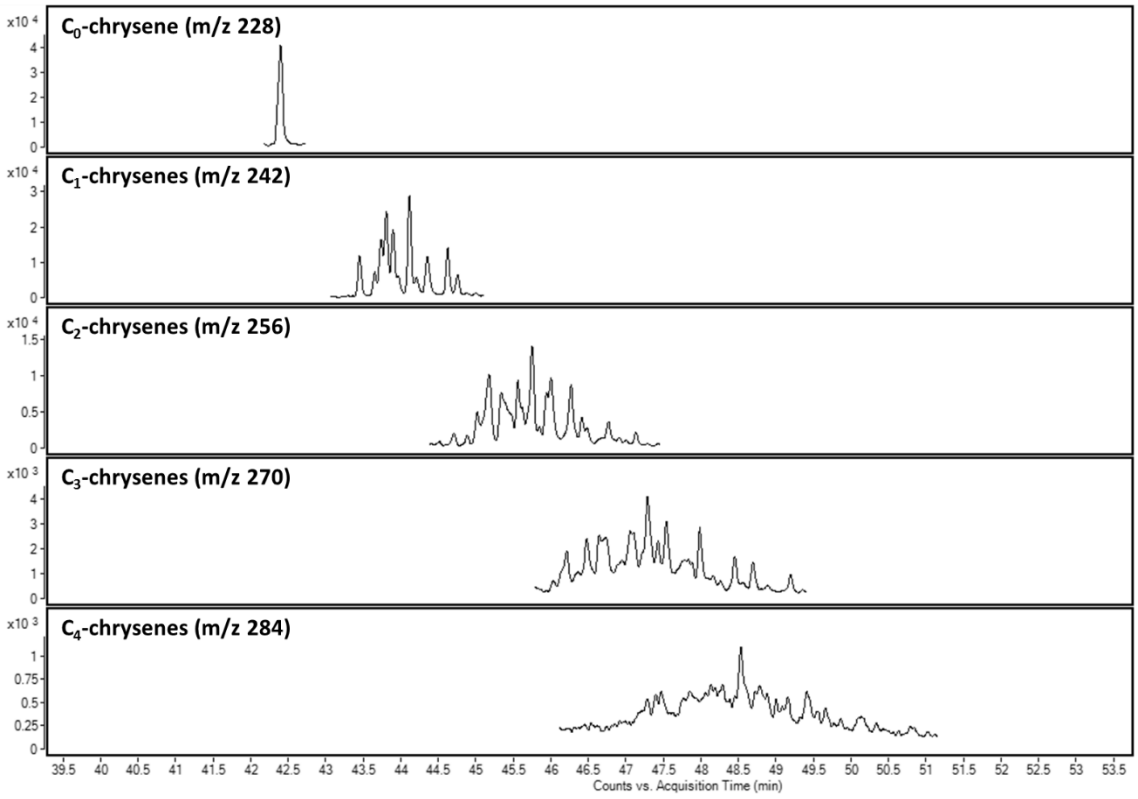

Figure A5 Extracted ion chromatogram of alkylated chrysene homologs in GB sample

Table A1 GC/MS/MS parameters used for PAH analysis

Compound	**TS**	**MRM Transitions (*m/z*)**	**CE (eV)**	**Type**
Biphenyl	1	154.0 → 152.0	25	Target
		154.0 → 153.0	25	
Naphthalene-d_8	1	136.0 → 108.0	19	SS
Acenapthylene	1	152.0 → 150.0	40	Target
		152.0 → 151.0	40	
Acenapthene-d_{10}	1	162.0 → 160.0	25	SS
Acenapthene	1	154.0 → 152.0	40	Target
		153.0 → 152.0	40	
Phenanthrene-d_{10}	2	188.0 → 160.0	19	SS
Anthracene	2	178.0 → 176.0	34	Target
Fluoranthene	3	202.0 → 201.0	30	Target
		202.0 → 200.0	50	
Pyrene	3	202.0 → 201.0	30	Target
		202.0 → 200.0	50	
p-Terphenyl-d_{14}	4	244.0 → 212.0	40	IS
Benzo(*a*)anthracene	4	228.0 → 226.0	38	Target
		228.0 → 224.0	38	
Benzo(*b*)fluoranthene	5	252.0 → 250.0	42	Target
		250.0 → 248.0	40	
Benzo(*k*)fluoranthene	5	252.0 → 250.0	42	Target
		250.0 → 248.0	40	
Benzo(*j*)fluoranthene	5	252.0 → 250.0	42	Target
		250.0 → 248.0	40	
Benzo(*e*)pyrene	5	252.0 → 250.0	42	Target
		250.0 → 248.0	40	
Benzo(*a*)pyrene-d_{12}	5	264.0 → 260.0	39	SS
Benzo(*a*)pyrene	5	252.0 → 250.0	42	Target
		250.0 → 248.0	40	
Perylene	6	252.0 → 250.0	40	Target
		250.0 → 248.0	40	
Dibenz(*a,h*)anthracene	6	278.0 → 276.0	42	Target
		276.0 → 274.0	38	
Dibenz(*a,c*)anthracene	6	278.0 → 276.0	42	Target
		276.0 → 274.0	38	
Indeno(1,2,3-*cd*)pyrene	6	276.0 → 274.0	42	Target
Benzo(*ghi*)perylene	6	276.0 → 274.0	42	Target

Note: TS-time segment; CE-collision energy; SS-surrogate standard; IS-internal standard

Table A2 GC/MS parameters used for alkylated PAHs and RRF standards

Compound	**Target Ion(*m/z*)**	**RRF standard**
C_0-Naphthalene	128	-
C_1-Naphthalenes	142	2-Methylnaphthalene
C_2-Naphthalenes	156	2,6-Methylnaphthalene
C_3-Naphthalenes	170	2,3,5-Methylnaphthalene
C_4-Naphthalenes	184	2,3,5-Methylnaphthalene
C_0-Phenanthrene	178	-
C_1-Phenanthrenes	192	1-Methylphenanthrene
C_2-Phenanthrenes	206	1-Methylphenanthrene
C_3-Phenanthrenes	220	1-Methylphenanthrene
C_4-Phenanthrenes	234	1-Methylphenanthrene
C_0-Dibenzothiophene	184	-
C_1-Dibenzothiophenes	198	Dibenzothiophene
C_2-Dibenzothiophenes	212	Dibenzothiophene
C_3-Dibenzothiophenes	226	Dibenzothiophene
C_0-Fluorene	166	-
C_1-Fluorenes	180	Fluorene
C_2-Fluorenes	194	Fluorene
C_3-Fluorenes	208	Fluorene
C_0-Chrysene	228	-
C_1-Chrysenes	242	Chrysene
C_2-Chrysenes	256	Chrysene
C_3-Chrysenes	270	Chrysene
C_4-Chrysenes	284	Chrysene
p-terphenyl-d_{14}	244	-